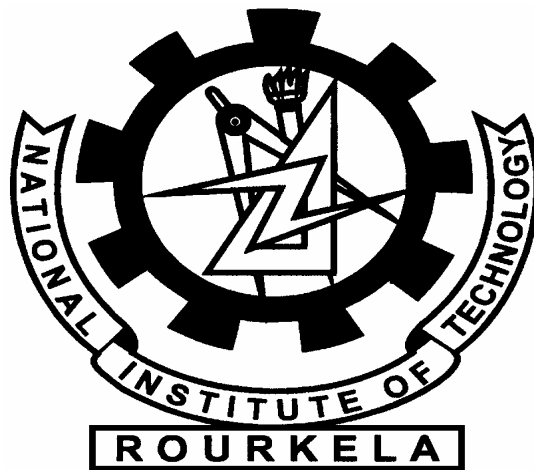A STUDY OF
RAIN ATTENUATION CALCULATION AND STRATEGIC POWER CONTROL
FOR
Ka-BAND SATELLITE COMMUNICATION IN INDIA

JAYADEV JENA

Department of Electrical Engineering (ESC)
National Institute of Technology, Rourkela-769008
India

A STUDY OF
RAIN ATTENUATION CALCULATION AND
STRATEGIC POWER CONTROL
FOR
Ka-BAND SATELLITE COMMUNICATION IN INDIA

*Thesis Submitted for the partial fulfillment
of the requirement for the degree of*

Master of Technology (Research)

In

Electrical Engineering
(Electronic Systems and Communication)

By
Jayadev Jena

Roll No. 608EE301

Under the guidance of

Prof. Prasanna Kumar Sahu

Department of Electrical Engineering
National Institute of Technology, Rourkela-769008
India

National Institute of Technology, Rourkela

Certificate

*This is to certify that the thesis entitled **"A Study Of Rain Attenuation Calculation And Strategic Power Control For Ka-Band Satellite Communication In India"** by Mr. Jayadev Jena, submitted to the National Institute of Technology, Rourkela for the award of **Master of Technology (Research)** in Electrical Engineering, is a record of bonafide research work carried out by him in the **Department of Electrical Engineering(ESC), National Institute of Technology, Rourkela** under my supervision. I believe that this thesis fulfills part of the requirements for the award of degree of Master of Technology (Research). The results embodied in the thesis have not been submitted for the award of any other degree elsewhere.*

<div align="right">

Prof. Prasanna Kumar Sahu
Department of Electrical Engineering
National Institute of Technology
Rourkela- 769008

</div>

Acknowledgement

ABSTRACT

The tremendous worldwide growth in the use of Internet and multimedia services prompted the ambitious planning for evolution of commercial and broadband satellite communication systems. The traditional C and Ku bands in satellite communications are getting crowded, So the systems are moving towards higher frequency ranges above 20 GHz. The Ka-band (18-40 GHz) frequency spectrum has gained attention for satellite communication. The inherent drawback of Ka-band satellite system is that increase in signal distortion resulting from propagation effects. Atmospheric attenuation in Ka-band is always severe, especially in the presence of rain. Thus, New technologies are required for Ka-band systems, such as multiple hopping antenna beams and regenerative transponders to support aggregate data rates in the range of 1 - 20 Gbps per satellite, which can provide DTH, HDTV, mobile and fixed Internet users with broadband connection. Currently in India C and Ku-band frequencies are being used for commercial satellite communications. In future Ka-band will be used for wideband applications. Keeping in view of the socio-economic and geographical diversities of India. Propagation studies are essential for estimation of attenuation, so that Ka-band satellite links operating in different parts of Indian region can be registered appropriately. Ka-band system is recognized as a new generation in communication satellites that encompasses a number of innovative technologies such as on board processing (OBP) for multimedia applications and switching to provide two way services to and from small ground terminals. To do this efficiently multiple pencil like spot beams are used. One distinct feature of this propagation being used to address this problem is Satellite Spot-Beam. To design effective satellite communication system, the arrangement of spot beam locations in Indian subcontinent, the study and analysis of link availability for Ka-band satellite communication in various geographically separated spot beams in India using statistical data is necessary. Based on global rain models integrated with the link budget, the study allows us to examine major system design issues encountered in Ka-band satellite communication that are susceptible to propagation impairments. This system can be flexible enough to increase power on specific transmissions to compensate for local weather conditions. This can make better use of the available bandwidth than C or Ku-band satellite, and more users can get higher level of services.

Key words: Satellite communication in India, Ka Band, Rain attenuation, OBP, Power control.

<u>**CONTENTS**</u>

Chapter 3

Prediction Models for Rain Attenuation

Chapter 4

Fade compensation and uplink power control

Chapter 5

Conclusion and Future works

LIST OF TABLES

LIST OF FIGURES

ACRONYMS

- ACTS   Advanced communications technology satellite
- BER   Bit error rate
- CDMA   Code division multiple access
- C/I   Carrier to interference ratio
- C/N   Carrier-to-noise ratio
- C/No   Carrier-to-noise density
- DAH   Dissanayake, Allnutt, and Haidara (rain attenuation model)
- DBSG   ITU-R Data Bank Study Group
- dBK   deciBel-Kelvin
- dBm   deciBel- milliwatts
- dBW   deciBel-watt
- DTH   Direct to home
- EIRP   Effective isotropic radiated power
- Eb/No   Energy per bit to noise density ratio
- EHF   Extreme high frequency
- erfc   Complimentary error function
- FDM   Frequency division multiplexing
- FDMA   Frequency division multiple access
- FEC   Forward error correction
- FMT   Fade mitigation techniques
- GEO   Geostationary Earth orbit
- GHz   Gigahertz
- G/T   Receiver figure of merit
- HPA   High power amplifier
- IEEE   Institute of Electrical and Electronics Engineers
- IMD-   Indian Meteorological Department
- ISRO   Indian Space Research Organisation
- ITU   International Telecommunications Union

- ITU-R   International Telecommunications Union, Radio communications
- ITU-T   International Telecommunications Union, Telecommunications Standards sector
- K   Degree Kelvin
- Ka-band -   Frequency band between 17.7 and 21.2 GHz (downlink) and 27-31 GHz (downlink) assigned to satellite communication
- Ka-   Kurtz above
- Ku -   Kurtz under
- Mbps   Megabits per second
- MCPC   Multiple channel per carrier
- MF-TDMA   Multi-frequency time division multiple access
- MPEG   Motion picture expert group
- NOC   Network Operation Centre
- OBP   On-board processing transponder
- QAM   Quadrature amplitude modulation
- QPSK   Quadrature phase shift keying
- S/N   Signal-to-noise ratio
- ST   Satellite terminal
- SS/TDMA   Satellite switched Time division multiple access
- TDMA   Time division multiple access
- TWTA   Travelling wave tube amplifier
- VSAT   Very small antenna (aperture) terminal

Introduction

1.1   Introduction

Satellite communication systems have become an essential part of world's communication infrastructure, serving billions of people with telephone, data, and video services. Despite the growth of fibre-optic links, satellite systems continue to dominate attracting fresh investment in new systems. The proposed systems must provide two-way interactive services to support data rates of 1 to 20 Gbps [48] per satellite. The International Telecommunication Union (ITU) has granted licenses to satellite organizations to operate broadband satellite systems in the Ka-band spectrum, which is often referred to as 30/20 GHz [29]. This paper assesses the future role of satellite communications in providing mobile, fixed Internet users with broadband connection in India. It analyzes Ka-band satellite communication link available in geographically dispersed zones through spot beam techniques in India. It is based on global rain models integrated with the link budget [29]. The rain models developed, allow us to examine major system design issues encountered in Ka-band or higher satellite communication bands   that are susceptible to propagation impairments.

Today's communications satellites offer extensive capabilities in applications involving data, voice, and video, with services provided to fixed broadcast, mobile systems, personal communications, and private network users. Worldwide, there have been considerable experiments on   Ka-band Satellites to solve the problem of saturation of the available orbital slots at C and Ku-band and to provide new services for the information age. Ka-band system is recognized as a new generation for communication satellites [47] [8] that encompasses a number of innovative technologies such as on board processing (OBP) for multimedia applications and switching to provide   two way services to and from small ground VSAT terminals[5]. To do this efficiently multiple pencil like spot beams are used. This paper proposes 16 spot-beam locations to cover Indian main land. The on board processing and switching (effectively the provision of the equivalent of a sophisticated telephone switch board on a satellite) are already employed in satellites providing mobile communications to handheld receivers in some western part of world.

1.2 Background and Motivation

The growing demand for advanced telecommunication services, due to an increase of traffic and the number of users, requires the extension of the capacity assigned to the services. Satellite systems can be very useful to this, because of their typical flexibility in terms of coverage area and the possibility of being utilized as private networks or for interconnecting public at large. Capacity enhancement can be achieved both the ways with new available spectrums and efficient use of the existing ones [52].

The satellite communication system providers are moving towards Ka-band and other higher frequency ranges, as the pre-allocated satcom bands have become crowded [8]. Ka-band satellite systems use uplinks at a frequency of about 30GHz and downlinks near 20GHz. More than a dozen Ka-band systems have been proposed for launch in this decade. One inherent drawback of Ka-band satellite systems is increase in signal distortion resulting from propagation effects [28]. Atmospheric attenuation in Ka-band is severe, especially in the presence of rain [7]. Tropospheric scintillation increases with frequency, creating fast amplitude variations and additional phase noise in the transmission [55]. The scintillation is generally enhanced by smaller antenna apertures and very small aperture terminals (VSATs), which are becoming very popular.

The NASA Advanced Communication Technology Satellite (ACTS) program has provided a means to investigate the problems associated with Ka-band satellite transmissions [7]. ACTS is the first Ka-band communication satellite in geostationary orbit (GSO) over the western hemisphere (September 1993). ACTS has served as a test bed for many of the new technologies needed for Ka-band systems, such as multiple hopping antenna beams and regenerative transponders [54].

During last five years Indian Space Research Organisation (ISRO) has started investigating the problems in Indian region. It had launched GSAT4 satellite on 15th April 2010 but the mission failed. So the investigation through this satellite as envisaged could not materialise. Here we have tried by collecting the standard data from Indian meteorology and the international agencies like ITU, NASA, journals and research papers, to compare the behaviour with the tropical countries reports to get a step ahead on the study of Ka band in Indian region [2].

1.3   Features of Ka- Band

Ka-band is having raw bandwidth of around 13 GHz (27-40 GHz) and some additional 9 GHz of K-band (18-27 GHz) typically used for Ka-band satellite downlinks, compares well with the 6 GHz of Ku-band [8][52].

The advantage of Ka-band over other forms of internet via satellite is that it only requires a dish antenna of size 65 cms×75cms. Additionally Ka-band uses spot beams for service via satellite, which makes better use of the available bandwidth than a C or Ku-band (12-18 GHz) satellite, i.e. more users can get higher level of services.

At Ka-band the propagation impairment strongly limits the quality & availability service in satellite communications [8]. Attenuation due to rain plays a significant role in tropical regions [20], especially with a great diversity of climatic conditions in India. Currently in Indian region C and Ku-band frequencies are being used for commercial satellite communication applications. In future Ka-band will be used for wideband applications. Propagation studies are essential for estimation of attenuation so that Ka-band satellite links operating in different parts of Indian region can be registered appropriately. The details of Ka band and its difficulties are discussed in chapter 2.

1.3.1 Ka-band Earth-GEO Links

In the last decades, satellite communications have been moving from lower frequency band, i.e., C-band (6/4 GHz) and Ku-band (14/12 GHz), to higher frequency band, i.e., Ka-band (30/20 GHz). Moving to higher frequencies [37] will offer several advantages [8]:

- Less congested spectrum: C-band frequencies have been used for a long time for satellite communications and is already saturated. Afterwards, satellite communications migrated to Ku-band frequencies, but have been filling up rapidly. Higher frequency band is hence needed badly to solve the problem.

- Reduced interference potential: Because Ka-band has not yet been used widely, cross interference is expected to be less.

- Higher data rates: Compared with C-band (downlink frequencies between 3.7 to 4.2GHz, and uplink frequencies between 5.925 to 6.425GHz) and Ku-band (uplink frequencies between 14 and l4.5GHz, and downlink frequencies between 11.7 and 12.7GHz), Ka-band offers wider bandwidths, and as a result, higher data rates.

− Smaller equipment size: The diameters of Ka-band antennas varies between 2 feet and 5 feet, while for C-band, large dish is required with diameter of about 6 feet, and for Ku-band, the diameter is between 2.6 and 5 feet.

1.3.2 Successful Ka band Missions

Ka-band satellite service on Earth-GEO (geostationary earth orbit) links was first introduced as early as the 1970's in Japan. Afterwards, ESA and NASA both showed interests in introducing higher frequency band, i.e., Ka-band, to satellite communications. Several significant measurement campaigns were conducted and contributed greatly to characterization of the propagation channel, investigating the propagation impairments, and developing/improving the prediction models and fade mitigation techniques for Ka band Earth-GEO links [54].

• The OLYMPUS experiment started in 1989 by ESA, and terminated in August 1993. During the satellite's lifetime, the OLYMPUS beacon signal for propagation research was received and analyzed at more than fifty locations covering all of Western Europe with different climatic regions, and a few in North America. [8][45].

• The ITALSAT program was initiated by the Italian Space Agency, with the purpose of demonstrating advanced technologies in the field of Ka-band propagation. ITALSAT was launched in December 1991 into a geostationary orbit. The propagation measurements were performed at the frequencies of 20, 40 and 50 GHz.

• The Advanced Communications Technology Satellite (ACTS) was conceived at the National Aeronautics and Space Administration (NASA). It was designed to obtain slant-path attenuation statistics for locations within the United States and Canada for use in the design of low-margin Ka-band satellite communication systems. ACTS provided beacon signals at 20.2 and 27.5 GHz for use in making attenuation measurements [54].

After the successful commercial application of Ku-band ,2000 onwards, there have been growing commercial interests in using Ka-band on Earth-GEO links to provide different kinds of service, especially low-price high-speed two-way broadband internet service [7][8]. Past successful events and future launches include Anik-F2 (Canada, 2004), WildBlue-1 (U.S., 2006), Spaceway system (U.S., 2005 and 2006), KA-SAT (Europe, 2010) and ViaSat (U.S., 2011) [48].

1.4 Rain and Attenuation

The attenuation is caused by the scattering and absorption of electromagnetic waves by drops of liquid water. The scattering diffuses the signal, while absorption involves the resonance of the waves with individual molecules of water. Absorption increases the molecular energy, corresponding to a slight increase in temperature [8], and results in an equivalent loss of signal energy. Attenuation is negligible for snow or ice crystals, in which the molecules are tightly bound and do not interact with the waves [7]. The attenuation increases as the wavelength approaches the size of a typical raindrop (water particles), which is about 1.5 millimetres. Wavelength and frequency are related by the relation $c = \lambda . f$, where λ is the wavelength, f is the frequency, and c is the speed of light (approximately 3 x 10^8 m/s). For example, at the C-band downlink frequency of 4 GHz, the wavelength is 75 millimetres. The wavelength is thus 50 times larger than a raindrop and the signal passes through the rain with relatively small attenuation. At the Ku-band downlink frequency of 12 GHz, the wavelength is 25 millimetres. Again, the wavelength is much greater than the size of a raindrop, although not as much as at C-band. At Ka-band, with a downlink frequency of 20 GHz, the wavelength is 15 millimetres and at V-band, at a downlink frequency of 40 GHz, it is only 7.5 millimetres. At these frequencies, the wavelength and raindrop size are comparable and the attenuation is quite large. Considerable research has been carried out to model rain attenuation mathematically and to characterize rainfall throughout the world. Many experimental measurements are done in western hemisphere related to this field. [7]

The standard method of representing rain attenuation is through an equation of the form (details in chapter 3)

$$L_r = \alpha \, R^\beta . \, L = \Upsilon \, L \tag{1.1}$$

Where, L_r is the rain attenuation in decibels (dB), R is the rain rate in millimetres per hour, L is an equivalent path length (km), and α and β are empirical coefficients that depend on frequency and to some extent on the polarization. The factor γ is called the specific rain attenuation, which is expressed in dB/km. The equivalent path length depends on the angle of elevation to the satellite, the height of the rain layer, and the latitude of the earth station. The rain rate enters into this equation because it is a measure of the average size of the raindrops. When the rain rate increases, *i.e.* it rains harder, the rain drops are

larger and thus there is more attenuation. Rain models differ principally in the way the effective path length *L* is calculated. Two authoritative rain models that are widely used are the Crane model and the ITU-R (CCIR) model [8][34]. The original Crane model is the global model which we have taken for our analysis for Indian region. A revision of this model that accounts for both the dense centre and fringe area of a rain cell is the so-called two component model (1.2)[7].

In the design of any engineering system, it is impossible to guarantee the performance under every conceivable condition. One sets reasonable limits based on the conditions that are expected to occur at a given level of probability. In the design of a satellite communications link one includes margin to compensate for the effects of rain at a given level of availability, details in chapter 4. The statistical characterization of rain begins by dividing the world into rain climate zones [29]. Within each zone, the maximum rain rate for a given probability is determined from actual meteorological data accumulated over many years.

1.5 Major Propagation Impairments on Ka-band Earth-Space Links

One major problem of using Ka-band on Earth-space links is that the propagation impairments become more severe at such high frequencies [18][19]. Free space loss is the dominant component of the propagation attenuation. It can be calculated by using the equation

$$L = 20 \log \left(\frac{4 \pi d}{\lambda} \right) \qquad \text{[dB]} \qquad (1.2)$$

Where, L is the path loss, d is the distance between the satellite and the earth station, λ is the wavelength of the signal in use. Attenuation by atmospheric gases depends on frequency, elevation angle, and altitude above sea level and water vapour density. It is relatively small compared to rain attenuation. Rain affects the transmission of an electromagnetic signal in three ways [7]:

- It attenuates the signal;

- It increases the system noise temperature;

- It changes the polarization.
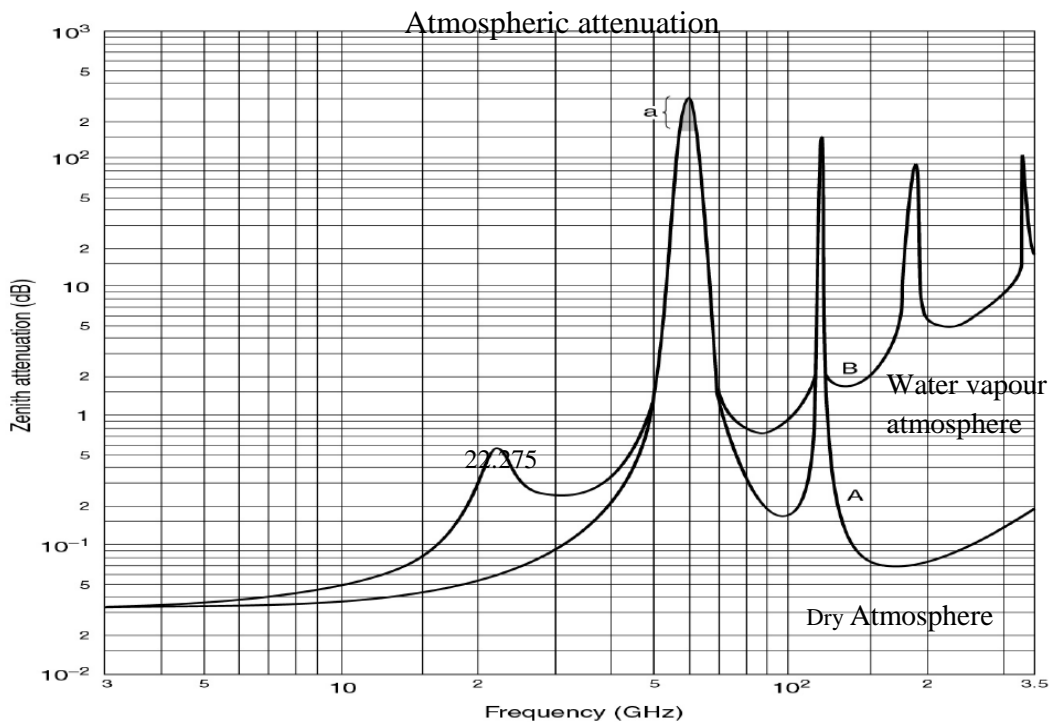
Figure 1.1 Total dry air and water-vapour zenith attenuation from sea level for standard atmosphere. Surface pressure 1013hPa, surface temperature 15 °C, surface water-vapour density: 7.5g/m^3 [14]

All three of these mechanisms cause degradation in the received signal quality and become increasingly significant as the carrier frequency increases. Frequency below 10GHz it may normally be neglected, however it is significant above 10GHz, especially for low elevation angles. Water vapour is the main contributor compared to gaseous attenuation in the frequency range below 30GHz with a maximum occurring at 22.275GHz, which is the resonance frequency of water particles with RF [8]. The attenuation due to oxygen absorption exhibits an almost constant behaviour for different climatic conditions, whereas the attenuation due to water vapour varies with temperature and absolute humidity. Rain fade is the signal degradation due to interference of rainfall or clouds with radio waves (RF). Attenuation due to rain is a dominant factor for determining link availability at frequencies above 10 GHz. It depends on temperature, drop size distribution, terminal velocity and the shape of the raindrops. Also Ka-band is affected by cloud in the path [45].

Gas attenuation is caused by gas molecules (oxygen and water vapour) absorbing energy from the radio waves passing through them. Gas attenuation increases with

increasing frequency, and is dependent on temperature, pressure, and humidity. ITU-R P.676-6 includes and approximate model of calculating the gaseous attenuation. Clouds and fog consist of water droplets (less than 0.1 mm in diameter), which absorb and scatter energy and causes reduction in signal amplitude. Although cloud attenuation is not severe, it usually presents for large percentage of the time. The method of obtaining cloud and fog attenuation is described in ITU-R 840 [26].

Raindrops absorb and scatter radio wave energy, resulting in rain attenuation, which is the major impairment for frequency bands above 10 GHz. Because of the smaller wavelength, transmission at Ka-band is more susceptive to rain attenuation, which could reach 40 dB at 30 GHz. Rain attenuation severely impairs the link performance, and therefore, fade mitigation techniques (FMT), such as power control and site diversity, are implemented to predict or compensate the rain fading [3].

1.5.1   Effect of scintillation

Scintillation, here defined as tropospheric scintillation, is a rapid and random fluctuation in one or more of the characteristics (amplitude, phase, polarization, and direction of arrival) of a received signal, which is caused by refractive index fluctuations of turbulence due to turbulent mixing of air masses with different temperatures, pressure and water vapour content. At low elevation angles and higher frequencies, scintillation could reach the value comparable to rain fading and impairs low margin systems. Such fast fluctuation could interfere with power control algorithms used to mitigate rain fading [7]. Determination of rain fading and scintillation are significant for estimating or designing the Earth-space links, as well as for the fade mitigation techniques.

For Earth-GEO links, both rain fading and scintillation occurring along the path has been well studied, and many prediction models have been developed and tested by being compared with the measurement data. The earth-space link is fixed for Earth-GEO links. Therefore, the range between the satellite and earth station, and the slant path through the atmosphere do not change, which make the prediction or calculation of the attenuation simple and straightforward. The analysis of rain and scintillation are analogous [55].

1.5.2 Attenuation levels effect on RF Bands

At C-band, the rain attenuation for an elevation angle of 50° and a maximum rain rate of 30 mm/hr is 0.1 dB. This is practically a negligible effect. At Ku-band, under the same conditions, the attenuation is 4.5 dB. This is a large but manageable contribution to

the link budget. However, at the Ka-band downlink frequency of 20 GHz, the attenuation is 12.2 dB. This would be a significant effect, requiring over 16 times the power as in clear sky conditions. At the uplink frequency of 30 GHz, the attenuation would be 23.5 dB, requiring over 200 times the power.

These losses simply cannot be accommodated completely at extreme end but can be compensated partially; discussed in chapter 4 and the accessibility would be much less. In practice, these high rain attenuations are sometimes avoided by using site diversity, in which two widely separated earth stations are used [12]. The probability that both earth stations are within the same area of rain concentration is small. But a parallel system would be indispensable, which will be too expensive. Alternatively, a portion of spectrum in a lower band may be used where needed. For example, a hybrid Ka-band/Ku-band system might be designed in which Ka-band provides ample spectrum in regions of clear weather, but Ku-band is allocated to regions in which the rain margin at Ka-band is exceeded [8].

1.5.3. Rain and temperature

The downlink system noise temperature increases due to rain. The figure of merit of the earth station receive antenna is the ratio of the antenna gain to the system temperature *G/T*. The effect of rain is to increase the system temperature and thus reduce the figure of merit. The antenna temperature is the integrated sky temperature weighted by the antenna gain. At a high angle of elevation, the clear sky temperature is typically about 25 K since the antenna looks at cold space. However, the temperature of liquid water is about 300 K. Thus the rain increases the sky temperature noteworthy. Therefore, the noise admitted to the earth station receiving antenna increases and causes further signal degradation. However, rain does not affect the system noise temperature of the satellite and uplink chain more, because its antenna looks at the warm earth. The rain layer acts very much like a lossy waveguide [31][22].

1.5.4. Rain and Polarisation

Rain changes the polarisation of the signal somewhat. Due to the resistance of air, a falling raindrop assumes the shape of an oblate spheroid. Wind and other dynamic force can cause the rain drop to be rotated at statistical distribution of angles. Consequently, the transmission path length through the rain drop is different for different signal polarisations and the polarisation of the received is altered. For a satcom system with dual linear polarisations, the change in polarisation has two effects. First, there is loss in signal strength

because of misalignment of the antenna relative to the clear sky orientation. Given by 20log(cosτ), where τ is the tilt angle relative to the polarization direction induced by the rain. Second, there is additional interference noise due to the admission of a portion of the signal in opposite polarisation.

1.6 Spot beam and its features
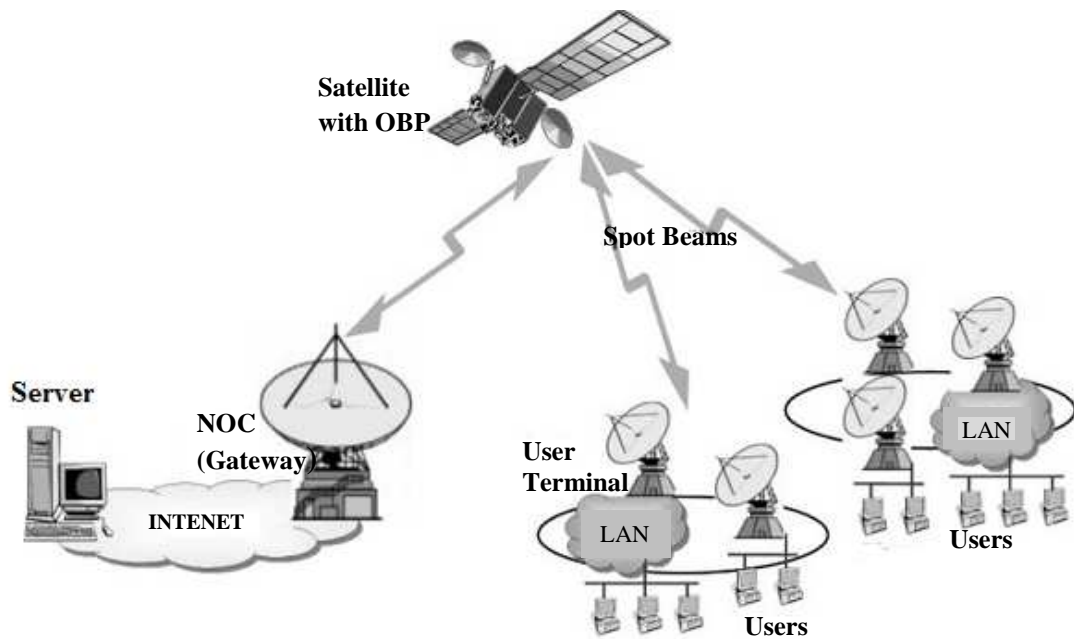
Figure1.2: Satellite communication system architecture. The satellite provides broadband service across multiple spot-beam locations.

Generally communication satellites transmitted with a very broad signal. The same signal that is received in the New Delhi is from the same source as the signal that is received in Chennai. Satellites that are not having "Spot Beams" send out a signal over very large areas, transmitting data across the foot print. But Spot Beams are different. It is similar to a searchlight focused on one area of the country. A typical Spot Beam has a radius of only 200-500Kms [19]. Depending on where you are in the country, you won't detect the beam unless you are in the focus. With this tool, the same frequency spectrum can be used with different source material, in different regions. In addition, the system is flexible enough to increase power on specific transmissions when needed to compensate for local weather condition. The transmission of regional TV channels is ideal since a signal focused on an area is a perfect fit for the application.

The Spot Beam technology is being applied on newer satellites using the Ka-Band (e.g.; GSAT-4 of ISRO, India). Spot Beam technology is also ideal for the transmission of video requiring ultra high bit rates such as HDTV. But more than 100 kilometres from the

signal centre in a populated region, it is possible that you will not be able to receive the HDTV Spot Beams. . The Spot Beam technology is being applied on newer satellites using the Ka Band [8]. There are several Ka band satellites in use that do not use Spot Beams: Advanced Communication Technology System (NASA, USA), Superbird and N-STAR (Japan), HOT BIRD 6 (Eutelsat, France), DFS Kopernikus (Germany), and Italsat (Italy), but the newer, more advanced satellites are using Spot Beam technology [48].

1.6.1 HDTV Spot Beams

High Definition TV Spot Beams with Ka band are often narrower in focus than the Ku/Ka band Spot Beams used for Standard Definition TV. If the user placed more than 50 miles from the signal center in a populated region, it is possible that one will not be able to receive the HDTV Spot Beams. It makes good business sense for them to maximize service in coverage area, but there are tradeoffs [47].

In low population density areas like north east beam, it makes sense to have the Spot Beams cover a 300-400Kms radius, because that enables more subscribers which results into more revenue. In metro cities it sometimes makes sense to focus the signal more narrowly for HDTV, and users are more densely packed together. However, due to different frequencies are used for adjacent Spot Beams, overlap usually can be managed.

1.6.2 Spot-Beam Satellites and Two-Way Communications

One advantage of Ka band is that it requires a smaller dish to offer very good performance. Ka band using Spot Beams is more efficient than a traditional C or Ku band satellites. The service is able to deliver significant improvements in performance. A Ka band satellite can provide as much as an 8X increase in capacity over Ku band satellites. The technology can provide upload speeds as fast as 16 Mbps and download speed as fast as 30 Mbps. Three Ka band satellites with Spot Beam technology are already in service in North America: Telesat Canada's Anik F2, WildBlue Communications Wildblue 1, and Hughes Network Systems SPACEWAY 3. According to Northern Sky Research, there are 15 million U.S. households without access to broadband Internet service. Spot Beam satellites operated by WildBlue and Telesat have already reached over 300,000 Internet subscribers in one year from their launch in 2005 [19].

1.7 Fade Mitigation Techniques

Mitigating the effects of rain attenuation has been an area of focus in the research community. The measures against signal degradation can be grouped into two as diversity techniques and compensation techniques. Diversity techniques, such as site and frequency-

diversity, avoid signal degradation by switching between the signals obtained at different receiver sites or between different frequency bands. Site diversity takes advantage of the fact that probability of high attenuation occurring simultaneously at two or more receiver sites is significantly lower than any single site. Therefore, signals obtained at multiple sites can be combined (at some central location) to improve the signal-to-noise ratio [12]. Frequency diversity makes use of the fact that signals suffer more from atmospheric attenuation as the frequency of operation increases. Hence, a Ka-band system may switch to lower frequency bands (C or Ku) when the attenuation due to rain exceeds a certain threshold. Other diversity techniques include time- and orbital-diversity [7][19]. But these all are too expensive and dependent.

Compensation techniques, such as adaptive coding and modulation, transmission rate reduction, and power control, avoid signal degradation by restoring the signal quality to the initial level. Adaptive coding involves changing the amount of redundancy introduced to the transmitted information as the quality of the link changes. The probability of successful transmission increases as the redundancy level is increased; however, transmission (bandwidth) efficiency decreases at the same time. Adaptive modulation schemes decrease the required SNR for achieving a target bit error rate (BER) by reducing the spectral efficiency (in bps/Hz) of the transmitted signal when fading occurs. A satellite system may switch between higher-order modulation schemes, such as 16-PSK,16 QAM, 64-PSK, or 254-QAM (quadrature amplitude modulation), under clear sky conditions, and lower-order modulation schemes like BPSK(binary PSK) and QPSK (quadrature PSK) under deep fading [25]. Data rate reduction, on the other hand, achieves an extra margin over the required signal-to-noise ratio by decreasing the information data rate whenever the system experiences deep fading. Finally, in adaptive power control schemes, transmitted power is adjusted dynamically based on the attenuation levels. Power control can be applied on the satellite downlink by changing the satellite effective isotropic radiated power (EIRP), or on the uplink, by controlling the power of earth stations. Adaptive power control (APC) is more efficient than providing fixed power margins, since severe attenuation occurs typically in short durations. APC can also be easily combined with other compensation techniques if larger fade margins are required [19].

While diversity and compensation techniques improve transmission quality of the users located inside the footprint of the satellite spot-beam, they do not take into account the interaction between the users, such as those belonging to the same spot beam. The

heterogeneity in spot-beam queues arises not only as a result of the load variation and the types of communication sessions, but also because of the variation of the physical channel conditions. This heterogeneity results in lower allocated session rates for active flows. We propose an optimization-based approach that controls system power with the goal of smoothing users across multiple spot beam locations.

Fade mitigation techniques (FMT) are implemented in the satellite communications system to avoid or compensate for attenuations, mainly for countering rain fading. Two major techniques are power control and site diversity [8]. The objective of power control is to make the received power stay constant, by varying the transmitted power in direct proportion to the attenuation, mainly rain fading, on the link. Site diversity is a technique implemented to overcome the effect of path attenuation during intense rain events. Effective power control and site diversity depend on the accurate prediction of fading along the propagation paths, and the understanding of spatial behaviour of channels [7]. Therefore, channel models, which are able to characterise the propagation channels or predict the fading along the propagation path, play a significant role in developing FMTs.

1.7.1 Rain rate and BER

For a digital signal, the required signal power is determined by the bit rate, the bit error rate, the method of coding, and the method of modulation. The performance objective is specified by the bit error rate. If the rain rate is exceeded a certain threshold, the bit error rate would increase at the nominal bit rate, or else the bit rate would have to decrease to maintain the required bit error rate within limit [48]. The acceptable availability defined by communication system design specifications, is 99.5% for a BER of 5E-7 or better for desirable quality signal with and without rain fade compensation.

1.8 Organization of the Thesis

The work carried out in this thesis is organized in the following manner.

Chapter-1   INTRODUCTION

The necessity of satellite communication using various frequency bands   is discussed, especially reference to the features of   Ka-band. The past success story of Ka-band relevant areas of importance including fundamentals of   rain attenuation are analytically discussed.

Chapter-2   SATELLITE COMMNICATION AND Ka-BAND

Chapter 2 describes the satellite fundamentals, Ka-band channel characteristics and the attenuation caused by atmospheric gases. This chapter reviews the features of Ka-band and its use in satellite communications. The satellite transponders along with various types of modulation techniques and multiple access techniques used in satellite communication systems are discussed. This also represents the importance of higher frequency utilisation, especially Ka-band implemented within the scope of the satellite communication in India. Here we have introduced the proposed spot beam model and its features.

Chapter-3   PREDICTION MODELS FOR RAIN ATTENUATION

Chapter 3 reviews the global rain attenuation models for the prediction of rain effects on satellite link. The complete step-by-step procedures for three models (Crane model, ITU-R model, Moupfouma model) are presented. The collected data from different corners of India and world are used in these models. Finally, the rain attenuation level for different rain rates is calculated.

Chapter 4   FADE COMPENSATION AND POWER CONTROL

This chapter contains different types of power distribution methods and redirection of data to all spot beams. The power control procedures and compensation of fading due to rain in satellite communication networks are the vital issues in Ka-band communication are discussed. The spot beams can be obtained by the steerable antenna [14] to deliver the data collected from the on board processor (OBP) in a TDM process. Here the power is estimated in every step on the basis of channel condition and the number of users accessing in the foot print of corresponding spot beam. Here it is proposed for the regulation of the minimum threshold power and radiating power levels, based on channel conditions of revenue generating stations by static or dynamic mechanism. The channel data rate can be decided statistically keeping the total outcome of the system constant among the spot beams. The algorithm for power adjustment gives an idea for compensation.

Chapter-5   CONCLUSION AND SUGGESTIONS FOR FUTURE WORK

This concludes the thesis. The conclusion is given based on the analysis of results from the previous chapter. Proposals and suggestions for future works are presented.

Satellite Communication and Ka- Band

2.1 Introduction

Satellite communication system is basically an electronic communication package placed in earth orbit, whose prime objective is to assist transmission of information from one point to another through space. Satellites form an essential part of global telecommunication systems carrying large amounts of voice, video, and data traffic, and offering a number of features such as covering very large areas of the earth, with the ability to provide instantaneous infrastructure particularly in underserved areas, as well as frequency reuse technique through On Board Processor (OBP).

The use of satellite systems becomes important in regions like India where areas are geographically diversified. With the advent of satellite technology in Asia pacific region, the services become widespread, lower frequency bands such as C and Ku become congested. It is becoming an inevitable alternative to adopt higher frequency band for satellite services. Ka-band and above are attractive bands, because they offer wider bandwidth, higher data rate, and smaller component size, such as very small aperture terminals and ultra small aperture terminals [48].

In parallel with these developments, rapid growth in Internet traffic around the globe is creating an exponential increase in the demand for transmission bandwidth appropriated for multimedia services. These services include high-speed data, high-resolution imaging, and desktop videoconferencing etc., all of which require large transmission bandwidths.

2.1.1 Satellite Communication Fundamentals

Satellite communication system is composed of the space segment and the ground segment. Satellite is capable of performing as a microwave repeater for Earth stations that are located within its coverage area, determined by the altitude of the satellite and the design of its antenna system. The arrangements of the basic orbit configurations are Geostationary Earth Orbit (GEO), Medium Earth Orbit (MEO), and Low Earth Orbit (LEO). The respective altitude ranges are 36000 km for GEO, 5000 km to 12000 km for MEO, and 500 km to 900 km for LEO. A geostationary satellite is stationary in an apparent position relative to the earth. This position is typically about 35,784 km away from the earth. Its elevation angle is orthogonal to the equator, and its period of revolution is synchronized with that of the earth in

inertial space. The radio paths between ground terminals from a fixed position with a fixed elevation angle to satellite. The ground antennas pointing to these satellites may need only limited or no tracking capability. A geostationary satellite has also been called a geosynchronous or synchronous orbit or simply a geo-satellite [7][8].

The coverage area is normally referred as a footprint. The size of the coverage area depends on the satellite aerial semi-beam width. The non- geostationary LEO and Medium Earth orbit (MEO) approaches require more movable satellites to achieve this level of coverage [31].

2.1.2 Frequency Spectrum

Microwave frequencies used for transmission to and from the satellite propagate along a line-of-sight path. GEO provide fixed satellite service (FSS) in the C and Ku bands of the radio spectrum. Some GEO use the Ku band to provide certain commercial services nowadays. The lower is the band, the better the propagation characteristics and lower is the available bandwidth, but higher is the band, the more bandwidth that is available and worse is the propagation characteristic. Therefore, the competition is keen for this spectrum due to its propagation characteristics.

Frequency Band	L	S	C	X	Ku	K	Ka	V
Range (GHz)	1-2	2-4	4-8	8-12	12-18	18-27	27-40	40-60

Table 2.1: Microwave Frequency bands and bandwidth ranges for Communication

International Telecommunication Union (ITU) oversees the orderly use of the electromagnetic frequency spectrum for satellite communication, as well as other telecommunications applications [31].

2.1.3 Satellite Communication Features

At the present scenario, with the rapid increase of information revolution there has been constant demand in expanding the broadband integrated services to be included in satellite links. Considering India's geographical features, it is reasonable to adopt a satellite platform which can meet day to day growing demands of internet services as well as the core. By using satellites one can obtain wide coverage, quick rollout of facilities compared to buried optic fibre cables unconstrained by natural conditions and distance. Compared to conventional terrestrial networks, satellite communications have the following attractive features:

● **Ubiquitous access**: services are available to whole regions within satellite footprints, including locations where terrestrial wired networks are not possible or economically viable.

● **Broadcast/multicast nature:** multimedia services will be benefitted from this feature of satellite networks.

● **High bandwidth**: satellite channels can deliver gigabits per second.

● **Flexible bandwidth-on-demand capability**: result in maximum resource utilization. On the other hand, the overall telecommunication market is growing rapidly. Exponential growth in the Internet, multimedia services using satellites are now in demand. Growth in international trade, reduced prices due to privatization of telecommunications services worldwide, access to the World Wide Web, therefore use of broadband satellite services viewed as a cost-effective solution for providing wide area coverage for developing countries.

2.2. The Ka-band Satellite System and Current Status

As early as in 1970's, researchers from the United States, Europe, and Japan started exploring the Ka-band (from 26.5GHz to 40GHz) spectrum. Japan was the first country to provide Ka-band services and at that time transparent "bent-pipe" transponders technologies introduced only. For the last two decades, a number of experimental satellites have been launched to explore the use of Ka-band [48].

In 1984 NASA formed an Advanced Communications Technology Satellite (ACTS) program to develop Ka-band satellite technologies. Its goals were to alleviate orbit congestion in lower bands, and to promote effective utilization of the spectrum to increase communication capacities [7][54]. The first Ka-band ACTS satellite that was launched in September 1993 demonstrated commercial-off-the-shelf (COTS) earth station equipment incorporating two-way frequency conversion and multimedia system integration technologies. During last decade Ka-band satellite communication systems became so popular because they could provide:

Large bandwidth and Data-Handling Capacity: The large amount of bandwidth availability in Ka-bands is the primary motivation for developing Ka-band satellite systems since lower frequency bands have become congested. This covers from 27.5 -31.5 GHz for

uplink and uses K –band frequency 17.5-21.5 GHz for down link [52]. So nearly 8 GHz for the whole satellite system.

• **Small antenna size:** Size of passive RF components is related to the wavelength used, leading to a reduction of size as higher frequencies are used [22]. On the other hand higher frequency introduces higher losses in the components, partly reducing this advantage. For a given gain and beamwidth, as the frequency goes up, the size of the antenna decreases. For a fixed antenna size, this will significantly reduce the interference from adjacent satellite systems. Obviously, the price of the smaller antenna will be lower, which makes broadband satellite service affordable to millions of commercial and residential end-users. On Ka- band a 60 cm diameter antenna or even less will be sufficient for the receiver.

• **Larger system capacity and Smaller Satellite Footprints:** Using an antenna of same size as at lower frequencies, satellite covers a smaller area while the effective isotropic radiated power (EIRP) in these areas is proportionally increased. This allows utilization of multiple beams making it possible to reuse assigned frequencies [49]. Ka-band satellites provide smaller foot prints using multi beam antenna[9] to increase the satellite power density and allow large frequency reuses, which leads to higher spectrum occupancy. Many user terminals can be served simultaneously.

• **Flexible bandwidth-on-demand:** This feature maximizes the bandwidth and resource utilization, and minimizes the cost to end-users.

On the other hand, Ka-band satellite links suffer degradation due to atmospheric propagation effects, compared to lower frequency bands. A main disadvantage of Ka-band frequency system is increase in tropospheric propagation impairments. These are, however, changing rapidly in time making it uneconomical to counter them by simply increasing transmitted power for extended periods of time. Therefore accurate predictions are required so that advanced fade mitigation techniques can be introduced.

The primary propagation factors are rain attenuation, wet antenna losses, depolarization due to rain and ice, gaseous absorption, cloud attenuation, atmospheric noise, and tropospheric scintillation. Among these factors, rain attenuation is the most challenging obstacle to Ka-band systems.

Many Ka-band satellites have demonstrated that signal strength drops drastically during heavy rain, but many strategies and techniques are available to mitigate fading. On the other hand very small hopping spot-beams are used to focus the satellites signal power on a

small area to over the effect and penetrate the rain. The satellite systems can also use coding to overcome transmission impairments. Another strategy is to lower bit rates during the period of rain. This approach would be unsuitable for many applications but might be satisfactory for some, such as Internet access. Uplink power control is another technique to mitigate the signal losses in heavy rain [54].

In recent years, due to the delayed market growth, wear and tear, consolidation, and immature Ka-band satellite industries, many companies with satellite licenses, have either postponed or cancelled their proposed satellite systems in fast hand for few years. Hughes Network Systems (HNS) is the only company with an FCC filing who did not cancel its proposed Ka-band satellite system. Hughes contracted Boeing to build the first Ka-band satellite of the Spaceway systems providing broadband communication services for the North American region. Boeing ultimately bought Spaceway. The satellite was launched in early 2004. Later few advanced countries added their name in this race in last decade.

Indian Space Research Organisation had prepared the GSAT4 satellite as an experimental satellite to study the real time behaviour of ka-band in Indian region, but the failure of launching takes India back a step [2].

2.3. Satellite System Fundamentals

There are two basic types of satellites, 1) Bent pipe or the conventional frequency translation (FT) satellite, which comprises the vast majority of past and current satellite systems, and 2) On-Board Processing (OBP) satellite, which utilizes on-board detection and re-modulation to provide two essentially independent cascaded (uplink and downlink) communications links.. The early satellite transponders were based on analog transmission, but most modern satellite systems deliver signals digitally to ensure reliability and accuracy in information transmission.

2.3.1. Bent-pipe or frequency translation (FT) Satellite System [8]

This satellite receives the uplink signal at the uplink carrier frequency, f_{up}, down-converts the information bearing signal to an intermediate frequency, f_{IF}, for amplification, up-converts to the downlink frequency, f_{dn}, and, after final amplification, re-transmits the signal to the ground service area. Figure 2.1 shows a functional representation of the conventional frequency translation transponder. No processing is done on-board with the FT satellite, except amplification to overcome the large path losses and frequency conversion to
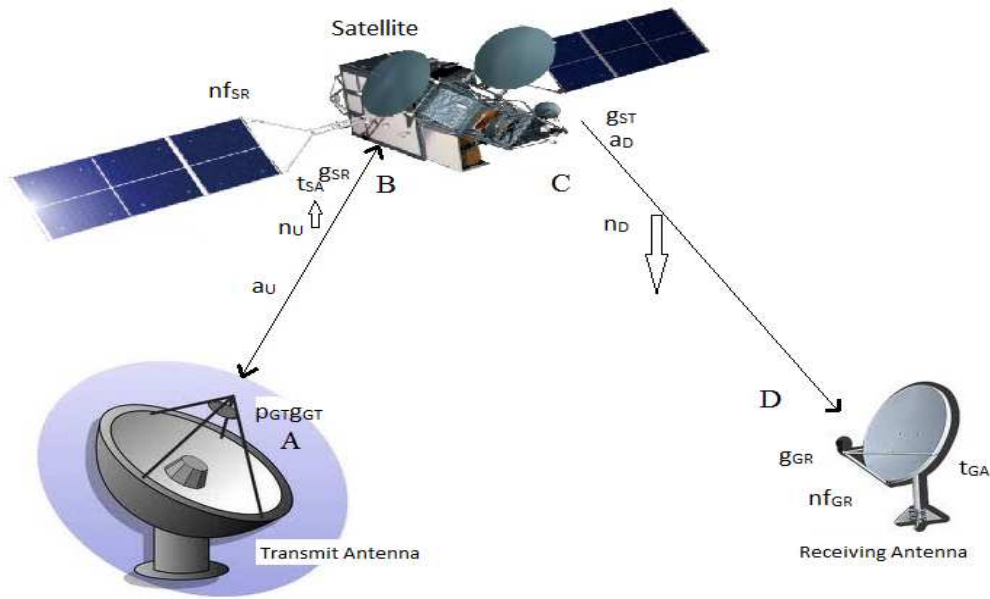
Figure 2.1: Overview of bent pipe transponder satellite link (G- Ground, S-Satellite)

(All symbols have their usual meaning)

separate the up and down links. Signal degradations and noise introduced on the uplink are translated to the downlink, and the total performance of the system is depends on both links. Generally, the transponder is transparent to the users since the transmitting signal from one earth station will "bounce" and arrive at another earth station with its characteristics unchanged. Usually, no change is made to the signal.

The conventional way of characterizing the satellite link behaviour using bent-pipe transponders is to use carrier-to-noise ratio (C/N). The C/N ratio represents the dB difference between the desired carrier signal power and the undesired noise power at the receiver. It also indicates the received signal quality for both analog and digital transmissions.

In satcom systems the C/N calculation is often called a link power budget. The C/N calculation in decibels is shown in (Eq.2.1) below.

$$\left.\frac{C}{N}\right|_{dB} = \left(P_t + G_t + G_r - L_p - A\right) - \left(K + T_n + B\right) - \text{other losses} \left[dB\right] \tag{2.1}$$

Where, P_t= Transmitted Power (dB), G_t=Gain of transmitting antenna

G_r = Receiving antenna gain of the satellite.

L_p= Path Loss=10 log$(4\pi R/\lambda)^2$ [dB], A= Rain attenuation [dB]

R= Transmission distance [m], λ = Wave length of the signal [m]

k= Boltmann's constant = 1.38×10^{-23} J/K= -228.6 dBW/Hz

T_n= Noise Tempreture [dBK] = 290K

B= Noise Bandwidth in which noise is measured [dBHz]

Other Losses such as Antenna pointing Losses, Atmospheric gaseous Losses, Power Amplifier back-Off, Link margin etc are also there. But these losses can be ignored in comparison to losses mentioned above.
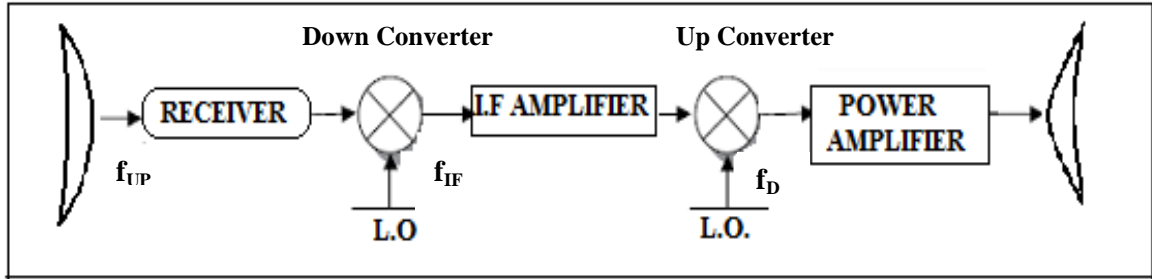
Figure2.2: Functional block diagram of a bent pipe transponder

Uplink:

The uplink refers to the signals delivered from an earth station to a satellite in space, and the downlink refers to the signal delivered from the satellite for the earth stations. For the uplink, the transmitted power is the power transmitted from an earth station to the satellite.

The received signal is always much weaker than the transmit signal since the signals passes through a long path in the sky. Path loss 'L_p' depends upon the distance between the transmitter and the receiver, and the operating frequency. The path loss for Ka-band GEO satellites about 200 dB, is large compared to those for satellites in lower orbits, and for those satellites operating in lower frequency bands.

The link performance equations for the FT satellite uplink, including the contributions of path loss and path noise has been presented in this section. The sum of P_t and G_t in decibels is presented as Effective Isotropic Radiated Power (EIRP). The EIRP is commonly specified in satellite communications and regulations. ITU and FCC have indicated the power limitations of transmitters in term of EIRP. The maximum EIRP permitted for an earth terminal is fixed for designing the outdoor unit and indoor unit of it.

The carrier power received at the satellite antenna terminals, point (**B**) on Figure 2.2, is

$$C_{SR} = \frac{P_T G_T G_R}{L_{UP} A_{UP}} \qquad [dB] \qquad (2.2)$$

Where, L_{up} is the uplink free space path loss, A_{UP} is the other uplink path loss, and G_T and G_R are transmit and receive antenna gains, respectively. The noise power at the satellite antenna, point (**B**), is the sum of three components, i.e. n_{SR} =Uplink Path Noise + Satellite Antenna Receive Noise + Satellite Receiver System Noise   the three components are

$$n_{SR} = k\, t_{UP}\left(1-\frac{1}{A_{UP}}\right)b_{UP} + k\, t_{SA}\, b_{UP} + k\, 290(nf_{SR}-1)b_{UP} \qquad (2.3)$$

Where, k is Boltzmann's constant, b_{UP} is the uplink information bandwidth, t_{SA} is the satellite receiver antenna temperature, nf_{SR} is the satellite receiver noise figure, and t_{UP} is the mean temperature of the uplink atmospheric path. Therefore, the uplink carrier-to-noise ratio, at point (B), is then given by

$$\left(\frac{c}{n}\right)_{UP} = \frac{c_{SR}}{n_{SR}} = \frac{P_T G_T G_{SR}}{L_{UP} A_{UP} k\left[t_{UP}\left(1-\frac{1}{A_{UP}}\right)+t_{SA}+290(nf_{SR}-1)\right]b_{UP}} \qquad (2.4)$$

This result gives the uplink carrier-to-noise ratio expressed in a form where the uplink path losses and noise contributions are found.

Downlink

The downlink carrier-to-noise ratio for the frequency translation satellite is found by following the same procedure that was used for the uplink, using the equivalent downlink parameters as defined in Figure 2.2. Thus, at point (D)

$$C_{GR} = \frac{P_{ST} G_{ST} G_{GR}}{L_{DN} A_{DN}} \qquad (2.5)$$

$$\left(\frac{c}{n}\right)_{DN} = \frac{c_{GR}}{n_{GR}} = \frac{P_{ST} G_{ST} G_{GR}}{L_{DN} A_{DN} k\left[t_{DN}\left(1-\frac{1}{A_{DN}}\right)+t_{GA}+290(nf_{GR}-1)\right]b_{DN}} \qquad (2.6)$$

This result gives the downlink carrier-to-noise ratio expressed in a form where the downlink path losses and noise contributions are exclusively displayed. The combine effect of both uplink and down link carrier to noise ratio is now expressed as

$$\left(\frac{c}{n}\right)_{C} = \frac{\left(\frac{c}{n}\right)_{UP}\left(\frac{c}{n}\right)_{DN}}{1+\left(\frac{c}{n}\right)_{UP}+\left(\frac{c}{n}\right)_{DN}} \qquad (2.7)$$

As the individual ratios are >> 1, by approximation 1 may be neglected and the equation reduces to and by rearranging in the form of carrier to noise density form the above equation can written as

$$\left(\frac{c}{n}\right)_{C}^{-1} \cong \left(\frac{c}{n}\right)_{UP}^{-1} + \left(\frac{c}{n}\right)_{DN}^{-1} \qquad (2.8)$$

$$\left(\frac{c}{n_{o}}\right)_{C}^{-1} \approx \left(\frac{c}{n_{o}}\right)_{UP}^{-1} + \left(\frac{c}{n_{o}}\right)_{DN}^{-1} \qquad (2.9)$$

A transponder is said to be uplink limited if its uplink CNR is more than downlink CNR and conversely, it is downlink limited if its downlink CNR is more than uplink CNR. It is possible that some transponders are uplink limited and others downlink limited, on the same satellite, depending on link parameters and the specific applications [41]. And the Energy to noise density ratio per Bit, (e_b/n_o) can be found by this relation. And the combine effect of uplink and downlink is given as

$$\left(\frac{c}{n_{o}}\right) = \frac{1}{T_{b}}\left(\frac{e_{b}}{n_{o}}\right) \qquad (2.10)$$

$$\left(\frac{e_{b}}{n_{o}}\right)_{C}^{-1} \approx \left(\frac{e_{b}}{n_{o}}\right)_{UP}^{-1} + \left(\frac{e_{b}}{n_{o}}\right)_{DN}^{-1} \qquad (2.11)$$

The probability of error for the overall end-to-end digital link is determined from the composite energy-per-bit to noise density described above. The parameters and ratios presented here and in the previous sections are expressed as numerical values, not in dB. The composite link performance for the bent pipe transponder is difficult to predict because of the interactions of the link parameters, as evidenced in the uplink and downlink results given by noise figure and CNR equations. It is possible to draw some general conclusions about composite link behaviour from the composite carrier-to-noise ratio results, as given by Equation (2.11).

i)   The overall performance or CNR is slightly less than the weaker link. Thus a satellite with dominant link will perform no better than the weaker link.

ii) When both uplink and downlink CNRs are same the overall system performs with a carrier-to-noise ratio of 1/2 either link or 3 dB below the dB value of either link. Thus, a satellite with equal uplink and downlink performance will operate with a composite value 3 dB below the value of each of the individual links.

CNR_{UP}	CNR_{DN}	CNR_C
20 dB	10 dB	9.6 dB
10 dB	10 dB	7 dB

Table2.2: System performance comparison for bent pipe transponder

As mentioned in the previous section, as heavy rain significantly degrades the link performance, the C/N ratio falls due to it. The permissible rain attenuation for a link depends on many factors, such as the link availability in an average year, earth station geographical location, and link operating frequency. The estimation of the rain attenuation can be calculated using the ITU recommended rain model and other models, which is presented in Chapter 3. Other factors affecting the link performance include antenna pointing losses, atmospheric gaseous losses, power amplifier back-off power, link margins, and implementation margins which have also been described briefly Chapter 3.

2.3.2. On-board Processing (OBP) Satellite System [7]

The OBP satellite system, consisting of regenerative transponders and on-board switching with multiple spot-beams, provides bandwidth on demand with low processing delay, flexible interconnectivities, and lowered ground station costs. A satellite that provides on-board demodulation and re-modulation of the information bearing signal is referred to as an on-board processing (OBP) satellite. The OBP satellite, also called a regenerative satellite or a smart satellite, provides two essentially independent cascaded communications links for the uplink and downlink. Figure 2.3 shows a schematic block diagram of the on-board processing satellite transponder. The information signal on the uplink at a carrier frequency, f_{UP}, after passing through a low noise receiver, is demodulated, and the baseband signal, at f_{BB}, is amplified and enhanced by one or more signal processing techniques. The processed baseband signal is then re-modulated on the downlink, at the carrier frequency, f_{DN}, for transmission to the downlink ground terminals. Degradations on the uplink can be compensated by the on-board processor, and are not transferred to the downlink.
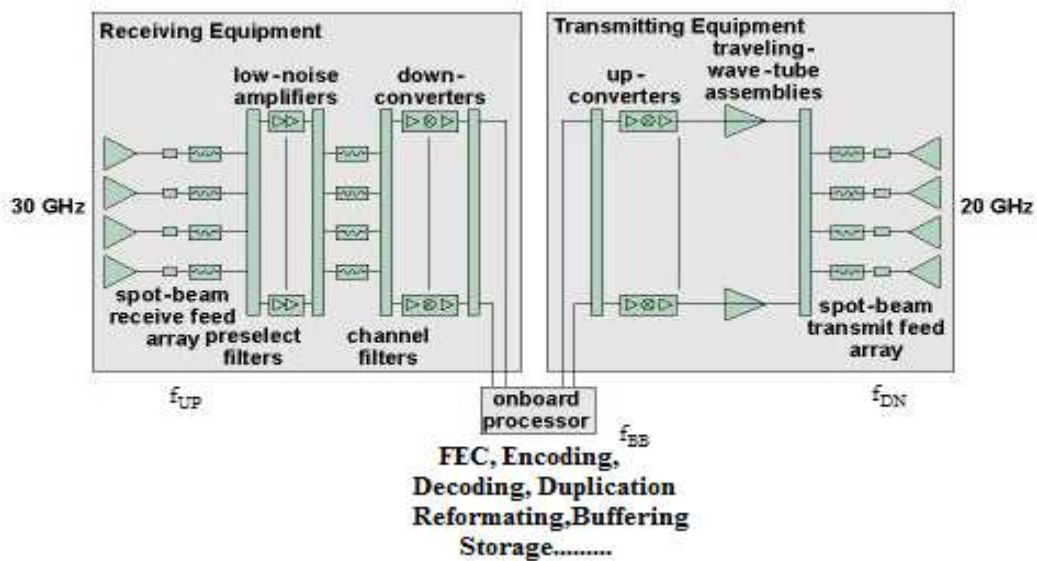
Figure2.3: On-board processing (OBP): transmitting and receiving equipment on board with satellite

In an OPB satellite system, both the uplink and the downlink system are independent to each other, and enable the designer to apply signal enhancing techniques to either or both the links in the satellite. On board the satellite employ digital transmission techniques, and can use a wide range of waveform modulation formats or access scheme. BER used in digital signals to measure the probability of bit error that may occur in a given time in the system.

OBP satellites offer several advantages over the conventional bent pipe satellite [54]. The performance of the uplink and downlink can be improved separately with forward error correction coding or other techniques. Noise induced on the uplink does not degrade the downlink because the waveform is reduced to baseband and regenerated for downlink transmission. The downlink can employ TDMA, so that the power amplifiers can operate at or near saturation to optimize power efficiency on the downlink. For example, a satellite can employ several FDMA carriers on the uplink to minimize ground station uplink complexity, demodulate on the satellite, add error correction coding, re-modulate, and combine into one TDMA downlink to provide optimum efficiency for downlink power [32].

(i)   OBP Uplink and Downlink

The downlink CNR or energy-per-bit to noise density, (e_b/n_o), for an onboard processing satellite system is essentially independent of the uplink CNR over the operating range of the transponder. The link equations for CNR previously given for bent pipe satellite are applicable to the on-board processing satellite uplink and downlink. Since on-board

processing satellites employ digital transmission, a more appropriate parameter is the energy-per-bit to noise density ratio, expressed as

$$\left.\left(\frac{e_b}{n_o}\right)_{UP}\right|_{OBP} = \frac{1}{r_{UP}} \frac{p_{GT} g_{GT} g_{SR}}{l_{UP} a_{UP} k \left[t_{UP}\left(1-\frac{1}{a_{UP}}\right)+t_{SA}+290(nf_{SR}-1)\right]} \qquad (2.12)$$

and

$$\left.\left(\frac{e_b}{n_o}\right)_{DN}\right|_{OBP} = \frac{1}{r_{DN}} \frac{p_{ST} g_{ST} g_{GR}}{l_{DN} a_{DN} k \left[t_{DN}\left(1-\frac{1}{a_{DN}}\right)+t_{GA}+290(nf_{GR}-1)\right]} \qquad (2.13)$$

Where, r_{UP} and r_{DN} are the uplink and downlink data rates, respectively.

Each link can be evaluated directly from the above equations and the resulting end-to end performance will generally be driven by the weaker of the two links. Additional on board processing could improve either or both links, however, and should be included in final performance conclusions.

(ii) Overall OBP performance:

The overall composite (or end-to-end) link performance for the OBP satellite is described by its bit error performance, or the probability of error, P_E, for a specified digital transmission process. The overall error performance of the on-board processing transponder will depend on both the uplink and downlink error probabilities.

Let P_{UP} is the probability of a bit error on the uplink (BER$_{UP}$) and P_{DN} is the probability of a bit error on the downlink (BER$_{DN}$).A bit will be corrected in the end-to-end link if either the bit is correct on both the uplink and downlink, or if it is in error on both links. The overall probability that a bit is correct, P_{COR}, is

$$P_{COR} = \left(1-P_{UP}\right)\left(1-P_{DN}\right)+P_{UP}P_{DN} \qquad (2.14)$$

Therefore,

P_{COR}= Probability of Correct Reception End-to- End

$(1-P_{UP})$ = Probability of Correct Bit on Uplink

$(1-P_{DN})$ =Probability of Correct Bit on Downlink

$P_{UP}P_{DN}$ = Probability of a Bit Error on Both Links

Rearranging terms,

$$P_{COR} = 1-(P_{UP}+P_{DN})+2P_{UP}P_{DN} \qquad (2.15)$$

The probability of a bit error on the end-to-end link is

$$P_E = (1 - P_{COR})$$

or, $\quad P_E\big|_{OBP} = P_{UP} + P_{DN} - 2P_{UP}P_{DN}$ (2.16)

The composite link probability of error will be dependent on the uplink and downlink parameters and their impact on the (e_b/n_o) for each link. A specific modulation must be specified to determine the relationship between the bit error probability and the (e_b/n_o) for each link. The composite error performance can then be determined. Different modulation schemes used in digital communications provide different BER performances. The overall error budget of the digital satellite systems using OBP is defined in (Eqn. 2.11) shown as:

$$BER_{overall} = BER_{UP} + BER_{DOWN}$$ (2.17)

Where, $BER_{UP,}$ BER_{DOWN} are Probability of bit error for Uplink and Downlink respectively.
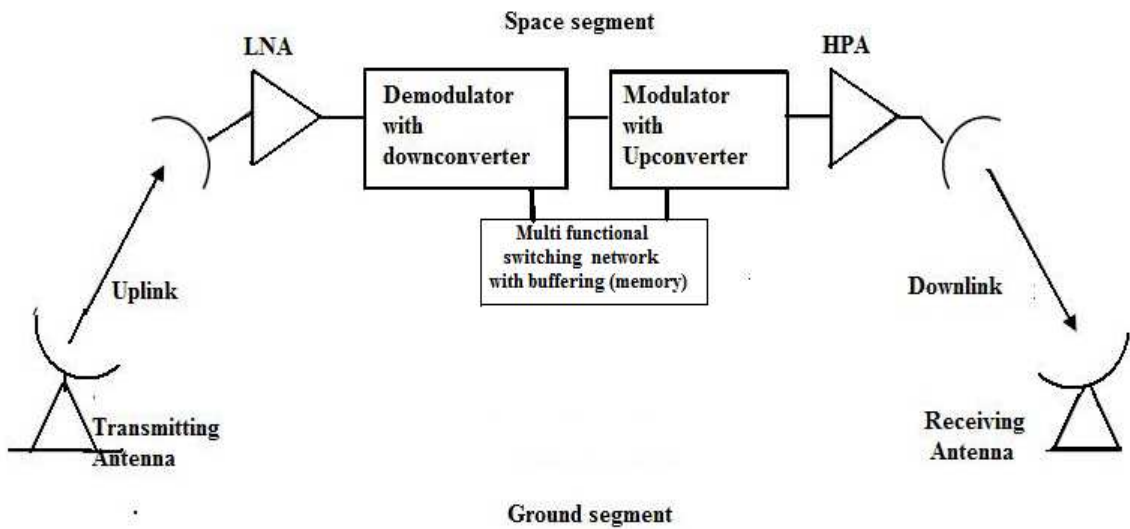
Figure 2.4: Functional blocks of an OBP satellite

On-board Processing Switches

There are four types of on-board switches: circuit switch, cell switch, fast packet switch and hybrid switch. Each on-board processing switch has its own particular features and technologies. Among four switches, the packet switch is the most popular selection for satellite networks because it provides both packet-based traffic and circuit-based traffic in Internet Protocol (IP) based networking environments. The Ka-band satellite system may

adopt packet-switch OBP in order to provide broadband internet services. Some advantages and disadvantages of packet switching are

- Self-routing/auto-configuration abilities,

- Flexible and efficient bandwidth utilization

- Can accommodate circuit-switched traffic

- Easy to implement autonomous private network

- But, for circuit switched traffic, higher overhead is required than circuit switching due to packet headers and Contention/congestion may occur.

2.4 Spot beam model and proposed features
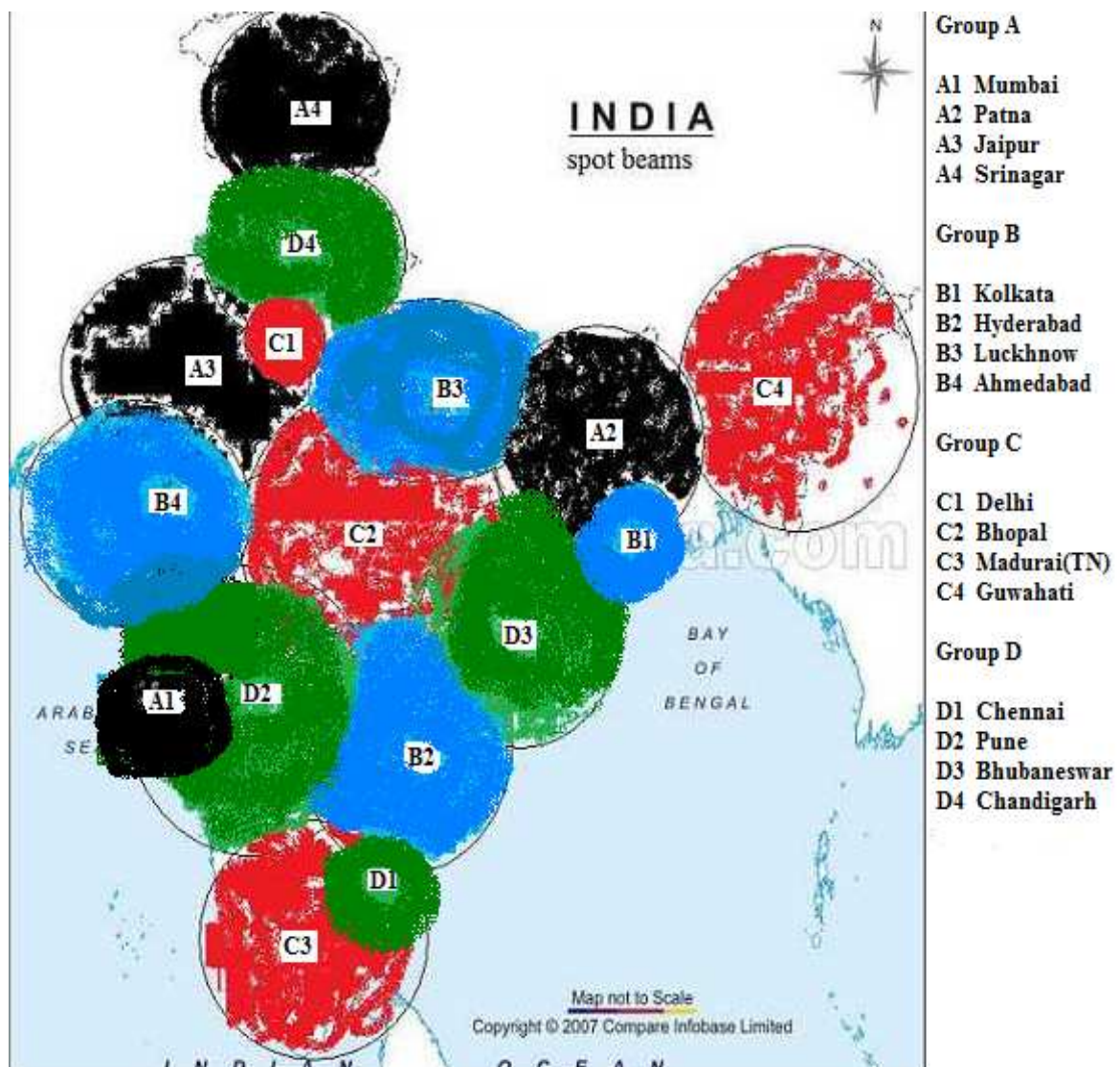
Figure 2.5: Outline of proposed spot-beam locations and grouping of disjoint beams for frequency re-use.

In general, communication satellites are transmitting with a very broader foot print. INSAT series Satellites that are not having "Spot Beams" and send out signals over very large areas, transmitting across India. Two cities in different part of India under one satellite foot print receive the same signal. But Spot Beams are different. It is similar to a spot light focused on one area of the country (figure 2.5).

A typical Spot Beam has a radius of only 200-500Kms. Depending on presence of density of user in this geographical area of the country, one won't detect the beam unless in the focus. So frequency reuse is possible for different spot beams in TDM. The Spot Beam technology has been applied on newer satellites using the Ka-Band (e.g.; GSAT-4 of ISRO, India) [2].

Spot Beam technology is ideal for the transmission of video requiring ultra high bit rates such as HDTV. The advantage of Ka-band over other forms of internet via satellite is that it only requires a 60 cm antenna. Additionally Ka-band uses spot beams for internet via satellite, which makes better use of the available bandwidth than a C or Ku-band satellite, i.e. more users can get higher level of services.

Here it proposes 16 spot-beam locations to cover Indian main land. Keeping view of the socio-economic status and population density, one metropolitan city will have a narrow beamwidth to cover limited area and high power gain footprint at every time slot. Beams are divided into four groups. In each group, 4 non-overlapped locations are present as seen in the figure 2.5. The total bandwidth of the satellite will be utilized for one group for a moment and after an interval the antenna switches to other group locations and so on. After covering all groups again it will restart the process from group A. Accordingly the OBP switching will provide data for each group in TDM process.

The on board processing (OBP) and switches are already employed in satellites providing mobile communications to handheld receivers in some western part of world. Here we are considering a ka band satellite system to provide cost-effective two-way voice, medium- and high-speed data, image, video (DVB-S) and video telephony communication services to both business and individual users in the Indian mainland. The proposed satellite broadband system provides higher capacity, intelligent routing, bandwidth on-demand, and value added services.

The uplink and downlink operating frequencies for proposed satellite system is same as proposed for GSAT4 by ISRO i.e., 29.6-30.2 GHz and 20.6-21.2GHz [2]. Only part of the uplink and downlink spectra was selected for the system design in this work. Here we are

considering a satellite position 83°E on GSO the position which is being used by ISRO for an INSAT satellite, to calculate effective geographical parameters. The analysis of geographical data, Rain rate Parameters and calculation of rain attenuation is discussed in chapter 3 for this 16 different locations, places taken as the geographical centre of the spot beams.

The proposed system requires multibeam antenna systems onboard or active phased array antenna system. Phased Array Antenna based communications links are anticipated to deliver high data rates without the risk of single point failure-prone motors used in reflector-based systems and are being used here for space-based communication applications due to their advantages in re-configurability [21] [4], faster scanning and switching [17], weight and power handling ability using digital signal processing (DSP). The phased array antenna can also electronically steer.

2.5. Beam forming with OBP System

On-Board Processing deals with the general topic of improving the received signal of the system in question before it is retransmitted to the desired user. Three forms of on-board processing take the form of regenerative repeaters, adaptive power control [46], and antenna beam forming. This is to investigate the area of digital beam forming method of on-board processing as applied to the geostationary satellite mobile communications environment at the Ka-band frequency. Digital Beam forming can cover the following advantages in a communications environment:

- Power can be efficiently focused on a target area to improve the efficiency.
- Adaptive beams may be dedicated to individual users using antenna arrays [4].
- The beamforming array can adapt to variations in the user traffic levels. [19]
- The increased efficiency of power usage could translate into reduced hardware requirements and payload expense.
- Frequency reuse may be increased as a result of narrower adaptive beams which reduce interference from adjacent channels.

- Beamforming may provide robustness to the system in the event of component failure. There are two general methods of beamforming being actively investigated in the present literature. The following sections briefly introduce the basic principles of these methods, and relate their application to the satellite system under investigation [43].

2.5.1 Reference-Based Beam forming

In reference based beamforming, a known signal which is highly correlated with the desired data and uncorrelated with interference signals is transmitted. This reference signal often takes the form of a known transmitted training sequence. Beamforming weights are calculated based on the reference signal using a variety of algorithms, the most common of which are Least Mean Square, and Direct Matrix Inversion. The major drawback of the reference-based beamforming method is the power and bandwidth resources that are taken up by the reference signal. In the satellite environment, this power cost is highly undesirable.

2.5.2 Location-Based Beamforming

In our proposed system this type of beam forming is suitable, which is the Location-based beamforming. This relies on knowledge of the direction of arrival of the desired signal and the interference signals. Using this information, optimum beam weights may be calculated to suppress the interference, and boost the desired signal. This technique is based on algorithms which reliably estimate the direction of both the desired and interference signals. This is often done on the basis of Eigen-vector analysis, such as the Multiple Signal Classification algorithm (MUSIC). Most of these direction estimation algorithms require accurate knowledge of the type of interference, and the geometry of the array. In the portable satellite communications environment, weather patterns are constantly changing, and the ability to characterize the system once deployed is difficult. These disadvantages would make facts of the interference environment difficult, and the array geometry calibration less robust.

2.6. Ka band Satellite Link Multiple Access Techniques

Since large amount of bandwidth are available on GEO Ka-band satellites, an appropriate bandwidth management technique is necessary. One of the best ways is to use a multiple access technique. In satellite communications systems, multiple accesses allow many earth stations to share a transponder even though their carriers have different signal characteristics [8].

Three common types of multiple accesses deployed in satellite communications systems are frequency division multiple access (FDMA), time division multiple access (TDMA), and code division multiple access (CDMA). A common hybrid solution is used by combining techniques such as FDM/TDMA. This proposes the earth station to use FDM for uplink and TDMA for downlink to maximize the bandwidth efficiency. FDMA and TDMA will be presented in the next section. CDMA satellite systems were proposed in recent years but here not considered.

2.6.1 Frequency Division Multiple Access (FDMA)

In general, FDMA separates the total system bandwidth into smaller segments/channels, and assigns each channel to a user. Each user transmits at a particular allocated frequency. Filters are used to separate the channels so that they do not interfere with each other. The disadvantage of a filter is that it cannot easily be tuned to change the bandwidth of channels or the channel frequency allocation. This makes inefficient use of transponder bandwidth and satellite capacity. Another drawback of FDMA is the non-linearity of the transponder power amplifier that generates intermodulation products between carriers. This degrades the link performance. In order to reduce such interference, the transmitting power of the satellite and earth station can be lowered. This is called back-off. Usually 2-3 dB back off power is needed when FDMA is used. On the other hand, FDMA becomes useful for uplink transmission when a hub network is used, since only one carrier occupying the total transponder bandwidth will be transmitted to the satellite.

2.6.2 Time Division Multiple Access (TDMA)

TDMA is a digital multiple access technique that allows signals to or from individual earth stations to be received or transmitted by the satellite in separate, non-overlapping time slots, called bursts. For uplinks, each earth station must determine the satellite system time and range so that the transmitted signal bursts are timed to arrive at the satellite in the proper time slots, even though it is very hard to synchronize many earth stations on earth with proper synchronization times. For downlinks, such precise timing is not required [8][7].

Compared with FDMA, TDMA offers the following features

− As only one signal is present at the receiver at any given time, there is no inter-modulation caused by non-linearity of satellite transponders. The satellite transponder can be driven nearly at saturation in order to provide maximum satellite power.

− The TDMA capacity does not decrease steeply with an increase in the number of accessing stations.

− The introduction of new traffic requirements and changes is easily accommodated by altering the burst length and position.

Each TDMA frame is formed by slots containing a preamble, guard time, and data information. The preamble contains synchronization and other essential data to operate the network. The guard time is used to prevent one station's transmissions from overlapping with

another station's following transmission time slot. For uplinks, the transmitted bursts/times of users are critical. They should arrive at the transponders in the required slots so that the required information can be extracted at the received earth stations without errors.

A typical time length of a TDMA frame is 2 ms, which reduces the proportion of overhead to message transmission time. Sixteen 8-bit words are typically used in a digital terrestrial channel. Figure 2.6 shows two TDMA frames consisting of preamble and satellite channel at each frame.
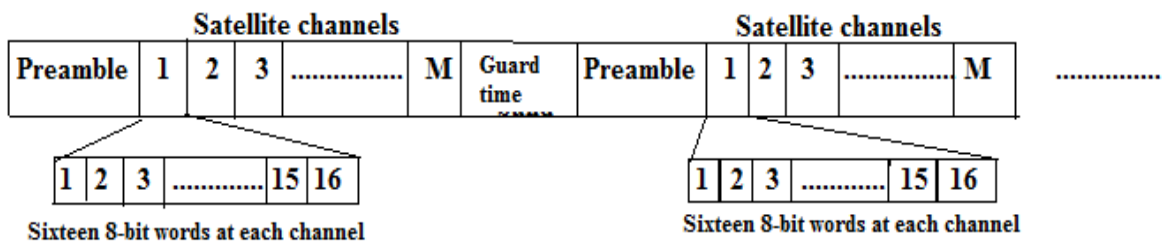
Figure 2.6: A TDMA frame for satellite channels.

At the receiver, higher data bit streams must be recovered using modulation techniques, which requires demodulation of RF signals, generation of a bit clock, sampling of the receive waveform, and recovery of bits. This process requires large storage of bits (at preamble and guard time slots), so that original signals can be reconstructed even though signal transmissions are delayed. In a GEO Ka-band satellite system, the delay time for one-way transmission is around 240-250 ms at the distance of 35,786 km between an earth station and the satellite. The earth station would have to be on the equator at the sub-satellite point.

2.7. Digital Modulation Techniques for Satellite Links

For efficient use of transponders and resources higher level of modulation e.g., QAM, M-PSK instead of QPSK and BPSK, higher compression standards like MPEG-4 to MPEG-7 for video, FECs can be used. A number of modulation techniques have been developed to optimize particular features of a digital transmission link. The desired bit error rate determines the minimum required C/N values for each modulation technique.

The types of digital modulations are divided into coherent and non-coherent types. At a given minimum C/N requirement, the BER performance of a coherent system is better than a non-coherent system. In addition, coherent modulation can incorporate both amplitude and phase information, although synchronization circuits and phase-locked loop circuits increase

the complexity of the system. On the other hand, non-coherent modulation is insensitive to the phase information, which degrades the BER performance. Since none of the satellite systems today uses non-coherent modulation, coherent modulation BPSK, QPSK, M-ary phase shift keying (M-PSK) modulations, and now Quadrature Amplitude Modulation (QAM) will be adopted for the link design of satellites.

2.7.1. Phase Shift Keying (PSK)

PSK modulation is the most commonly used digital modulation in digital satellite communications systems. The BER is often referred to the probability of bit error, P_e. Probability of bit error is calculated from the characteristics of the type of modulation used and the energy per bit per noise density (E_b/N_o), which can also be obtained directly from the C/N values. To simplify the BER calculation, inter-symbol interference is assumed to be zero and that ideal root raised cosine filters are used at the transmitter and receiver.

The greater is the E_b/N_o value, the lower the probability of bit error. For an ideal system, the E_b/N_o can be represented as:

$$\frac{E_s}{N_o} = \left(\frac{C}{N} \right)\left(\frac{B_n}{R_s} \right) \quad \text{or} \quad \frac{E_b}{N_o} = \left(\frac{C}{N} \right)\left(\frac{B_n}{R_b} \right) \tag{2.18}$$

Where, E_s = Energy per symbol [J], E_b= Energy per bit [J]

N_o = single sided noise power spectral density [W/ Hz]

C = carrier power [W], N = noise power [W]

R_s = symbol rate [symbol per second (sps)] =$1/T_s$, T_s = symbol duration [sec]

B_n = noise bandwidth [Hz]

BPSK consists of one bit per symbol. BPSK is used in some satellite links although it is considered to have low bandwidth efficiency compared to QPSK. QPSK is widely used in satellite links, transmits two bits per symbol. Since two bits are sent per symbol, the symbols have four possible states. Since QPSK carries twice information per symbol than BPSK, it needs an extra 3 dB of C/N to achieve the same P_e of BPSK.

Higher numbers of bits per symbol can also be sent using an Mth order modulation scheme, called M-ary Phase Shift Keying (M-ary PSK). M stands for the number of possible states. M has to be greater or equal to 4. This can generally be used for any multi-level

modulation scheme. Bandwidth efficiency is a critical consideration when a higher level of modulation schemes is adopted. The bandwidth efficiency for any modulation usually is defined as

$$\eta = \frac{R_b}{B}$$
$$(2.19)$$

Where, η = bandwidth efficiency [bits/s/Hz]

B = bandwidth of transmitted signal [Hz]

2.7.2. Quadrature Amplitude Modulation (QAM)

QAM is combination of four phase states of QPSK with multiple carrier amplitudes. For instance, 16-QAM is a modulation in which each symbol represents 4 bits and has 16 possible states. Taking M=16 as an example, 16-PSK needs an extra 4 dB of C/N to achieve an error probability of 10^{-6} compared to 16-QAM. Thus, the BER performance of 16-QAM is much better than 16-PSK, as shown in Figure 2.7. Therefore, many new generations of Ka-band satellites designed for data services, Internet access will use 16-QAM between the satellite and hub, so that lower BER values can be maintained.

Modulation Type	Probability of Bit Error Rate	Relative Symbol rate (Rs)
BPSK	$P_e = Q\left[\sqrt{\dfrac{2E_b}{N_o}}\right] = \dfrac{1}{2}erfc\sqrt{\dfrac{C}{N}}$	R
QPSK	$P_e = Q\left[\sqrt{\dfrac{2E_b}{N_o}}\right] = \dfrac{1}{2}erfc\sqrt{\dfrac{C}{2N}}$	½ R
M-ary PSK (MPSK)	$P_e \approx erfc\left[\sqrt{\dfrac{C}{N}sin^2\dfrac{\pi}{M}}\right]$ for M ≥ 4	R_b/N
M-ary QAM (MQAM)	$P_e = \dfrac{2\left(\sqrt{M}-1\right)}{\sqrt{M}}erfc\left[\sqrt{\dfrac{3}{2(M-1)}\left(\dfrac{C}{N}\right)}\right]$	R_b/N

Table 2.3: Coherent signal Modulation Methods and theoretical error equations [44]

Table 2.3 presents the above modulations' probability error theoretical equations and symbol rate relationships that will be used for the system design. Table 2.4 provides the required C/N values for M-ary PSK and M-ary QAM at the given probability of errors equal to 10^{-6}.

M-ary PSK Modulation	Symbol rate (R_s)	Desired C/N(dB) at BER=10^{-6}	M-ary QAM Modulation	Desired C/N(dB) at BER=10^{-6}
2-PSK(BPSK)	R	10.76	-	-
4-PSK(QPSK)	½ R	13.53	4-QAM	13.77
8-PSK	$R_b/3$	19.12	8-QAM	17.53
16-PSK	$R_b/4$	24.97	16-QAM	20.02
32-PSK	$R_b/5$	30.95	32-QAM	24.36

Table 2.4: Comparison of C/N for M-ary PSK and M-ary QAM
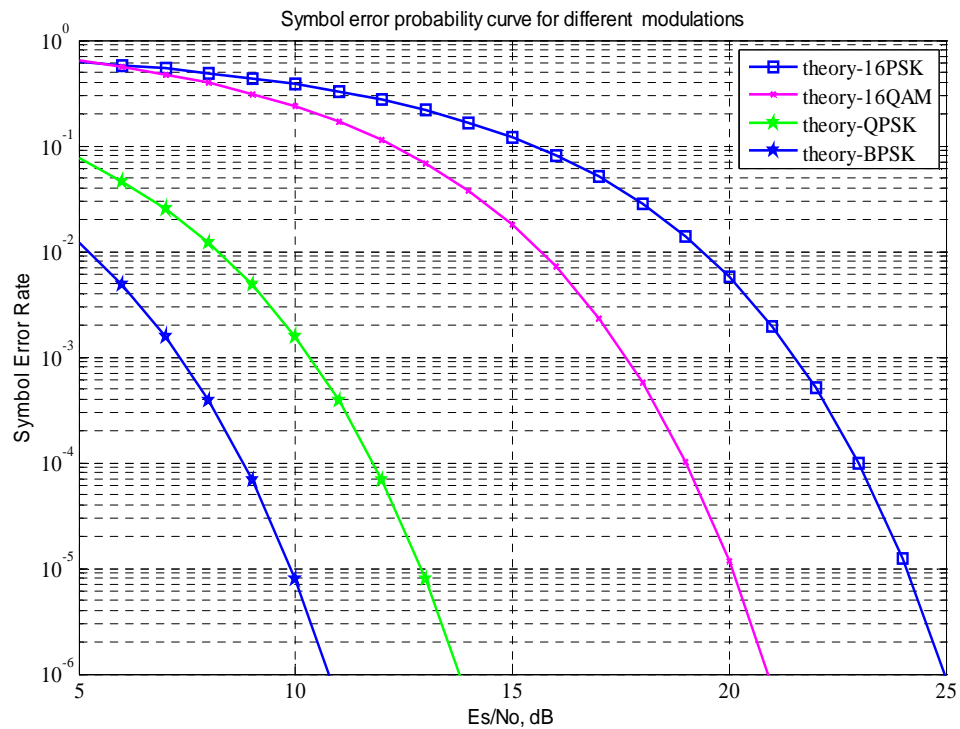
Figure2.7: Comparison of BER performance for various digital modulation techniques.

From Figure 2.7 above, it can be concluded that when a higher number of bits per symbol in a type of modulation is used, a higher C/N value is required to achieve the same probability of error compared to those in lower number of bit per symbol. The higher order modulations in Table2.4 require higher C/N values that may be more difficult to achieve in a satellite link. Thus, using forward error correction (FEC) or uplink control power to get better BER for a given C/N maybe a preferable method, as described in the next section.

2.8. Forward Error Correction (FEC)

FEC not only used to optimize the link budget and maximize the power bandwidth efficiency, but also can provide a flexible tradeoff between the BER and the occupied bandwidth. With various selections of coding and code rates, FEC can be used to relax the link budget parameters or to improve the BER of a given link, especially at a small earth station with limited antenna size. FEC is an error correcting method for a transmission link. Using redundancy added to the information bits, the receiver can detect and correct transmission errors and corrupted signals. In addition, no feedback is required from the receiver. The common codes that are used in satellite modems include Viterbi codes, Reed Solomon codes, Turbo codes, convolution codes, etc. [44].

2.9. Link Budget Calculation

The link budget is a calculation which shows the expected carrier to noise ratio (CNR) of the system under the specified conditions. This ratio is directly related to the Eb/No as discussed. From this calculation a prediction of the bit error rate and the reliability of service can be determined. The following sections outline the values chosen for the input parameters and the calculations [57].

i)   **Hardware Specifications & Frequency Parameters**

Hardware losses for both the uplink and the downlink are estimated at 2.0 dB for the receiver and 0.2 dB for each feed. The satellite gain is calculated using the designed parabolic antenna. The power for each downlink signal is limited to 1 Watt due to power constraints on the satellite. The earth antenna gain was set at 0 dB and the earth transmitter is given a power of 1 Watt. In this way the design of the satellite system alone can be evaluated and the necessary gain needed from the earth station to make the system feasible can be determined.

Frequencies in the Ka frequency band are chosen because this band communication is our main aim. There is a large amount of available bandwidth which can support high data rate services. Frequency has a direct effect on the power of the received signal due to rain attenuation and free space loss. Free space loss increases at a rate of inverse distance squared. The frequency scaling method presented is used for frequencies +/- 1 GHz for the up and downlink frequencies of 30 and 20 GHz.

ii)   Target Latitude and Longitude

The target latitude and longitude are selected based on the coverage area of the feed with the worse gain as calculated in the antenna design i.e., the proposed geographical spot beam locations. The geographical coordinates of feed # 1 correspond to 10^oN   Latitude and 78^oE Longitude. The satellite Latitude position must be situated on the equator 0° in order to maintain a geostationary position. The Longitude position of the satellite is chosen to be 83° E. (This is the geographic centre of the coverage area.)

iii)   Height above Sea Level

A target's height above sea level affects the attenuation due to the free space loss, as well as the effect of rain on the slant path of the signal. A height of 0.2 km is selected for the elevation of the target.

iv)   Outage Percentage

The outage percentage is a statistical calculation which is used to predict the percentage of time that atmospheric attenuation exceeds a certain threshold. This calculation is based on the CCIR attenuation model as presented in chapter 3. The model is dependent on the geographic parameters as well as the frequency of the signal. An outage percent probability of 0.01 % is used for this system. The 0.01% level is the value derived from measured systems by ITU DBSG5. Other percent outage levels must be calculated indirectly using a scaling method. The 0.01 % level gives a statistical prediction that the attenuation due to rain will exceed the calculated threshold only 0.01 % of the year [57].

v)   Antenna Gain Reductions

For an antenna design having a beam width of 0.2^o and servicing a location having an elevation angle of 20° the antenna gain reduction is found to be 0.5 dB [31].

vi)   System Interference and Channel Guard Bands

In the FDMA system, no interference from other users was modelled. This is due to the fact that all users occupy a unique frequency and from the fact that channels are spaced with 1 MHz guard bands at the upper and lower edges of each channel. Broadband front-end filtering would provide additional attenuation to interfering signals. The narrow beamwidth of the antenna and low side lobe levels tend make user   signals in other geographic areas very weak relative to the desired signal. For this reason, the FDMA system is seen to be noise-limited.

vii)   Temperature Parameters

Summer temperatures are estimated for the system to give a worst-case scenario. Temperatures selected based on those found in literature and through personal communication with system operators and designers. The selected parameters are presented in chart form in the link analysis summary. The temperature values chosen significantly affect the amount of attenuation which results from the downlink degradation factor.

viii)   Pulse Design and base band channel

A BPSK pulse is used to transmit data. This scheme simplifies the recovery of the message signal at the receiver. To minimize inter-symbol interference a 100 % raised cosine pulse is selected. This effectively doubles the bandwidth of the system. The increase in bandwidth is not seen as a problem due to the large amount of unallocated bandwidth in the Ka band. The basic information rate is selected for 2 Mbps. The 2 Mbps rate will allow for high data rate transfer as well as image transmission.

Satellite receiver loss(dB)	2	Earth feed temp (^{o}K)	300
Satellite feed loss (dB)	0.2	Sat Feed temp (^{o}K)	200
Satellite Gain (dB)	48	Earth Temp (^{o}K)	300
Satellite Power (dB)	0	Satellite Temp (^{o}K)	200
Earth Receiver Loss (dBW)	2	Sky Temp (^{o}K)	2
Earth feed loss (dB)	0.2	Medium temp(^{o}K)	290
Earth Gain (dB)	0	Ground Temp (^{o}K)	300
Earth Power (dBW)	0	Guard band (MHz)	1
Target Latitude (deg)		Base band (MHz)	2
Target Longitude (deg)		Outage (%)	0.01
Satellite Longitude(deg)	83	Aperture Degradation (dB)	0.5
TEC (/m^2)	10^{17}	Interference Noise (dB)	0.0
Height above M.S.L (km)	0.2	H$_2$O Vapour Density (g/m^3)	7.0

Table 2.5: Typical Link Budget Parameters FDMA Systems.

ix) Ionospheric Effects

The major parameter controlling the effect of the ionosphere is the Total Electron Count (TEC/m^3) and the frequency. The TEC value of 10^{17} is used. The ionospheric effects are not seen as significant with respect to signal distortion. The reason for the small influence of the ionosphere on the ka band signal is due to the inverse frequency dependence on the degradation parameters. The ionospheric effects are not considered further.

x) E_b/N_o Requirements

The E_b/N_o level is selected to give a Bit error rate (BER) of 10^{-5} for BPSK pulses. This level corresponds to an E_b/N_o of 10. Additional gain from beam forming and coding would be expected to increase this level to give data quality performance of 10^{-6} or better.

Calculation frequency	19 GHz	20 GHz	21 GHz	29 GHz	30 GHz	31 GHz
Satellite EIRP(dBW)	45.8	45.8	45.8	45.8	45.8	45.8
Earth EIRP(dBW)	2.2	2.2	2.2	2.2	2.2	2.2
Elevation Angle(deg)	22.59	22.59	22.59	22.59	22.59	22.59
Free Space Loss (dB)	210.69	211.14	211.56	214.37	214.66	214.95
O_2 Attenuation	0.15	0.15	0.16	0.26	0.27	0.29
H_2O Attenuation (dB)	0.42	0.66	1.04	0.44	0.42	0.40
Gaseous Loss(dB)	0.57	0.81	1.21	0.70	0.69	0.70
Rain Attenuation(dB)	11.33	12.98	14.76	23.21	25.39	27.69
System Temp (^{o}K)	572.70	578.96	583.49	485.99	485.97	485.96
DWN Degradation(dB)	2.15	2.03	1.84	0.00	0.00	0.00
Noise Power(dB)	201.02	200.97	200.94	201.73	201.73	201.73
Noise Bandwidth(MHz)	8	8	8	8	8	8
Total Loss(dB)	228.24	230.47	232.87	241.71	244.17	246.76
Total Gain (dB)	43.6	43.6	43.6	43.6	43.6	43.6
CNR, E_b/N_o (dB)	49.64	51.91	54.35	62.39	64.86	67.45
Channel Bandwidth (MHz)	10	10	10	10	10	10
Number of Channels	200	200	200	200	200	200
Bandwidth Available(GHz)	2	2	2	2	2	2
Required E_b/N_o (dB)	10	10	10	10	10	10
E_b/N_o Margin(dB)	59.64	61.91	64.35	72.39	74.86	77.45
Max Dispersion(deg)	0.027	0.027	0.027	0.027	0.027	0.027
Max.Dispersion (psec)	0.008	0.008	0.008	0.008	0.008	0.008
Phase delay(deg)	24.24	24.24	24.24	24.24	24.24	24.24
Group delay (psec)	6.734	6.734	6.734	6.734	6.734	6.734

Table2.6: Typical Link Budget Calculations at different frequencies of FDMA systems

2.9.1 Comparison with L Band Voice System

There is significantly loss resulting in the broadband scenario proposed as compared to voice band systems which operate at lower frequencies. In order to illustrate the source of these differences, a comparison shown with the 9.6 kbps voice band.

Parameter	Uplink			Downlink		
Frequency	**1.6 GHz**	**30 GHz**	**Difference**	**2.0 GHz**	**20 GHz**	**Difference**
Bit Rate	9.6 kbps	2 Mbps		9.6 kbps	2 Mbps	
Free Space Loss	188.38	214.66	26.38	190.11	211.14	21.03
Noise Power(dB)	158.34	141.73	22.61	157.11	140.96	22.15
Weather Attenuation(dB)	0.1	26.08	25.98	0.1	13.79	13.69
Total Major attenuation factor(dB)	30.14	105.01	74.87	33.1	89.97	56.87

Table 2.7: Uplink and downlink performance Comparison: Ka band system Vs L band system.

As this analysis shows that the major factors contributing to the system attenuation in compared to the lower frequency and data rate system are the free space loss, the noise power (which is a function of the data rate and noise power bandwidth) and the attenuation due to weather. The values affecting the magnitude of this attenuation are the result of the desired frequency band of the service required. Practical receiving antennas are limited to a gain of approximately 50 dB due to size constraints, construction and pointing errors. It is anticipated that beam forming will allow for an increase in the signal to noise ratio which would make this system less costly.

2.10. Summary

This chapter provided a literature review of satellite communications technology. It presented comparisons between the conventional bent-pipe transponder and on-board processing transponders. It discusses different types of multiple access techniques: FDMA, TDMA, and CDMA. Coherent modulations were compared, such as BPSK, QPSK, M-PSK, and QAM. Different modulation selections with link power budget design will be presented when the terrestrial-satellite integration network is determined in Chapter 3. FEC and UPC are alternative solutions in providing a desired BER performance to be discussed in chapter 4. A typical link budget is presented and a comparison is done with the old satellite systems L band.

Prediction Models for Rain Attenuation

3.1 Introduction

The rapid growth of satellite services using higher frequency bands such as the Ka-band has highlighted a need for estimating the combined effect of different propagation impairments. It is necessary to identify and predict the overall impact of every significant attenuation effect along any given path. Accurate predictions of the propagation impairments that affect link quality are essential for the reliable design of satellite communications.

Rain attenuation plays a more important role in satellite communication than other atmospheric losses when Ka-band is in use especially in tropical and sub tropical regions. Extensive rain characteristic prediction and modelling have been made all over the world. Most of these predictions and models are of statistical nature. Some popular models are Crane model (1980), ITU-R model (1982), Moupfouma model (1984), and modified ITU model as DAH model (1997) [3][8].

This chapter surveys a review of previous researches of rain attenuation on the communication system links and includes the discussion of latest developments in the modelling over terrestrial and slant path. Emphasis is placed on calculation of rain attenuation in 16 spot beam areas as proposed using above prediction models. The ITU-R worldwide model for rain attenuation and effective path length along horizontal reduction factor and vertical adjustment factor models are presented in detail and analysed.

3.1.1 Rainfall Impact on Satellite Link

Satellite signal propagation above 10 GHz over an atmosphere is a subject of impairment and phenomena such as, gaseous attenuation, cloud and fog attenuation, in addition to rain attenuation. These are degrading the intensity of satellite signal on the path, since the influence of the impairment on the microwave propagation increases with the frequency, the concern of this thesis is to understand of this influence, which allow these bands channels to use to provide high quality satellite services.

According to Olsen R.L. (1978), hydrometeors in the form of rainfall dominate the influence of the atmosphere on the satellite transmission [55]. The problems become more

acute for systems operating in tropical regions, where rainfall rate can adversely affect the satellite link. Rain can cause uncontrolled variations in signal amplitude, phase, polarization and angle of arrival, which result in a reduction in the quality of analog transmissions and an increase in the bit error rate of digital transmissions [7]. Figure 3.1 shows hydrometeor absorption is the dominant phenomenon causing power loss in the lower spectral part. This constitutes the main disadvantage of satcom operating at the Ku, Ka, or V frequency bands.
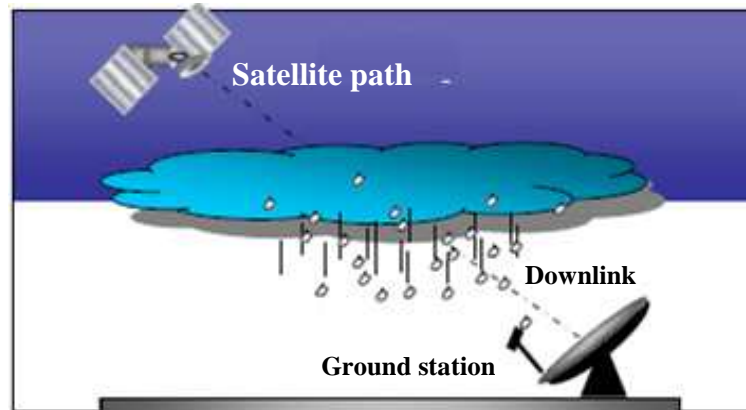
Figure 3.1: Hydrometeors affecting the satellite path.

The prediction of rain attenuation for the radio systems operating over 10 GHz can be improved through a better knowledge of the spatial-temporal structure of rain. The rain structure depends on the other factors such as rain cell diameter and rain height. A different type of rain shows different spatial structure and thus different impact on the radio systems. Rain rates studies have been conducted by number of researchers throughout the world. In most of the prediction models the actual knowledge of rain structure characteristics is not used directly but absorbed into some parameters of empirical formulas.

3.1.2 Rainfall Structure and Types

India has a great diversity in geographical parameters. A variety of climatic conditions, deserts, heavy rain regions and affected by oceanic winds. Rainfall is a natural, time varying phenomenon having complex structure due to its variability in space, duration and frequency of occurrence. In general, rain can be classified into four types (ITU-R, 1994), Stratiform, Convective, Monsoon, and Tropical rainfalls. Each type has its special characteristics which are varying, such as rain intensity and rainfall time duration as discussed below.

Stratiform rain is characterized by medium and low intensity with long duration in the mid-latitude regions, extending homogeneous to several hundreds of kilometers

horizontally, with vertical heights values follow from the 0°C isotherm heights (ITU-R, 2002). Stratiform rain results from the formation of small ice particles in the upper troposphere layers. As they fall, these particles join together to form bigger nuclei. The growing nuclei become unstable and as they pass through the melting layer turn into raindrops that fall down to earth surface [34].

Convective rain with high rain rates for short durations and extending over much smaller horizontal extent, usually few kilometers, but can extend much greater vertical heights because of convective upwelling up to 9-10 km. Convective rain is associated with clouds that are formed, in general, below the 0°C isotherm and are stirred up by strong winds. Differences in the troposphere pressure, water drops are created arid as they grow in size, until gravity precipitates them, with intermittently strong vertical velocities [23].

Monsoon precipitation is a sequence of bands of intense convection followed by intervals of stratiform precipitation. Convective rain displays considerable horizontal variability with cells and regions of higher intensity. Widespread stratiform rain may contain weak convective elements, relatively uniform regions of lower reflectivity with a melting layer and surround by convective showers. Tropical rainfall is predominantly convective and characterized by high intensity rain rates, which occur over limited extensions and with short duration where precipitation is surrounding the centre and in several outer spiral bands. These bands show a mixture of convective and stratiform structure. During precipitation, a stratiform structure develops, which extends over wider areas with light intensities [28].

3.1.3 Principal Sources of Rainfall Data

Principal sources of data for studying rainfall are represented by rain gauges or and their networks, meteorological ground based radars of Indian meteorological department (IMD), and space born sensors flying on satellites mainly from ISRO sites. Rain gauge data represent the most common source of information about the rainfall in a site, available for long time periods for proposed locations. The models for description of rain structure and the prediction of propagation impairments based on rain gauge data hourly recorded by IMD weather stations across the countries with 36 subdivisions. Besides this the long time statistical stored data of ITU databank, previous rain attenuation papers, have the key role for analysis and validation.

3.2 Indian Climate and Rainfall Distribution

In global position India is placed north of equator ranging from 8-42° North latitude and 70-97° East longitude. The tropic of cancer crosses horizontally in the middle ($23^{1/2}$N), with mean sea level temperature. It characterized by non-uniform temperature, high humidity and plentiful rainfall which arise mainly from the Southwest monsoon and North east monsoon over the country. Although the winds are light, heavy and variable, some uniform periodic changes in the wind flow patterns exist. Based on these changes, the seasons can be distinguished such as the south-west monsoon, north-east monsoon and two shorter inter-monsoon seasons. As a result of season's variation for the same location the significant change of rainfall rate intensity is varied in time and space which represented the random variables in spatial and temporal characteristics which can be described using cumulative distribution function.

One-minute rain rate cumulative distribution ($R_{0.01}$) is the probability P ($R \geq r_o$) that one minute rainfall intensity R (mm/hr) exceeds a threshold value r_o (mm/hr) for a time period T. It is expressed as

$$P(R \geq r_o) = N_o / N_T \tag{3.1}$$

Where N_o is the number of rain rate data more than r_o and N_T the total number of minute in time period T. [8]

3.3 Rain Attenuation Modelling

The evaluation of prediction models for satellite and microwave systems requires a detailed knowledge of the attenuation statistics for each ground terminal location at the specific frequency (20/30 GHz) of interest. Due to non availability of Ka- band satellite signal in these footprints and failure of GSAT-4 mission, it would obviously be an impossible task to collect experimental data for all the frequencies, locations, and elevation angles under consideration for operational satellite systems. Therefore, a more reasonable approach is to use the predictive models based on and in agreement with data from various national and international organisations. The possibility of predicting rain attenuation statistics on the path from rainfall intensity data has been a subject of considerable interest during the past researches, and has stimulated an extensive series of theoretical and experimental studies. The purpose of this chapter is to perform a systematic assessment of these methods on the basis of attenuation modelling which are discussed in the following sections [27][18][60].

3.3.1 Effect of elevation angle

The elevation angle from the earth station to the satellite, φ is determined from

$$\varphi = \cos^{-1}\left(\frac{r_e + h_{GSO}}{d} \sqrt{1 - \cos^2(B)\cos^2(L_E)} \right)$$ (3.2)

Where,

r_e =Equatorial radius = 6378.14 km;

h_{GSO} =Geostationary altitude = 35, 786 km;

d = Range, in km;

B = Differential longitude, in degrees;

and L_E =Earth station latitude, in degrees.

The elevation angle is important because it determines the slant path through the earth's atmosphere, and will be the major parameter in evaluating atmospheric degradations such as rain attenuation, gaseous attenuation, and scintillation on the path. Generally, the lower the elevation angle, the more serious the atmospheric degradations will be, because more of the atmospheric airmass is present to interact with the radiowave on the path to the satellite [15]. The airmass is more as the angle is less seen in figure 3.2. It approximates the atmosphere by a single layer of oxygen and a single layer of water vapour.
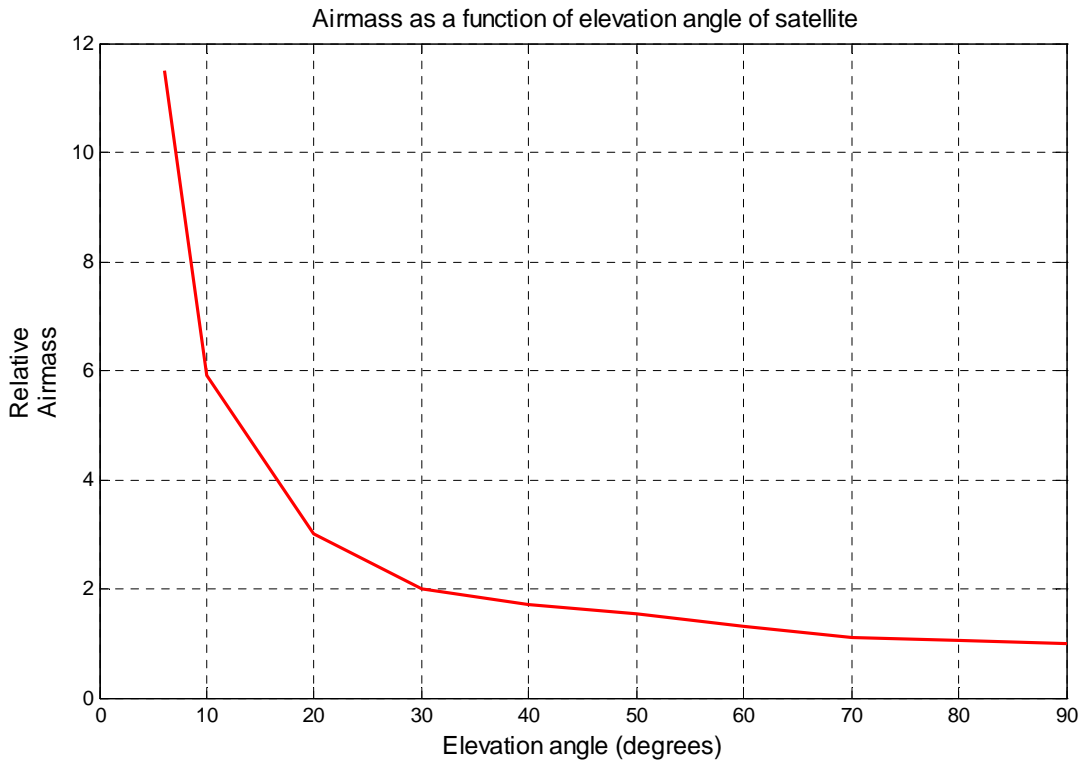
Figure 3.2: Relative Airmass of atmosphere as a function of elevation angle.

Total attenuation is calculated by multiplying path length with the specific absorption of each of the layers. Main advantage of this method is that only surface meteorological data are needed, disadvantage is lower accuracy, especially at low elevation angles. So ITU-R did not recommend using it for elevation angles lower than 5° [7].

In addition to the frequency dependence shown in figure 3.3 attenuation by atmospheric gases as well as other attenuation mechanisms described later is highly dependent on elevation angle. Lower elevation angle results in much longer path length through the atmosphere, thus increasing the attenuation [14]. Figure 3.3 shows dependence on different elevation angles for Ka-band frequencies calculated utilizing the reference standard atmosphere and high latitudes (>45°) from ITU-R Recommendation. P.835-4. Effect of the water vapour content change through the year is also shown in the figure. The difference between summer and winter values is more prominent at downlink frequencies as these are closer to the water vapour resonance frequency.
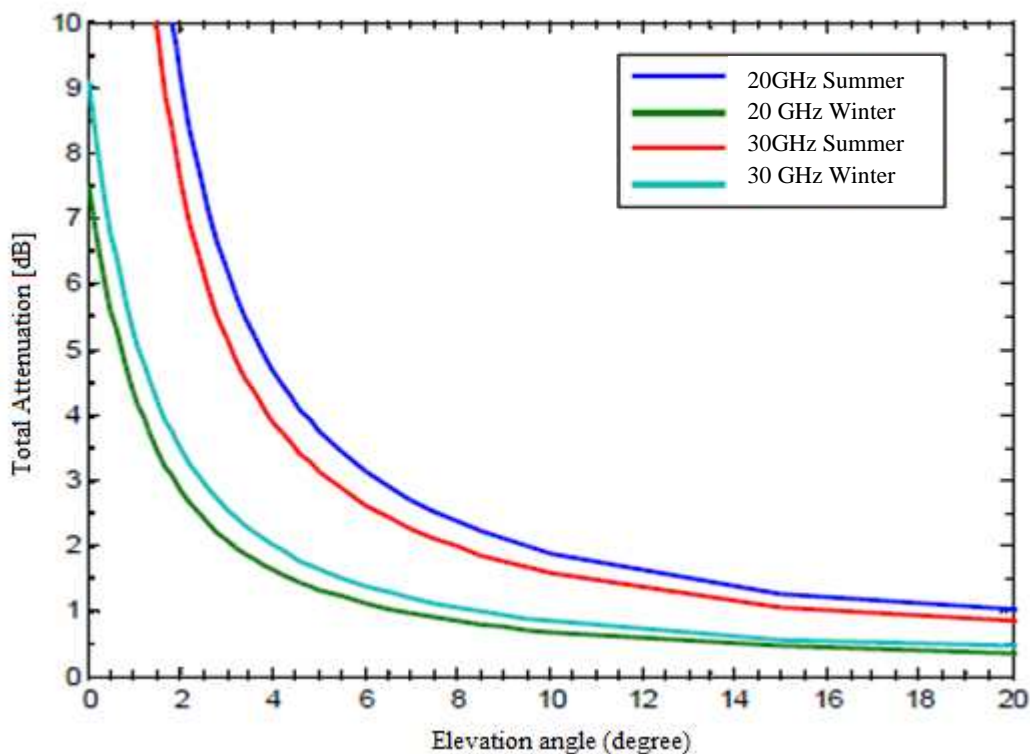
Figure 3.3: Total attenuation by atmospheric gasses with changing lower elevation angles and different frequencies, using summer and winter reference atmospheres [ACTS experiment][54].

The specific attenuation at three different elevation angles are seen in the figures 3.4-3.6 and found that it increases as the angle decreases using ITU database, details discussed later.
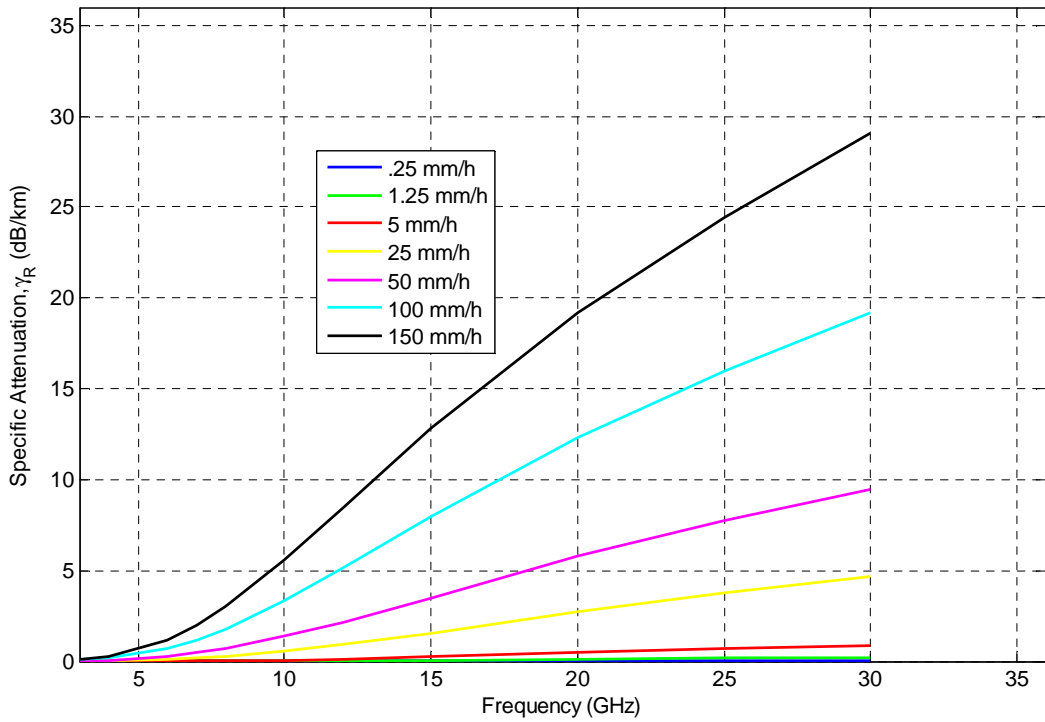
Figure3.4: Specific attenuation due to rain at an elevation angle of 30$^{\text{o}}$
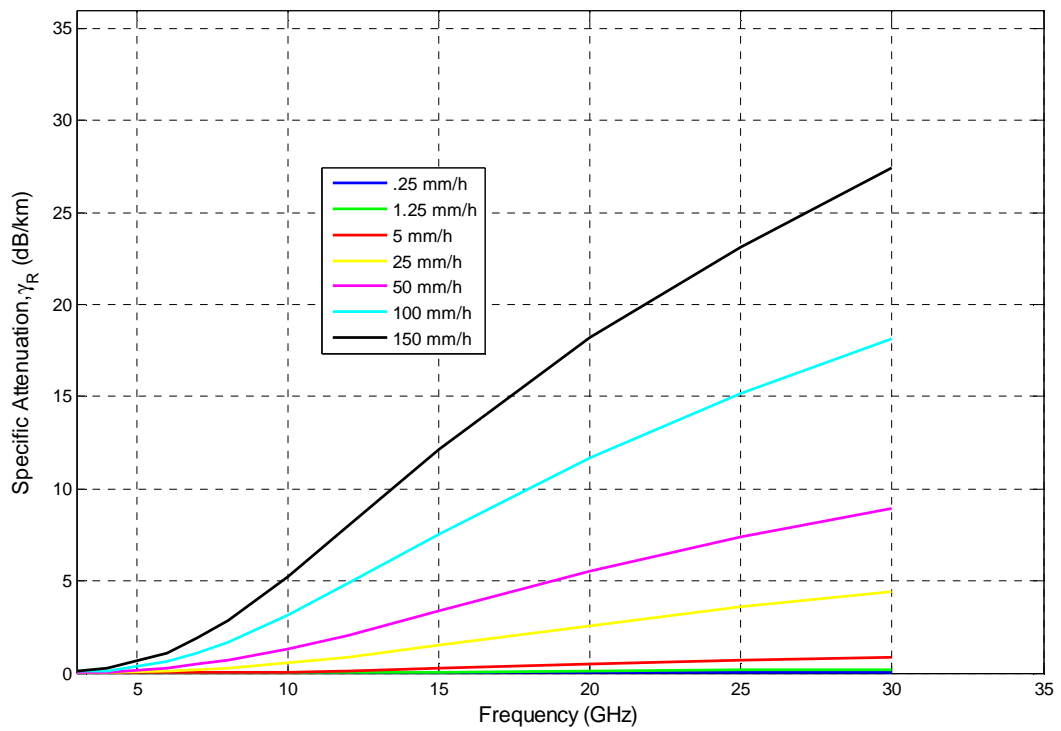
Figure 3.5: Specific attenuation due to rain at an elevation angle of 60$^{\text{o}}$.
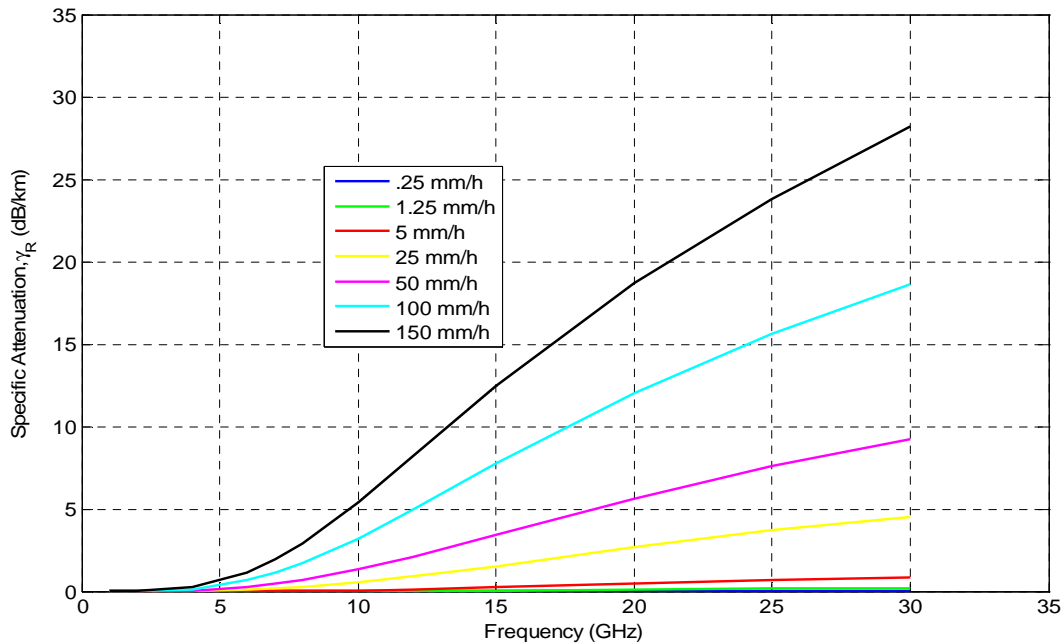
Figure 3.6: Specific attenuation due to rain at an elevation angle of 45°.

3.3.2. Statistical basis of link performance study

In general, the basic radio wave propagation mechanisms are not deterministic, and can only be described on a statistical basis. It is often necessary, and advantageous, to specify certain communications link system parameters on a statistical basis. This is particularly useful when considering parameters affected by transmission impairments in the atmosphere. Statistically based performance parameters are usually specified on a percent of time basis, i.e., the percent of time in a year, or a month, that the parameter is equal to or exceeds a specific value. Rain attenuation and some other atmospheric effects parameters are often specified on a percent of time basis [50][59]. The two most often used time periods for rain related parameter specifications are yearly (annual) and worst month. Most propagation effects prediction models are specified on an annual (8769-hour) basis. Broadcasting services, including the broadcasting satellite service (BSS), often specify on a worst month (730-hour) basis. The worst month denotes the calendar month where the transmission impairments, primarily rain attenuation, produce the severest degradation on the system performance. Parameters affected by rain attenuation, for example, carrier-to-noise ratio or signal-to-noise ratio, would have worst month values in July or August for most regions of India, in monsoon months when heavy rain occurrence is most probable. The parameter is presented on the linear scale of a semi-logarithmic plot, with the percent of time variable placed on the logarithmic scale.[7]

Several terms are used in specifying the percent of time variable, including outage, exceedance, availability, or reliability. If the percent of time variable is the percent of time the parameter is equalled or exceeded, P, then (100 – P) display represents the availability or reliability of the parameter.

Exceedance or Outage P (%)	Availability or Reliability (100-P) (%)	Outage time	
		Annual Basis (hour or minutes per year)	**Monthly** (hour or minutes per year)
0	100	0 hr	0
10	90	876 hr	73 hr
1	99	87.6 hr	7.3hr
0.1	99.9	8.76 hr	44 min
0.05	99.95	4.38hr	22 min
0.01	99.99	53 min	4 min
0.005	99.995	26 min	2min
0.001	99.999	5 min	0.4 min

Table 3.1:   Annual and monthly outage for specified percentage of time and availability.

Here a link availability of 99.99 % corresponds to a link with an expected outage of 0.01 %, or 53 minutes, on an annual basis. The BSS generally specifies link parameters in terms of an outage of '1% of the worst month', corresponding to 7.3 hours outage or 99% link availability during the worst month. Most propagation prediction models and measurements are developed on an annual statistics basis. It is often necessary to determine worst month statistics for some specific applications, such as the BSS, from annual statistics, because annual statistics may be the only source of prediction models or measured data available.

The ITU-R has developed a procedure in Recommendation ITU-R P.841-4 for the conversion of annual statistics to worst-month statistics for the design of radio communications systems. The recommendation procedure leads to the following relationship:

$$P = 0.30 \ P_w^{1.15} \tag{3.3}$$

Where, P is the average annual time percentage exceedance, in percent, and P_w is the average annual worst month time percentage exceedance, also in percent.

3.3.3 Development of Rain Attenuation Studies

The classical development for rain attenuation began with studies by early researches immediately after World War II till present [7]. Basically, most of rain attenuation studies are based on three assumptions which are:

− As the wave propagates through the volume of rain, its intensity decays exponentially.

− The raindrops are assumed to be spherical water drops which cause attenuation. This attenuation is due to both energy absorption losses in the raindrops and to scattered energy by water droplets from the incident radiowave.

− Each drop's contributions are independent of the other drops, and the contributions of the drops are additive.

The prediction techniques based on the use of rain gauge cumulative distribution of rain rate are measured at a point. The problem of spatial in-homogeneity of rainfall intensity is taken into account by using an effective path length, where the path is divided into small volumes of spherical and uniformly distributed water drops of rain as radio wave propagate through it, the reduction and the dispersion occurs on the signal amplitude caused by each rain drops, which is known as rain attenuation, as shown in Figure 3.7.
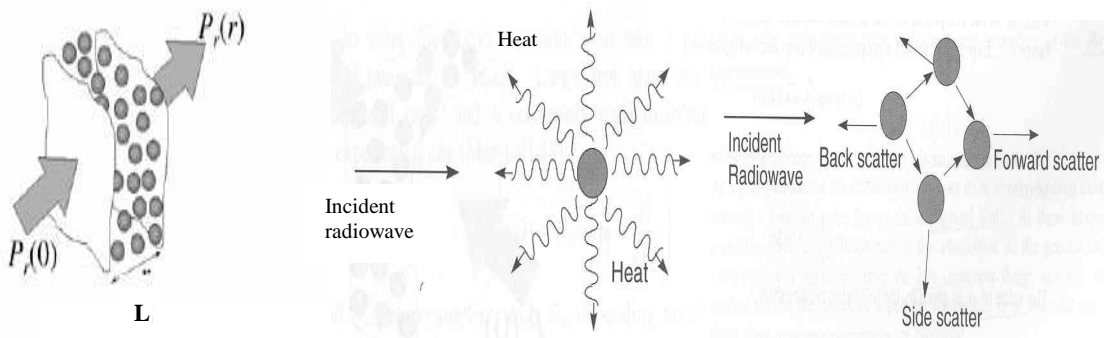
Figure 3.7: Volume of spherical uniformly distributed raindrops, dispersion and scattering of RF energy on collision with water particles.

According to Ippolito (1986), the total attenuation (*A*) in the direction of wave propagation in (dB) can be expressed as in equation (3.4). Where γ is the specific attenuation (dB/km) along the rain volume (km), and the total rain attenuation is integrating the specific attenuation over the path. On the other hand, the path is divided into small incremental volumes, where the rainfall is approximately uniform. The rainfall rate in each small volume is associated with a corresponding attenuation called specific attenuation [29].

$$A(dB) = \int_0^L \Upsilon dl \qquad (3.4)$$

$$A(dB) = \Upsilon(dB/Km) \times L_{eff} \ (Km) \qquad (3.5)$$

The problem of predicting attenuation by rain is quite difficult, because of non-uniform distribution of rainfall rate along the entire path length. Extensive efforts have been undertaken to develop reliable techniques by researchers, which is explored in effective

path length approach (Crane, 1980). According to ITU-R (1994), the effective path length is the length of a hypothetical path obtained from radio data dividing the total attenuation by the specific attenuation exceeded for the same percentage of time as in equation (3.5).

The details of L_{eff} are discussed in the next section. The attenuation of the wave, usually expressed in decibel (dB) value as,

$$A(dB) = 10 \log_{10} \left(\frac{P_t}{P_r} \right) \tag{3.6}$$

Where, P_t is the transmitted power and P_r is the received power and value is negative as P_t is greater than P_r.

According to ITU-R, the microwave engineers should design a desired availability of microwave link at 99.99% of the time that determines the required amount of link margin to counter the extreme rain attenuation condition. Therefore, the link is allowed to experience outage of 0.01% of the time throughout the year. Specific attenuation and effective path length are the main elements for all the prediction models, the discussions for these elements are provided in the following sub-sections.

3.3.4 The Effective Path Length (L_{eff})

The major problem in the estimation of rain attenuation studies relates with determining the effective path length. A large portion of the significant research accomplished on the effects of rain on the microwave and the satellite communication links have been involved with the determination of techniques and models to characterize the slant path from measurable quantities [20].

The effective path length is used to account for in-homogeneity of rain along the propagation path, According to Ponte (1985), and Lin (1979), the effective path length L_{eff} depends on the actual path length L and the reduction factor , $r(p)$ and its expressed as

$$L_{eff} = L_s \times r(p) \qquad [km] \tag{3.7}$$

An effort has been developed to give a better understanding of the effective path length concept and its dependence on meteorological factors and link parameters. Almost all of these reduction factors were derived in purely empirical method at a number of geographical locations (Crane,1993). According Dissanayake (1989), based on radiometric rain attenuation measurements in Peru, the most probable cause for the overestimation of attenuation is the path reduction factor, which is not applicable to climates dominated by tropical rainfall climate. Several models were proposed to define the effective path as discussed in the following subsection. Here we have tried to analyse the geographical data

of different locations of India taking account that our satellite may be placed at 83°E in the GSO. Accordingly the elevation angle is varies almost from 47° to 80°.

3.3.5 The Effective Rain Height

At a certain height above ground level snow and ice precipitation are converted into rain precipitation is called the effective rain height [34]. The region around this height is called the melting layer. During periods of light rain and for low elevation angles, the melting layer contributes significantly to the total slant path attenuation as verified by the relevant prediction model.
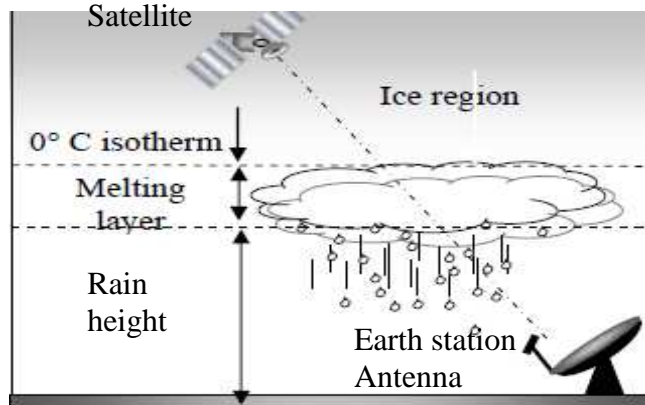
Figure 3.8:   Rain height and different rain layers.

For Indian region the elevation angle are ranges from 47° to 80° to the proposed satellite position at 83° E and the horizontal projection of the slant path can be calculated using the path geometry theories proposed by ITU-R. The rain height is the only factor that can affect the slant path length. The effective rain height is the rain height for the slant rainy path that affects the satellite link.

Spot beam	Madurai	Chennai	Hyderabad	Mumbai	Pune	Ahmed abad	Jaipur	Delhi
Elevation angle (degree)	79.8	74.3	72.23	70.65	71.28	60.7	57.5	56
Height above MSL (metre)	100.58	6.7	525	10.15	560	52	431	233
Latitude N, Longitude E	9°.72' 78°.10'	13°.11' 80°.23'	17°.28' 78°.36'	18°.70' 72°.65'	18°.35' 73°.75'	23o.0' 72°.55'	27°.0' 75°.70'	28°.50' 77°.22'
Spot beam	Chandigarh	Srinagar	Lucknow	Gawhati	Kolkata	Patna	Bhopal	Bhuba neswar
Elevation(deg)	53.4	49.3	58.6	58	62.8	60	62	66
Height above MSL (metre)	350	1730	123	55	6.5	54	50	45
Latitude N, Longitude E	30°.60' 76°.63'	35°.05' 74°.65'	26°.65' 81°.0'	26°.12' 91°.61'	22°.45' 88°.32'	25°.44' 85°.18'	23°.26' 77°.40'	20°.20' 85°.65'

Table 3.2: Approximated geographical parameters of 16 spot beam locations and elevation angle (degree) to satellite placed at 83° E (ISRO) of GSO

The effective rain height can be calculated using the total measured attenuation along the path divided by the attenuation per one kilometre. The vertical variation of rain specific attenuation can be taken into account to improve the prediction of rain attenuation along slant paths.

3.4   Effective Terrestrial path length

For the microwave link path which is known as terrestrial path and low elevation slant path angle, the horizontal reduction factor is taken into account for inhomogeneous distribution of rainfall horizontally [39]. Which cause the effective path length is shorter than the actual path length. The following section represents the most published horizontal reduction models in tropical region.

3.4.1. Moupfouma Reduction Factor Model [60]

According to Moupfouma (1984) an empirical model for predicting rain induced attenuation on terrestrial paths using effective path length is proposed based on studies in Congo, Japan, U.S and Europe for various path parameters and length. The mathematical expression for horizontal reduction factor r(p) expressed as follows

$$r(p) = \frac{1}{(1 + 0.03 \times ((P/0.01)^{-\beta}) \times (L_s))}$$

(3.9)

The β coefficient is given as a result of a best fit by

$$\beta = 0.45 \qquad 0.001 < P < 0.01,$$

and $\qquad \beta = 0.6 \qquad\ 0.01 < P < 0.1$

Where, f is the frequency in GHz.

L_s is the path length in km.

P (%)   is percentage in time of the year.

3.4. 2 CETUC Reduction Factor Model [20]

Pontes (1993), has proposed based on use of point rainfall cumulative distribution as function for the prediction of rain attenuation. Basically the model built based on data collected at Brazil sites and then adapted for application on a global basis considering experimental data from 281 measurement sites, available in the ITU-R data bank. The model is more practicable by taking the equivalent rain cell diameter into account concept to deal with the effective path length.   The mathematical formula for the model [37] is represented as

$$r(p) = \frac{1}{(1 + \text{pathlength(km)}) / L_o)}$$

(3.10)

Here L_o is the rain cell diameter proposed using the measured attenuation and the ITU-R specific attenuation as

$$L_o = u\,[1 + Rainrate^{(v - w\log(p))}] - 1 \tag{3.11}$$

Where the coefficients values are given as $u = 200$, $v = 0.425$, $w = 0.089$.

The length L of the equivalent rain cell is modelled as the function of the probability level P % and the point rain rate exceeded at this probability level. Based on measurements conducted at Malaysian site, Kareem (2000) has proposed new values for the confections as $u = 1500$, $v = 0.4856$, $w = 0.1530$.

3.4.3 Garcia Reduction Factor Model [20]

According to Garcia (2004), the database used to derive the prediction method is an extension of the ITU-R database of rain attenuation in terrestrial links, to which results of measurements carried out in the South-eastern region of Brazil have been added. The following empirical expression for r(p), against these parameters, was obtained using a nonlinear regression algorithm

$$r\,(p) \;=\; 3.445 \times (\,L\, - 0.164\,) \times (\,R_P\,(-0.369 + 0.115\, /\, Ls\,)) \tag{3.12}$$

Where, R_P is the rain rate exceedance measured using point rain fall rain gauges,

Ls, is the path length in km.

According to Kareem (2003), the effective path length for long path (more than 1km) addresses the horizontal inhomogeneity of rainfall distribution along the whole path. For practical assumption by study the effective path which expresses the actual path interacted with the rainy cell diameter concept. But, almost the previous researchers used the specific attenuation for one km. [29]

In Malaysia previous researchers have experimented taking a terrestrial microwave path of length 11.87 km, at 7 GHz and found the effective path length to be around 2.2 -2.9 km as average of all the measurements for all the paths as maximum length of the effective rain cell diameter. The next section will discuss the comparison of this predicted attenuation with other models based on horizontal reduction factor concept against measurements at several locations in tropical regions. The collected measured rain attenuation data obtained along different length microwave links operating at approximately 7 and 15 GHz are compared with predicted rain attenuation obtained using different models.
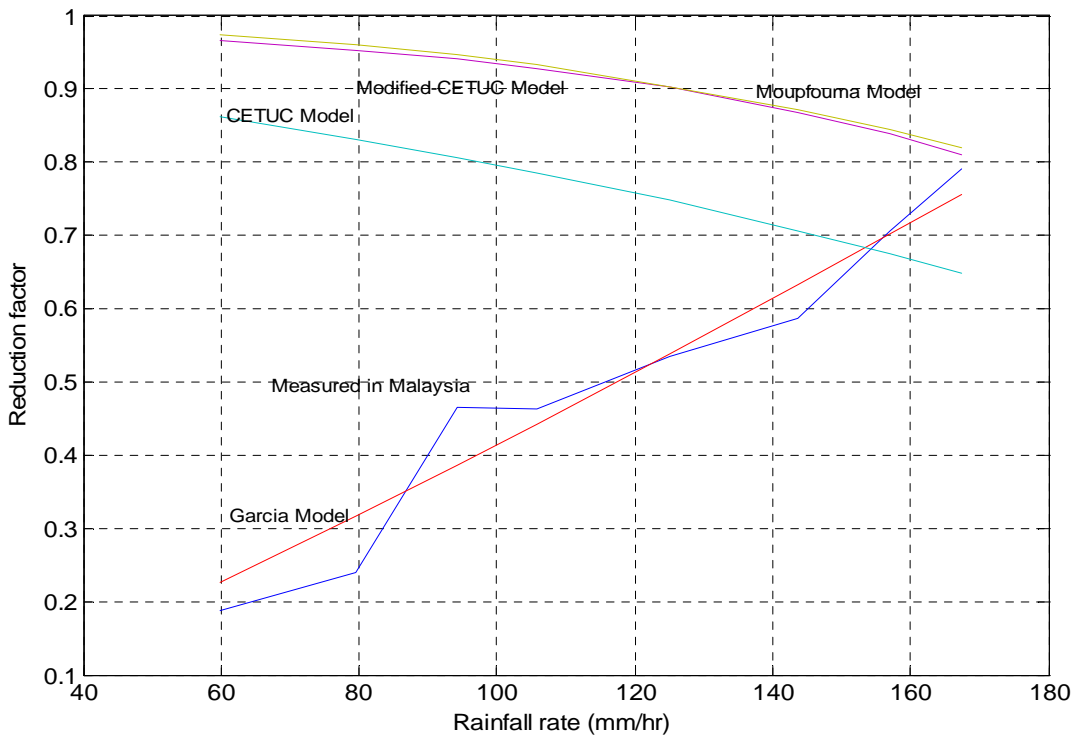
Figure 3.9: Comparison of different reduction factor models
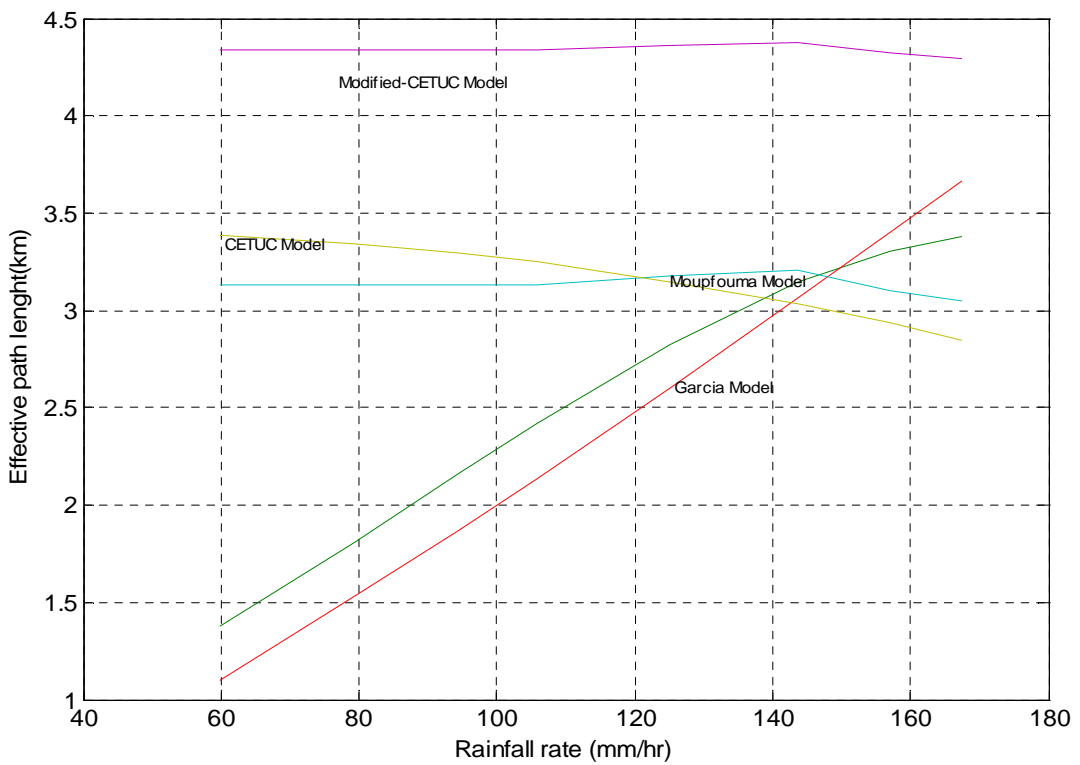
Figure 3.9a: Comparison of the effective path length for different models

The figure 3.9-3.9a shows the comparison of the effective path models. The CETUC, modified CETUC and Moupfouma prediction models show overestimate of the effective path for low rainfall rate intensity (less than100 mm/hr). Whereas, Garcia model shows underestimate along all the intensity of rainfall rate. In case of Garcia model, the assumption of use of the measured rain rate with the ITU-R specific attenuation was biased the model to has linear increase as the rainfall rate increase, which causes cell diameter to have slowly increase in length, and is practically not compatible with the measurements of rain cell size distribution. But the rain cell diameter in tropical was supposed to increases as rain fall rate increases.

3.5 Slant Path Prediction Models

The attenuation can be measured quite accurately by means of satellite beacon signals and radiometers. The propagation experiments are carried out only in a few places in the world and for a limited number of frequencies and link geometry, their results cannot be directly applied to all sites. For this reason, several attenuation models based on physical facts and using available meteorological data have been developed to provide adequate calculations in all regions of the world.

When designing a link budget for a satellite system, the atmospheric condition between the ground station and a space station is critical. A good (a clear sky day) or bad (a rainy or cloudy day) atmospheric environment would determine how the signals propagate between ground and space stations. The amounts of rain attenuation depending on the rain's characteristics, including raindrop sizes, raindrop temperatures, raindrop intensities, raindrop distributions, rain fall rates, and rain locations. The ITU provides a rain model [29] that is used to predict the attenuation due to precipitation and clouds along a slant propagation path for a percentage ranges from 0.001% to 5% of an average year. Here we have applied all 16 beam location data to predict the attenuation in Indian region, which is discussed below. On the basis of this model world is classified into 14 different rain zones. A,B,C,D,E,F,G,H,J,K,L,M, and N. India is comes under K and N. The south India is having more rain fall then north India. The rain fall rates and Percentage of time in a year is given in table 3.3a and 3.3b. Figure 3.10 shows the different rain zones defined by ITU-R in Asia pacific region.
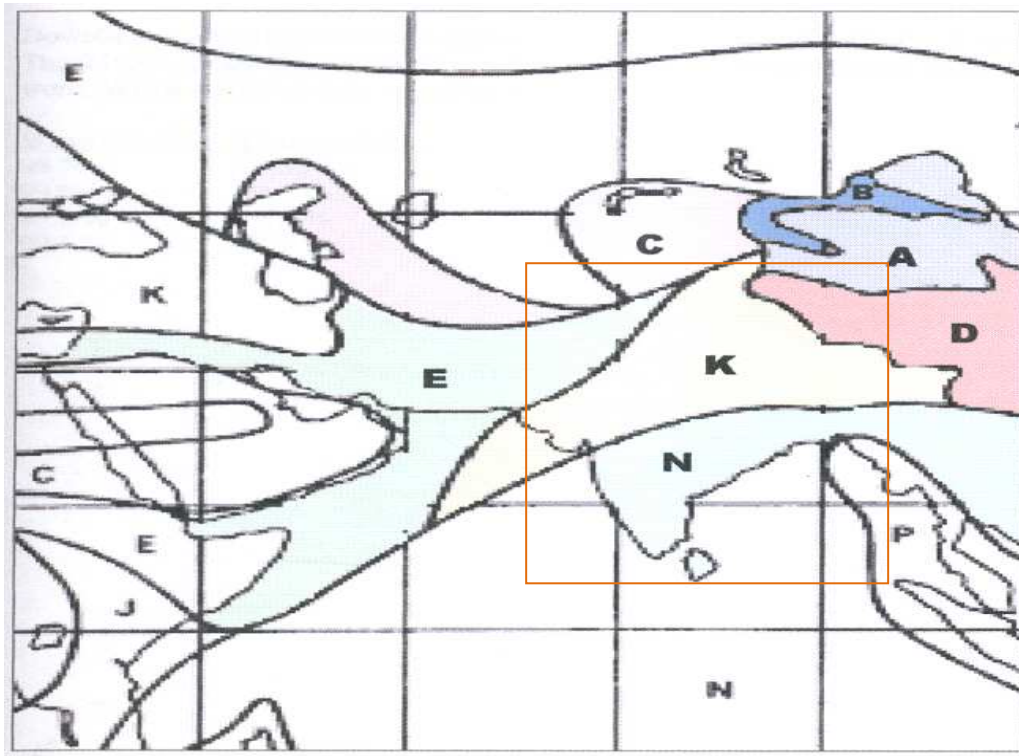
Figure 3.10: Different rain zones defined by ITU-R in Asia pacific region [from ITU-R].

Percentage of time in year	10	0.3	0.1	0.03	0.01	0.003	0.001
Rainrate exceeded (mm/hr) Region K Region N	1.5 5	4.2 15	12 35	23 65	42 95	70 140	100 180

Table 3.3a: Cumulative distributions of annual rain rates for regions K and N, (Source ITU-R).

Name of the spot beam	Mumbai	Patna	Jaipur	Srinagar	Kolkata	Hyderabad	Lucknow	Ahmeda bad
Rainrate exceeded 0.01% of time in year (mm/hr)	99.7	77.7	56.8	37.9	99.6	60.0	75.3	51.2
Name of the spot beam	Delhi	Bhopal	Madurai	Gawhati	Chennai	Pune	Bhuban-eswar	Chandi Garh
Rainrate exceeded 0.01% of time in year (mm/hr)	69.1	64.8	91.6	86.6	81.1	79.9	82.8	69.8

Table 3.3b: Cumulative distributions of annual rain rate for different spot beam locations, (Source ITU-R).

In particular, the prediction of rain induced attenuation starting from the cumulative distribution of rainfall intensity has been the subject of a major effort carried out by many researchers [6]. Several methods have been developed and tested against available data to relate the site climatic parameters to the signal attenuation statistics.
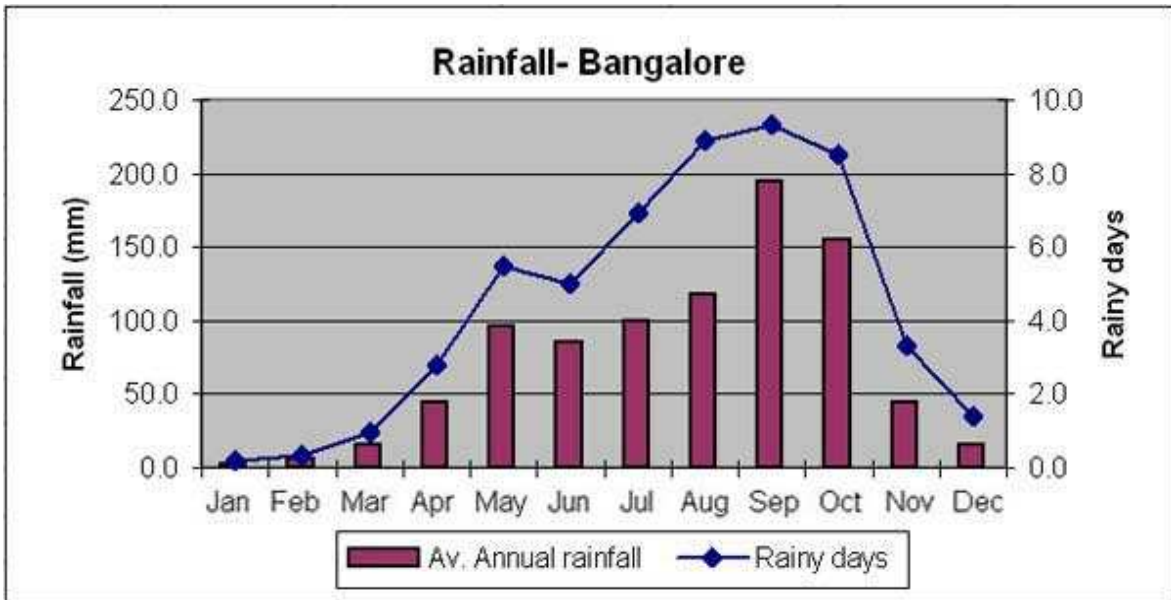
Figure 3.11a: 25 years average rain fall in Bangalore (1981-2005), Source IMD, Pune.
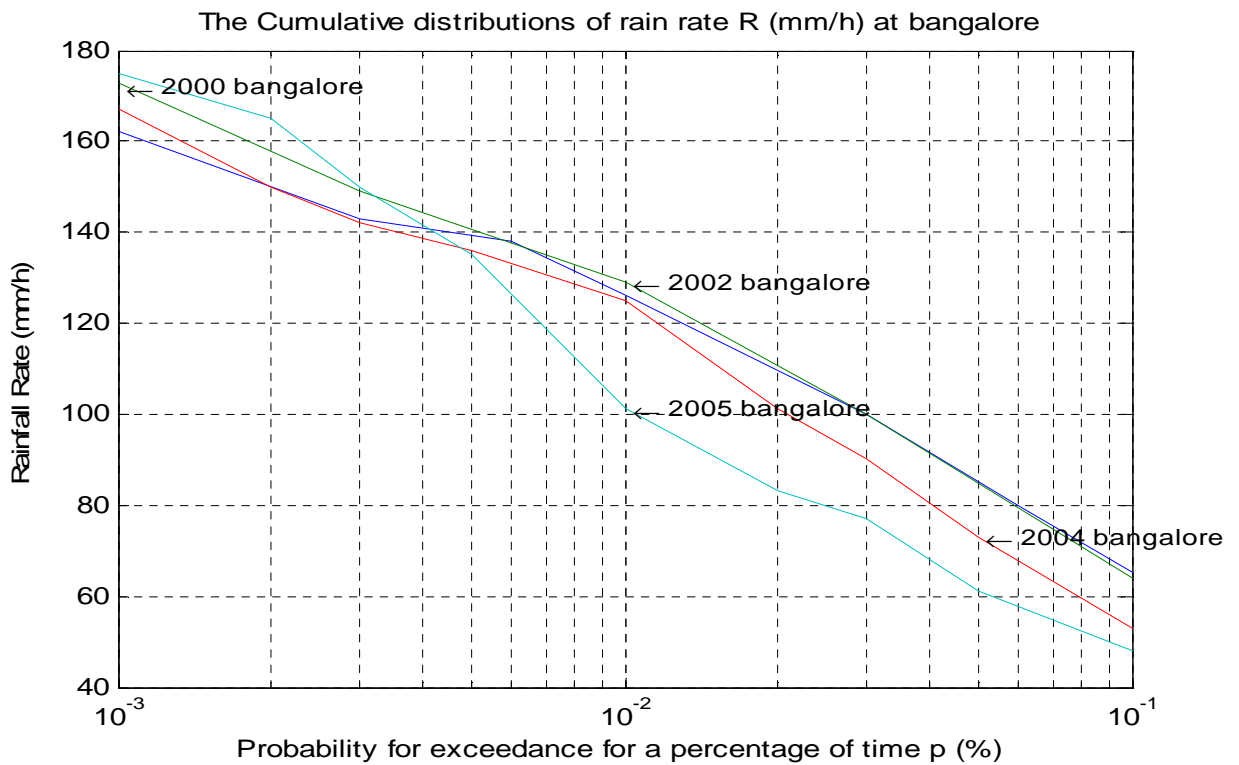
Figure 3.11b: The rain fall rate in Bangalore during 2000-2005.

Above figure 3.11a shows a 25 years average variation of rain fall data in different months in a south Indian city Bangalore. It shows in the end of monsoon season the rain fall exceeds 180 mm. In fact the rain rate exceeds 150mm/hr for the time less than 0.001% time in a year and more than 100 mm/hr for a period 0.01% of time in a year. Figure 3.11b shows rain fall rate for duration of four years. But according to ITU data base experts a continuous monitoring of six year database is required as the climatic condition is not uniform for years.

According to ITU-R the following rain prediction model which is among the best performing, are briefly described below. Here we have collected some rain fall data from IMD data bank for Bangalore and compared with the ITU data.

3.5.1 ITU-R Slant Path Prediction rain attenuation Model

The ITU-R rain attenuation model is the most widely accepted international method for the prediction of rain effects on communication systems [31]. The model was first approved by the ITU in 1982 and is continuously updated, as rain attenuation modelling is better understood and additional information becomes available from global sources. The ITU-R model has, since 1999, been based on the DAH rain attenuation model, named for its authors (Dissanayake, Allnutt, and Haidara) [50]. The DAH model has been shown to be the best in overall performance when compared with other models in validation studies. This section describes the ITU-R model as presented in the version of   ITU-R P.618-7, 2003 recommendation [26]. The rain attenuation depends on many parameters, including the given earth station elevation angle, latitude, and height above sea level, operating frequency, and effective earth's radius. The ITU rain model can be used for operating frequencies up to 55 GHz.
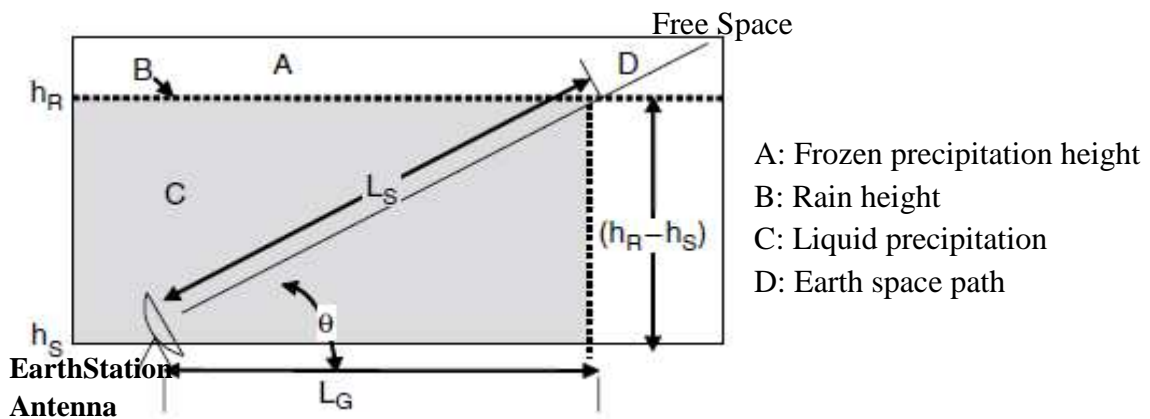
Figure 3.12: Schematic Presentation of an Earth-to-Space Path showing the Parameters are the Input into the ITU-R Rain Attenuation Prediction Procedures.

Figure above shows an earth-to-space path giving the parameters that are used at the ITU-R rain attenuation prediction procedures. The ITU model procedure consists of 10 steps. Each step defines certain parameters before the rain attenuation is calculated.

Step 1: The rain height (h_R) has to be determined. The values of h_R can be calculated from the earth station latitude.

$$h_R = \begin{cases} 3.0 + 0.028\,\phi, & 0^o < \phi < 36^o \\ 4.0 - 0.075(\phi - 36) & \phi \geq 36^o \end{cases} \quad \text{[km]} \quad (3.13)$$

Where, ϕ is the earth station latitude.

Step2:, The slant-path length (L_s) is defined in equation (3.14) below as long as the elevation angle (θ) is greater or equal to 5° .If the elevation angle (θ) is less than 5°, equation 3.15 should then be adopted.

$$L_s = \frac{(h_R - h_s)}{\sin\theta} \quad \text{[km]} \quad (3.14)$$

$$L_s = \frac{2(h_R - h_s)}{\left(\sin^2\theta + \frac{2(h_R - h_s)}{R_e}\right) + \sin\theta} \quad \text{[km]} \quad (3.15)$$

Where,

h_R = rain height [km] (typical value = 4 km)

h_s = height above mean sea level of the earth station [km]

θ = elevation angle [degrees]

R_e = effective radius of the earth [8500 km].

If ($h_R - h_s$) is less than or equal to zero, the predicted rain attenuation for any time percentage is zero. Thus, the rests of the steps in this section are not required. Otherwise, step three described below should be followed.

Step 3: The relationship between the horizontal projection, L_G, and L_s can be derived from the model Figure 3.4 and defined as the following equation.

$$L_G = L_s \cos\theta \quad \text{[km]} \quad (3.16)$$

L_S can result in negative values when the rain height is smaller than the altitude of the ground receiver site. If a negative value occurs, L_s is set to be zero.

Step 4: The rainfall rate ($R_{0.01}$) exceeded for 0.01% of an average year (with an integration time of 1 min) is defined from a long-term statistical data collection and measurements. Figure (3.13) below presents the overall rain climate zone all round the world ITU [28].

The climate zone map is used for both propagation predictions and interference calculations. The international Telecommunication Union (ITU) has divided the globe into 14 rainfall climatic zones and categorized India as Region N and K, partially with very high rain precipitation. According to ITU-R version, rain intensity that will cause the interruption of a communication link for 0.01% per year is 145 mm/hour.

Figure 3.13: ITU Rain zones. India comes under the area 3, Source ITU [7].
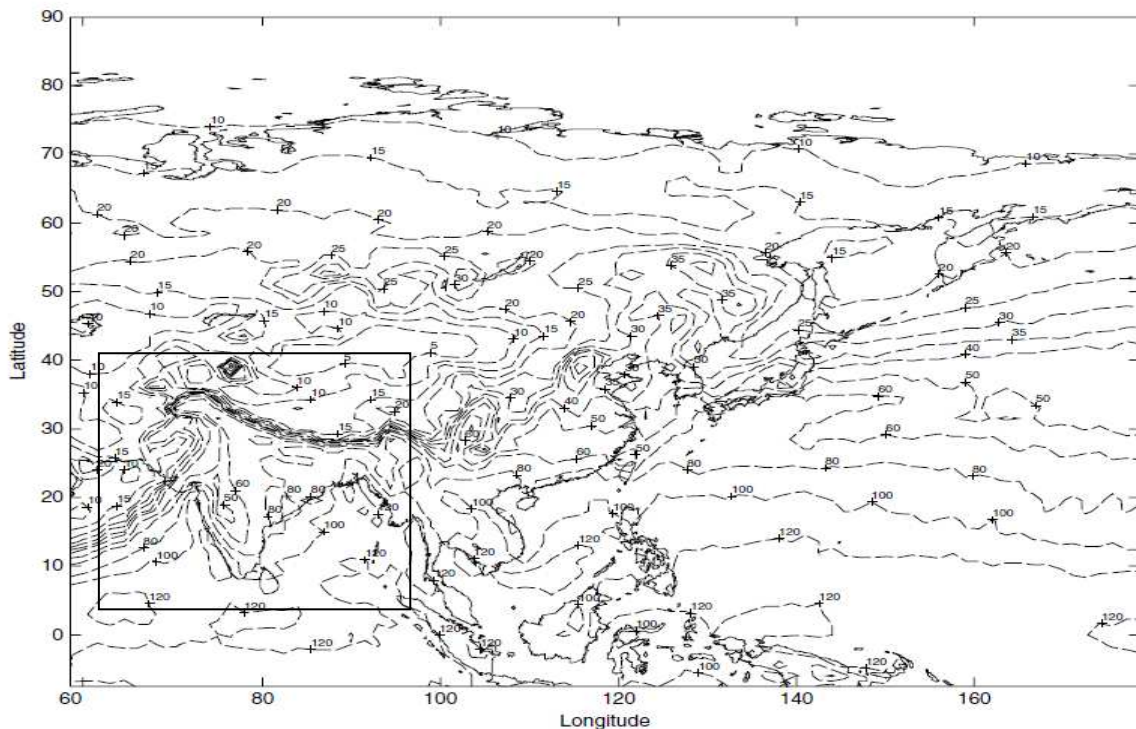
Figure 3.14:   Rain intensity exceeded for 0.01% of an average year [ITU].
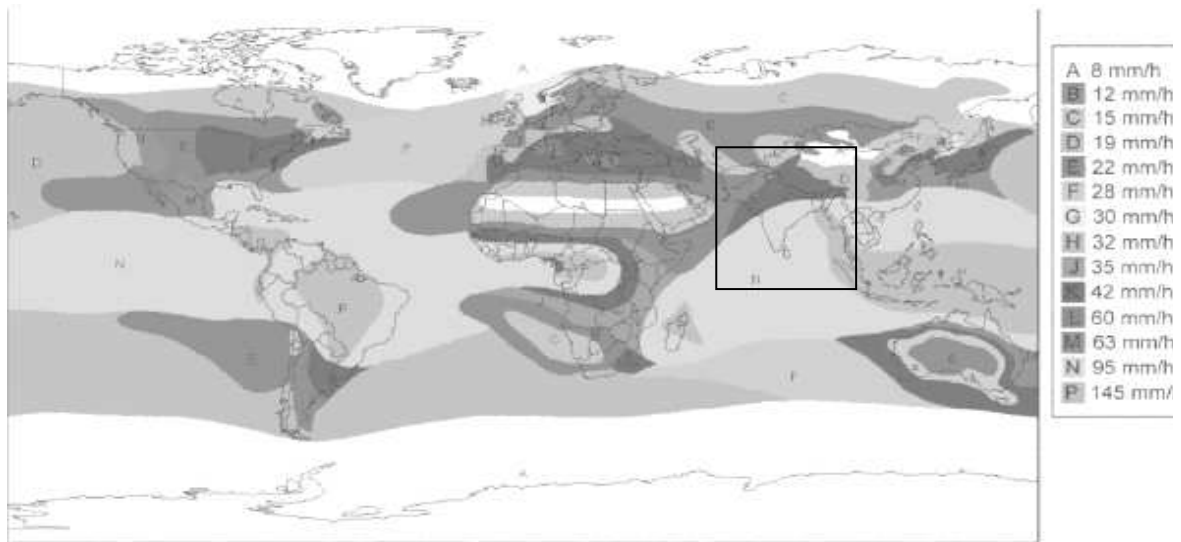
(Source: ITU-R P.837-4 for area 3)

Step 5: The rainfall intensities can also be found to correspond to particular time zones at the given percentage of time that is required for a satellite system link. Table 3.4 shows the rainfall rate intensities correspond to particular rain climatic zones in Figure (3.14) of step 4. For instance, the climatic zone code for South India is N and the rainfall rate intensity for 0.01% of the total amount of hours for an average year is 95 mm/hr. For comparison table 3.4b shows measured values in Indian city Amritsar by previous researchers.

% of time in a year	A	B	C	D	E	F	G	H	J	K	L	M	N	P	Q
0.001	22	32	42	42	70	78	65	83	55	100	150	120	180	250	170
0.003	14	21	26	29	41	54	45	55	45	70	105	95	140	200	142
0.01	8	12	15	19	22	28	30	32	35	42	60	63	95	145	115
0.03	5	6	9	13	12	15	20	18	28	23	33	40	65	105	96
0.1	2	3	5	8	6	8	12	10	20	12	15	22	35	65	72
0.3	0.8	2	2.8	4.5	2.4	4.5	7	4	13	4.2	7	11	15	34	49
10	0.1	0.5	0.7	2.1	0.6	1.7	3	2	8	1.5	2	4	5	12	24

Table3.4a: Rainfall rate exceeded in mm/hr corresponding to different ITU-R climate zones.

% time rain rate exceeded	0.001	0.003	0.01	0.03	0.05	0.08	0.1	0.3	0.5
Measured Rain rate (mm/Hr) 2001	110.5	88.5	62	39.7	29.5	16.3	12.6	2	0.75
ITU-R	150	105	60	33	24	15	15	7	4

Table3.4b: Rain rate measured at Amritsar during year 2001 which belongs to L region [24]**.**

Step 6: After the rainfall intensity is defined for a particular location and satellite system link availability for an average year, a specific attenuation (γ_R) can be determined using equation (3.17) below

$$\gamma_R = k\left(R_{0.01}\right)^{\alpha} \qquad [\text{dB/km}] \qquad (3.17)$$

Where, $R_{0.01}$ = point rainfall rate for the location for 0.01% of an average year [mm/hr]

   α , k = regression coefficient for estimating specific attenuation

and α and k are variable of frequency, elevation angle, and polarisation tilt angle. The overall k and α can be calculated from equation (3.18) and (3.19) below from the vertical (V) and horizontal (H) polarization values of k and α, given in Table 3.5. In addition, k and α can also be calculated for other frequencies by an interpolation technique.[7] k and α are calculated using regression coefficients k_H, k_V, α_H, and α_V at the frequency of interest from the following equations:

Frequency (GHz)	k_H	k_V	α_H	α_V
1	0.0000259	0.0000308	0.9691	0.8592
2	0.0000847	0.0000998	1.0664	0.9490
4	0.0001071	0.0002461	1.6009	1.2476
8	0.004115	0.003450	1.3905	1.3797
10	0.01217	0.01129	1.2571	1.2156
12	0.2386	0.02455	1.1825	1.1216
15	0.04481	0.05008	1.1233	1.0440
20	0.09164	0.06911	1.0586	0.9491
25	0.1571	0.1533	0.9991	0.9491
30	0.2403	0.2291	0.9485	0.9129
35	0.3374	0.3224	0.9047	0.8761
40	0.4431	0.4274	0.8673	0.8421

Table 3.5: Regression Coefficients for Estimating Specific Attenuation, γ_R [ITU P-838-3].

$$k = [k_H + k_V + (k_H - k_V) \cos^2\theta \cos 2\tau]/2 \qquad (3.18)$$

$$\alpha = [k_H\alpha_H + k_V\, \alpha_V + (k_H\alpha_H - k_V\alpha_V) \cos^2\theta\cos 2\tau]/2k \qquad (3.19)$$

Where, θ is the path elevation angle and τ is the polarization tilt angle with respect to the horizontal, for linear polarized transmissions. $\tau = 45°$ for circular polarization transmissions. Table 3.5, provides values of the regression coefficients for representative frequencies from 1 to 40 GHz. Regression coefficients for other frequencies, from 1 to 1000 GHz, can also be estimated. According to DHA model data, the values of k and α used for Ka-band analysis are

$$k = 0.0534 \quad \text{and} \quad \alpha = 1.0976 \qquad \text{for} \quad f = 18.45 \text{ GHz}$$
$$k = 0.1517 \quad \text{and} \quad \alpha = 1.0217 \qquad \text{for} \quad f = 28.25 \text{ GHz}$$

After all the necessary parameters have been defined and introduced previously, the horizontal reduction factor, $r_{0.01}$, for 0.01% time of an average year is

$$r_{0.01} = \frac{1}{1 + 0.78\sqrt{\dfrac{L_G\gamma_R}{f}} - 0.38\left(1 - e^{-2L_G}\right)} \qquad (3.20)$$

Where, f = Operating centre frequency [GHz]

L_G = horizontal projection calculated earlier.

This is to point out that a number of regional models have been developed by taking a short (300 meters,1 km etc.) microwave link as path length to calculate the specific attenuation but all have taken the same power law equation for final calculation. They are basically different in their k and α value. These values are presented in figure 3.15a, 3.15b.
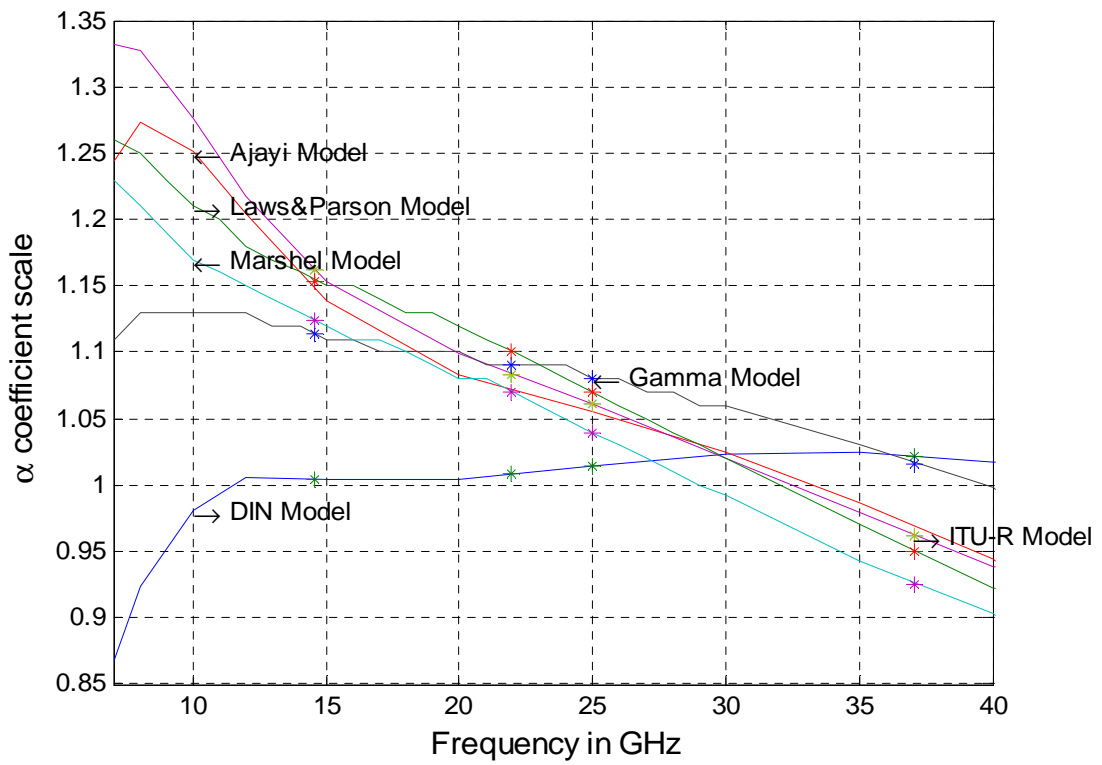
Figure 3.15a: Comparison of coefficient 'α' for Specific attenuation models with ITU.
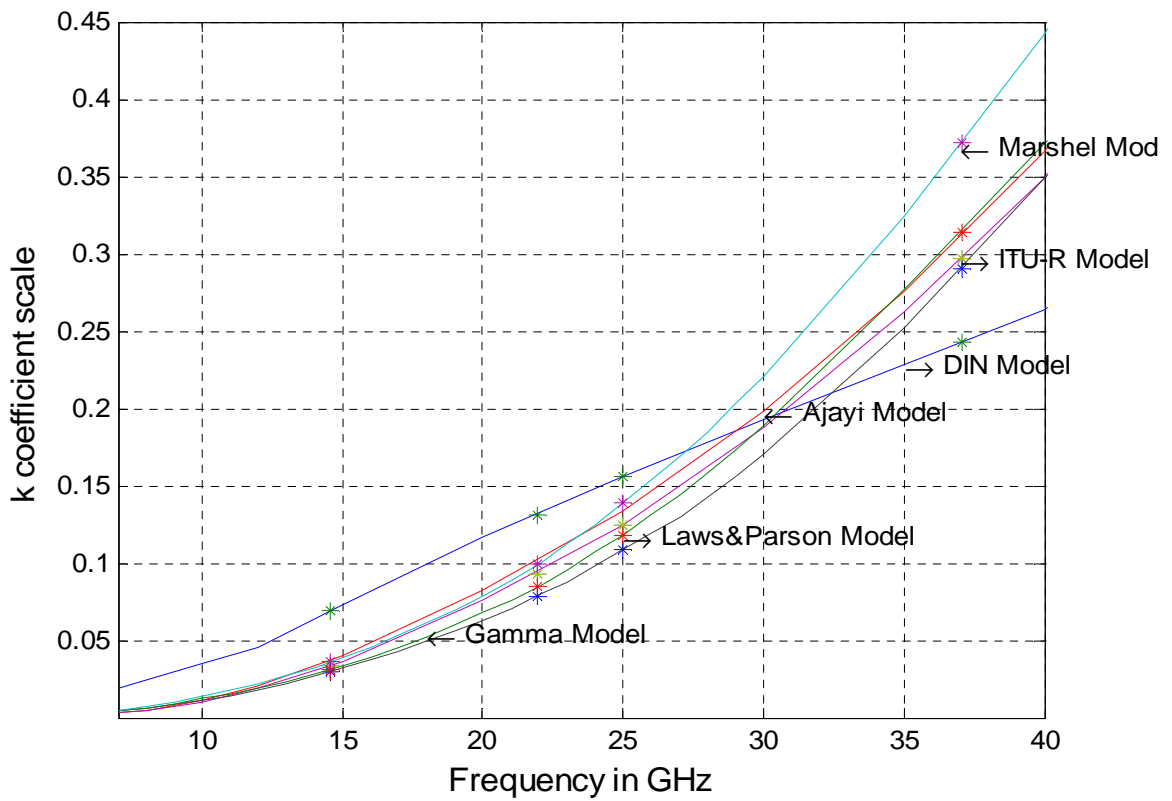
Figure 3.15b: Comparison of coefficient 'k' for Specific attenuation models with ITU.

Step 7: The vertical adjustment factor, $v_{0.01}$, for 0.01% of the time, can be calculated by a couple of sub-steps below. The values for ζ, L_R, φ and χ are found as follows:

$$\xi = tan^{-1}\left(\frac{h_R - h_s}{L_G r_{0.01}}\right) \qquad [degree] \qquad (3.21)$$

If, $\zeta > \theta$, equation (3.22) should be used to find L_R, otherwise equation (3.23) is used

$$L_R = \frac{L_G r_{0.01}}{\cos\theta} \qquad [km] \qquad (3.22)$$

$$L_R = \frac{(h_R - h_s)}{\sin\theta} \qquad [km] \qquad (3.23)$$

Step 8: The latitude of the earth station (φ) is then used to determine the χ value. If $|\varphi| < 36°$, eqn. (3.24) should be used to obtain the χ value; otherwise, the χ value equals to zero.

$$\chi = 36 - |\phi| \qquad [degrees] \qquad (3.24)$$

This now shows the vertical adjustment factor ($v_{0.01}$) that can be presented as the following equation, when the ζ, L_R, φ and χ values are determined.

$$r_{v0.01} = \frac{1}{1 + \sqrt{\sin\theta}\left[31(1 - e^{-\theta/[1+\chi]})\dfrac{\sqrt{\dfrac{L_r\gamma_R}{f^2}} - 0.45}{}\right]} \qquad (3.25)$$

Step 9: The effective path length (L_E), which will be used to calculate the rain attenuation prediction, can be obtained from following equation when L_R was given previously.

$$L_E = L_R v_{0.01} \qquad [km] \qquad (3.26)$$

Step 10: The predicted attenuation exceeded for 0.01% of an average year, $A_{0.01}$, is determined from

$$A_{0.01} = \gamma_R L_E \qquad [dB] \qquad (3.27)$$

The estimated attenuation to be exceeded for other percentages of an average year, in the range 0.001% to 5%, may then be estimated from the rain attenuation to be exceeded for other than 0.01% of an average year can be calculated by (Eq. 3.28).

$$A_p = A_{0.01}\left(\frac{p}{0.01}\right)^{-(0.065 + 0.033 ln(p) - 0.045 ln(A_{0.01}) - \beta(1-p)\sin\theta)} \qquad [dB] \qquad (3.28)$$

P is the desired percentage of an average year other than 0.01%, and β can be calculated based on the desired p value, and the given φ and θ values, shown in Table 3.5.

If p≥ 1% or |φ| ≥ 36°	β= 0
If p < 1% and |φ|< 36° and θ ≥ 25°	β=-0.005(|φ| - 36)
Otherwise	β=-0.005(|φ| - 36)+1.8-4.25sin(θ)

Table 3.6: Parameter Status of p, φ, and θ to find 'β' Value

This method provides an estimate of long-term statistics due to rain. Large year-to-year variability in rainfall statistics can be expected when comparing the predicted results with measured statistics [ITU-R P.678-1]. Obviously, the uplink rain attenuation is much higher compared to that on the downlinks. Therefore, the uplink must be designed carefully. In addition, other interference (adjacent satellite interference, antenna pointing losses, needed implementation margin and link margin, etc.) will also degrade both uplink and downlink performance.

3.5.2 Crane Global Model: Rainfall Rate vs. Attenuation

Robert.K.Crane (1980) rainfall rate model divided the world into eight regions based on total rain accumulation and the number of thunderstorm. Satellite and precipitation data were used to extend the climate over the ocean, and India is come under G, H, and D3 region [37].

The modified Crane global prediction model will be discussed in detail in this section because of its accuracy, the ease with which it can be used with a calculator, and global application. This model is based on the geophysical observations of rain rate, rain structure, and the vertical variation of atmospheric temperature. Therefore, the total path attenuation that may be exceeded for P percent of the year is a function of the point rain rate distribution, the vertical extent of the rain, and rain rate distribution along the path.

Figure 3.16 shows the global map of the rain rate for Asian climate regions, including the ocean areas. The rain climate regions are divided into four types of polar, temperate, subtropical and tropical region. India is pointed as a sub-tropical region. The point rain rate distributions for the rain climate regions of the Crane model are given in Table 3.7.
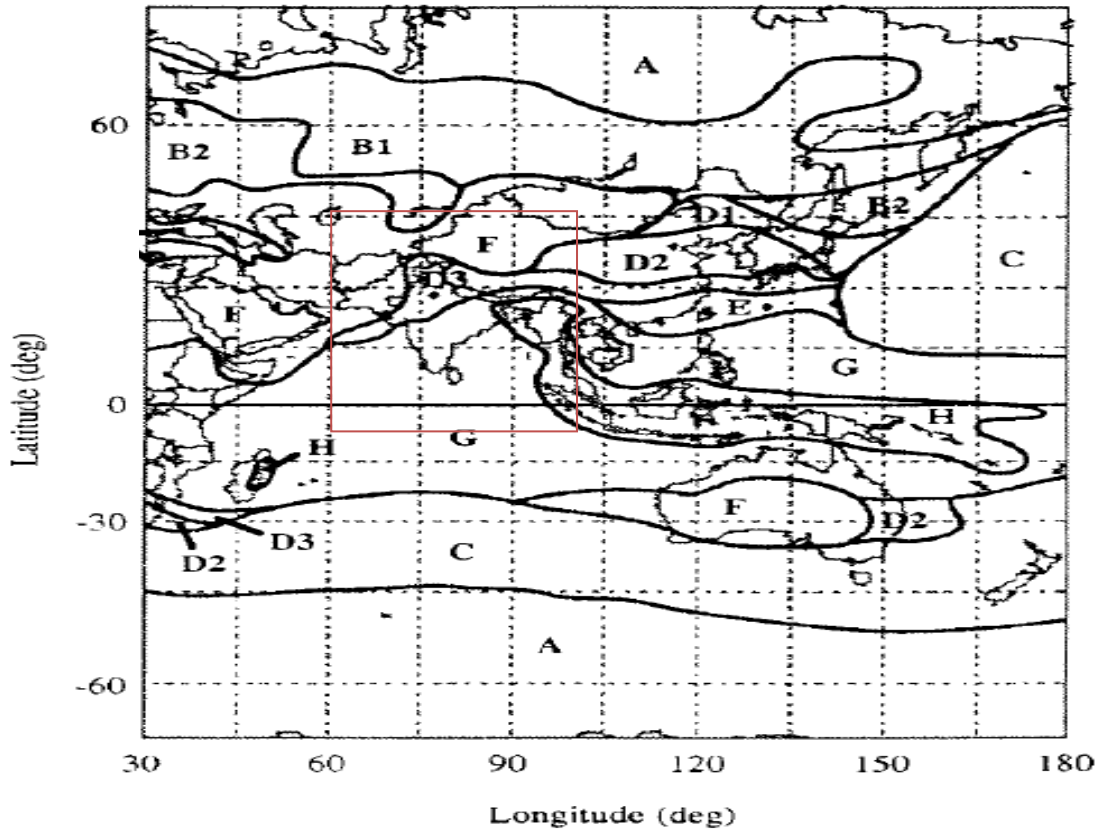
Figure 3.16: Different rain climatic zones of Global Crane model for Asia [37].

Rain rate exceeded. Percent of year	Rain rate distribution values per rain climate region (mm／hr) R_p											
(P%)	A	B	B1	B2	C	D1	D2	**D3**	E	F	**G**	**H**
0.001	28.1	52.1	42.6	63.8	71.6	86.6	114.1	**133.2**	176	70.7	**197**	**542.6**
0.002	20.9	41.7	32.7	50.9	58.9	69	88.3	**106.6**	145.4	50.4	**159.6**	**413.9**
0.005	13.8	29.2	22.3	35.7	41.4	49.2	62.1	**78.7**	112	31.9	**118**	**283.4**
0.01	9.9	21.1	16.1	25.8	29.5	36.2	46.8	**61.6**	91.5	22.2	**90.2**	**209.3**
0.02	6.9	14.6	11.3	17.6	19.9	25.4	34.7	**47**	72.2	15	**66.8**	**152.4**
0.03	5.5	11.6	9	13.9	15.6	20.3	28.6	**39.9**	62.4	11.8	**55.8**	**125.9**
0.05	4	8.6	6.8	10.3	11.5	15.3	22.2	**31.6**	50.4	8.5	**43.8**	**97.2**
0.1	2.5	5.7	4.5	6.8	7.7	10.3	15.1	**22.4**	36.2	5.3	**31.3**	**66.5**
0.2	1.5	3.8	2.9	4.4	5.2	6.8	9.9	**15.2**	24.1	3.1	**22**	**43.5**
0.3	1.1	2.9	2.2	3.4	4.1	5.3	7.6	**11.8**	18.4	2.2	**17.7**	**33.1**
0.5	0.5	2	1.5	2.4	2.9	3.8	5.3	**8.2**	12.6	1.4	**13.2**	**22.6**
1	0.2	1.2	0.8	1.4	1.8	2.2	3	**4.6**	7	0.6	**8.4**	**12.4**
2	0.1	0.5	0.4	0.7	1.1	1.2	1.5	**2**	3.3	0.2	**5**	**5.8**
3	0	0.3	0.2	0.4	0.6	0.6	0.9	**0.8**	1.8	0.1	**3.4**	**3.3**
5	0	0.2	0.1	0.2	0.3	0.2	0.3	**0**	0.2	0.1	**1.8**	**1.1**

Table 3.7: Rain rate exceeded in Percent of time in a year, Indian region highlighted.
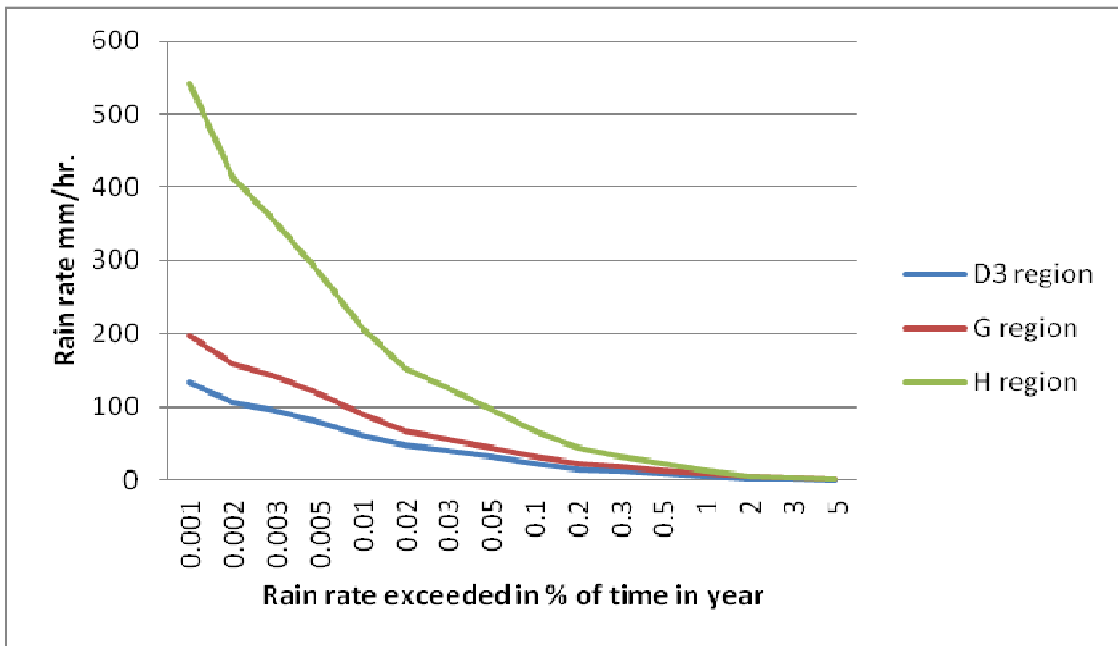
Figure 3.17: Rain rate exceeded in Percent of time in a year (P%), Indian regions D3, G,H. [7]

The rain attenuation over an average year for the Crane global model is calculated as the following steps.

Step1 : Obtain the annual rain rate distribution R_p.

    (a) Determine from the climate regions given by the maps of Figure 3.16.

    (b) Look up the appropriate rain rate distribution values listed in Table 3.7**.**

Step 2: The rain height H, used for the global model is a location dependent parameter based on the $0^{°}$ isotherm (melting layer) height. The rain height is a function of station latitude φ and percent of time in an average year p. Figure 3.18 gives the rain height, H, for probabilities of 0.001, 0.01,0.1, and 1 %, for station latitudes from 0 to $70^{°}$. Table 3.8 shows the rain height for probability values of 0.001 and 1.0%. Rain height values for other probability values can be determined by logarithmic interpolation between the given probability values.
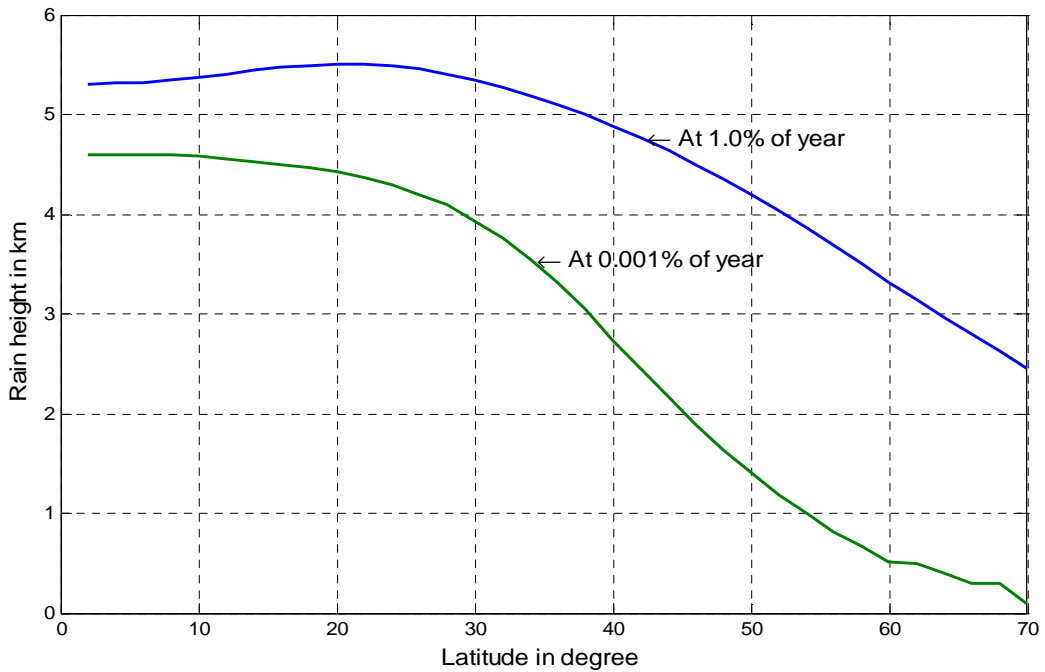
Figure3.18: Rain height for the global rain attenuation model.

It shows that India is within the latitude of 8-38° N, and the rain height ranges from 3 to 4.6 km for 0.001% of time in a average year. The detail is given in the following table.

Ground station latitude φ(degree)		≤ 2	6	8	10	14	18	20	24	26	30	34	36
Rain height H (km)	At 0.001% in a year	5.30	5.32	5.34	5.37	5.44	5.49	5.50	5.50	5.46	5.35	5.19	5.10
	At 1.0% in a year	4.60	4.60	4.59	4.58	4.53	4.47	4.42	4.37	4.20	3.94	3.55	3.31

Table 3.8: Rain heights for Global rain model, for 0.001% and 1.0% of time [59][7].

Step 3: Determine the surface projected path length. The horizontal (surface) path projection of the slant path, D, is found from the following. Determine the 0°C isotherm height H, then calculate the projected surface path length D. and Determine the 0° C isotherm heights for p = 0.001%, 0.01%, 1%.

$$D = \frac{H - H_0}{\tan \theta}, \qquad \theta \geq 10^o$$

$$D = (r_e + H_0)\psi \qquad \theta < 10^o \tag{3.29}$$

$$\psi = \sin^{-1}\left\{ \frac{\cos \theta}{r_e + H}\left[-(r_e + H_0)\sin \theta \right.\right.$$

$$\left.\left. + \sqrt{(r_e + H_0)\sin^2 \theta + 2r_e(H - H_0) + H^2 - H_0^2} \right]\right\} \tag{3.30}$$

Where,

H_0 : the height of ground station above mean sea level.

θ : the elevation angle to the satellite.

r_e : the effective radius of the earth $= 8500$km.

For Indian region, the elevation angle is greater than 45° and $H_0 = 5$ to 1700 m.

Step 4: Determine the specific attenuation coefficients. The specific attenuation is based on the relationship

$$\gamma_R = a - R^b \qquad \text{[dB/km]} \qquad (3.31)$$

Where, γ_R is the specific attenuation in (dB/km) and a and b are frequency dependent specific attenuation coefficients. The a and b coefficients are calculated using the ITU-R regression coefficients k_H, k_V, α_H, and α_V, previously provided in Table 3.5, and Figures 3.15a and 3.15b. The a and b coefficients are found from the regression coefficients from equations 3.18 and 3.19 respectively.

The specific attenuation coefficients 'a' and 'b' at different operating frequencies can also be considered as follows

$$a = 4.21 \times 10^{-5} f^{2.42} \qquad 2.9 \le f \le 54 GHz$$
$$a = 4.09 \times 10^{-2} f^{0.699} \qquad 54 \le f \le 180 GHz$$
$$b = 1.41 f^{-0.0779} \qquad 8.5 \le f \le 25 GHz$$
$$b = 2.63 f^{-0.272} \qquad 25 \le f \le 164 GHz$$

(b) Determine following four empirical constants from R_p.

$$d = 3.8 - 0.6 \ln R_p \qquad (3.32)$$

$$x = 2.3 R_p^{-0.17} \qquad (3.33)$$

$$v = 0.026 - 0.03 \ln R_p \qquad (3.34)$$

$$u = \frac{\ln\left[x \exp(vd)\right]}{d} \qquad (3.35)$$

Step 5: Calculate the mean slant path attenuation value A, at each probability of rain R_p and D.

(a) If $\quad 0 < D \le d \quad$ (Km)

$$A = \frac{aR_p^{\ b}}{\cos\theta}\left[\frac{\exp(ubD)-1}{ub}\right] = \frac{aR_p^{\ b}L}{D}\left[\frac{\exp(ubD)-1}{ub}\right] \quad \text{[dB]} \quad (3.36)$$

(b) If $d < D \le 22.5$ (Km)

$$A = \frac{aR_p^{\ b}}{\cos\theta}\left[\frac{\exp(ubd)-1}{ub} - \frac{x^b\exp(vbd)}{vb} + \frac{x^b\exp(vbD)}{vb}\right] \quad \text{[dB]}$$

$$= \frac{aR_p^{\ b}\ L}{D}\left[\frac{\exp(ubd)-1}{ub} - \frac{x^b\exp(vbd)}{vb} + \frac{x^b\exp(vbD)}{vb}\right] \quad \text{[dB]} \quad (3.37)$$

(c) If $D > 22.5$ Km, calculate A with D=22.5 but use the rain rate R_p at the value

$$P' = \frac{22.5}{D}p \ \text{ instead of } R_p.$$

Step 5: The Crane global model provides for an estimate of the upper and lower bounds of the mean slant path attenuation. The bounds are determined as the standard deviation of the measurement about the average and are estimated from the following table:

Percent of time in year	1.0	0.1	0.01	0.001
Standard deviation	±39	±32	±32	±39

Table 3.9: Standard deviations of the measurements about the average. [7].

For example, a mean prediction of 20 dB at 0.01% yields upper/lower bounds of ±32% or ± 6.4 dB. This results in a prediction range for the path attenuation, from the global model, of 26.4 to 13.6 dB, with a mean value of 20 dB.

The figures 3.19a -3.19d shows the predicted rain attenuation using ITU and Crane models for 16 beam locations as specified. The rain attenuation increases as the percentage of time decreases from 0.1% to 0.001% in a year. The ITU curves shows that the attenuation exceeds 20 dB towards 60 dB for duration less than 0.01%. But Crane model overestimates to 100dB for a less time. For a comparison we have collected the data in various tropical sites like Malaysia, Singapore and shown the predicted attenuation for different frequencies in figures 3.20-3.21, the attenuation for Ka band is ranges from 20-50 dB. Figure 3.22 shows data collected by DBSG3 of ITU in different tropical sites like Brazil, Peru, and Indonesia at Ku band. This shows the rain attenuation ranges from 5-20 dB for a duration 0.01% of time and up to 30 dB for 0.001% of time.

Figure 3.19a : Rain attenuation in group-A Spot-beam locations.

Figure 3.19b: Rain attenuation in group-B Spot-beam locations.
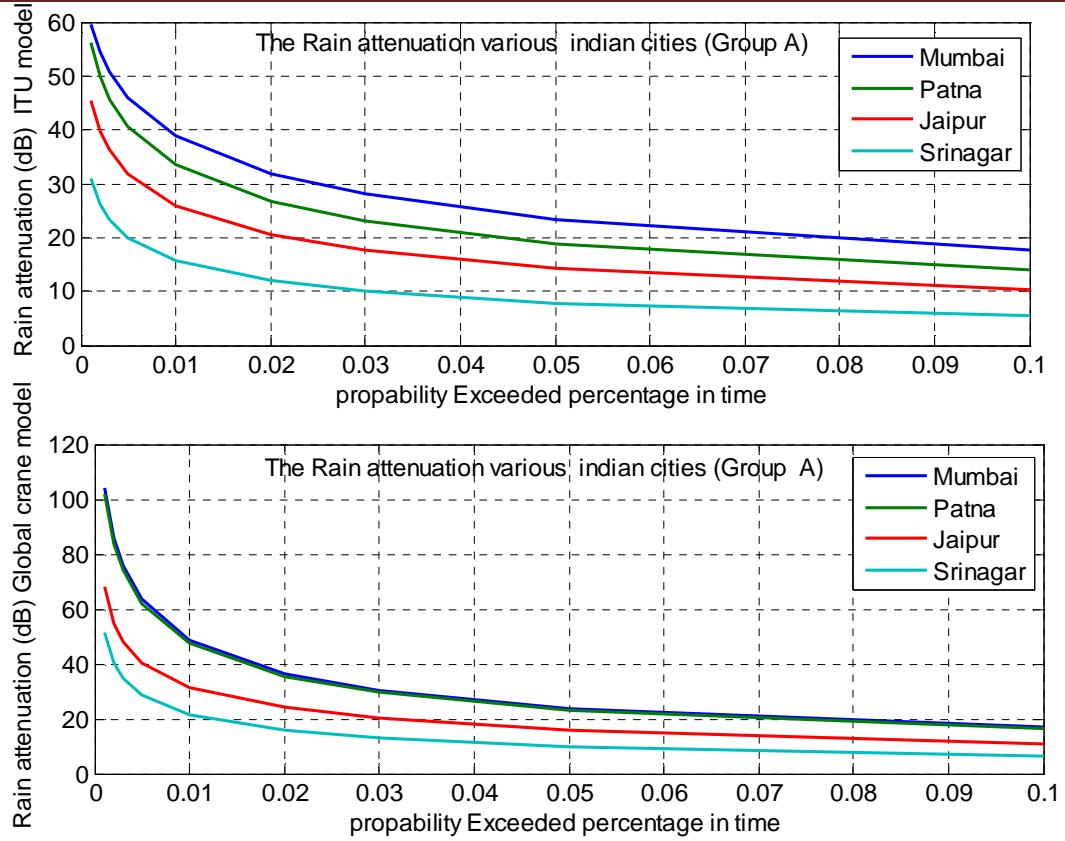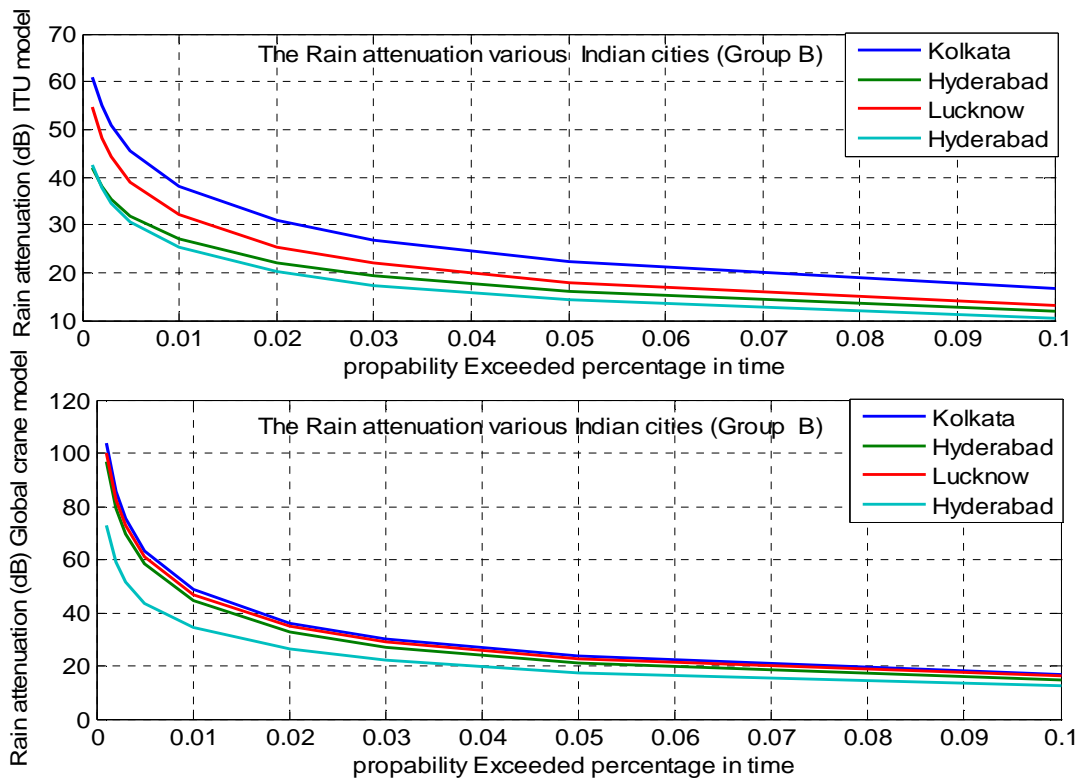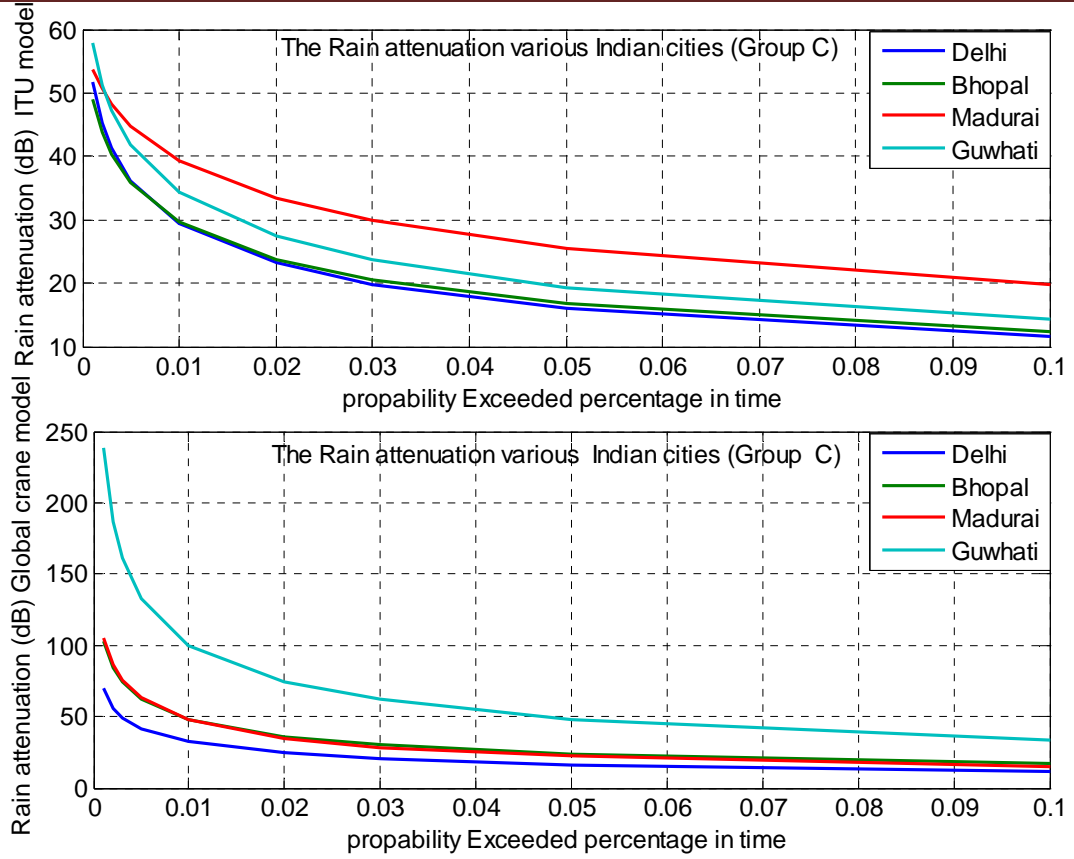
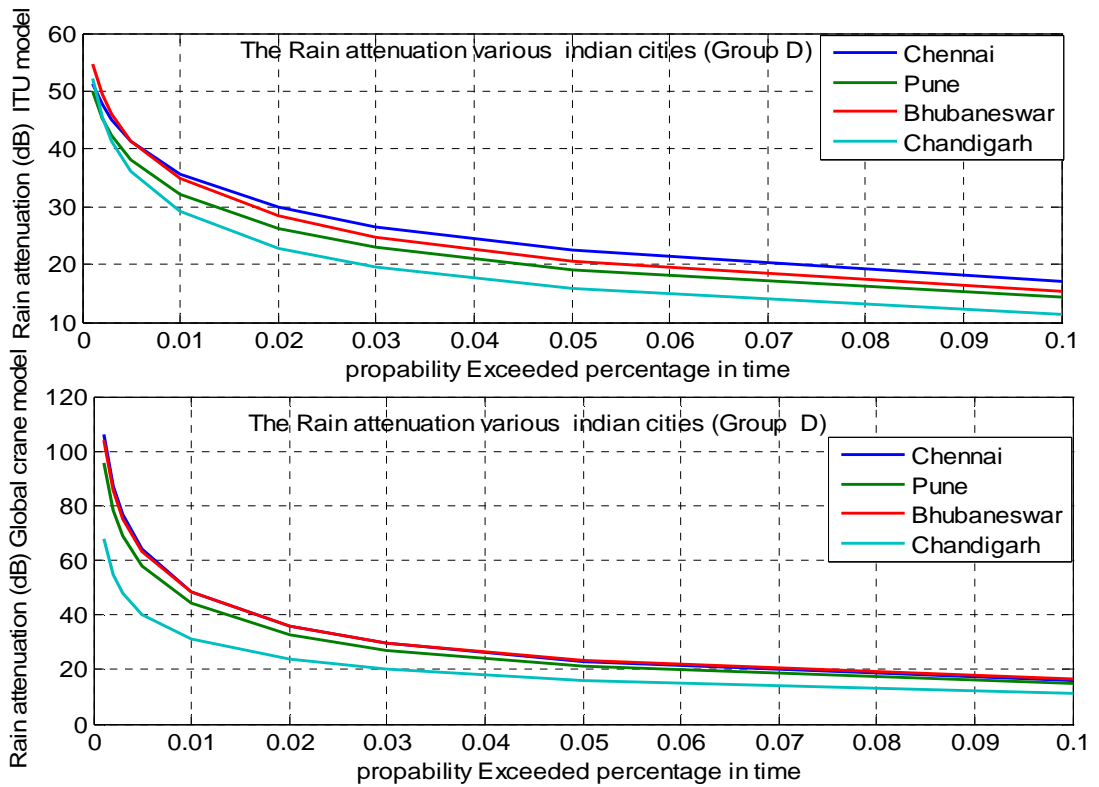**Figure 3.19c: Rain attenuation in group-C Spot-beam locations.**

Figure 3.19d: Rain attenuation in group-D Spot-beam locations.
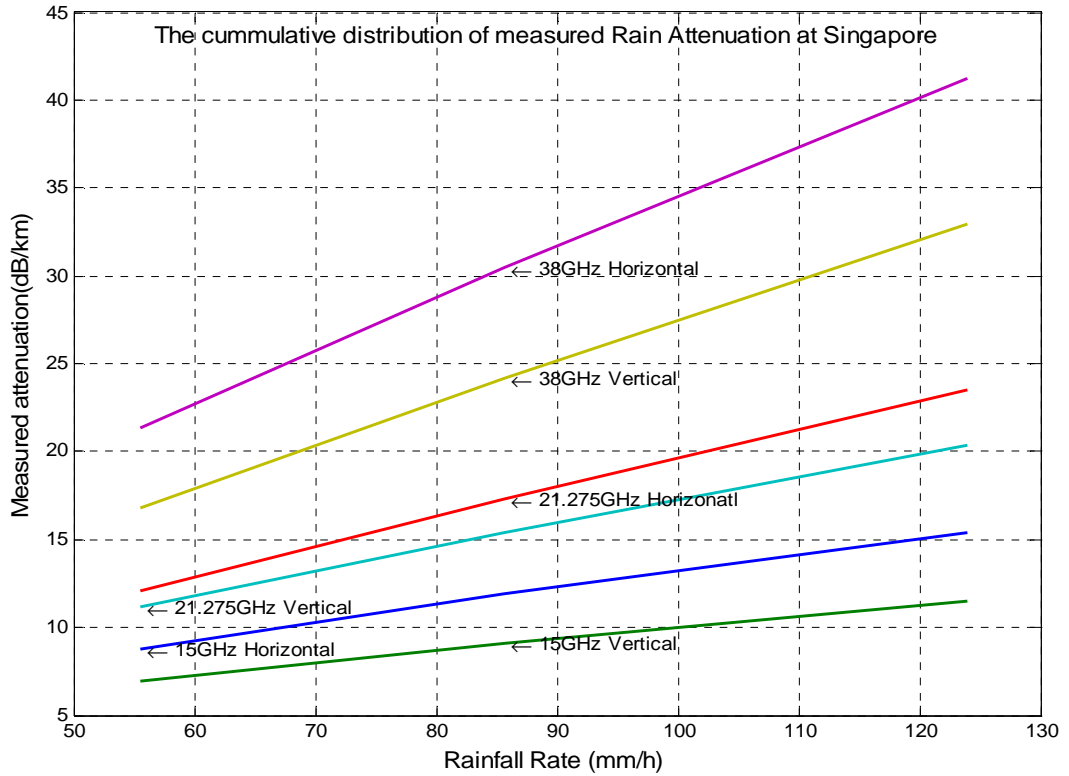
Figure 3.20: The measured rain attenuation in Singapore, used for a short path 1.1 (Km) microwave link.
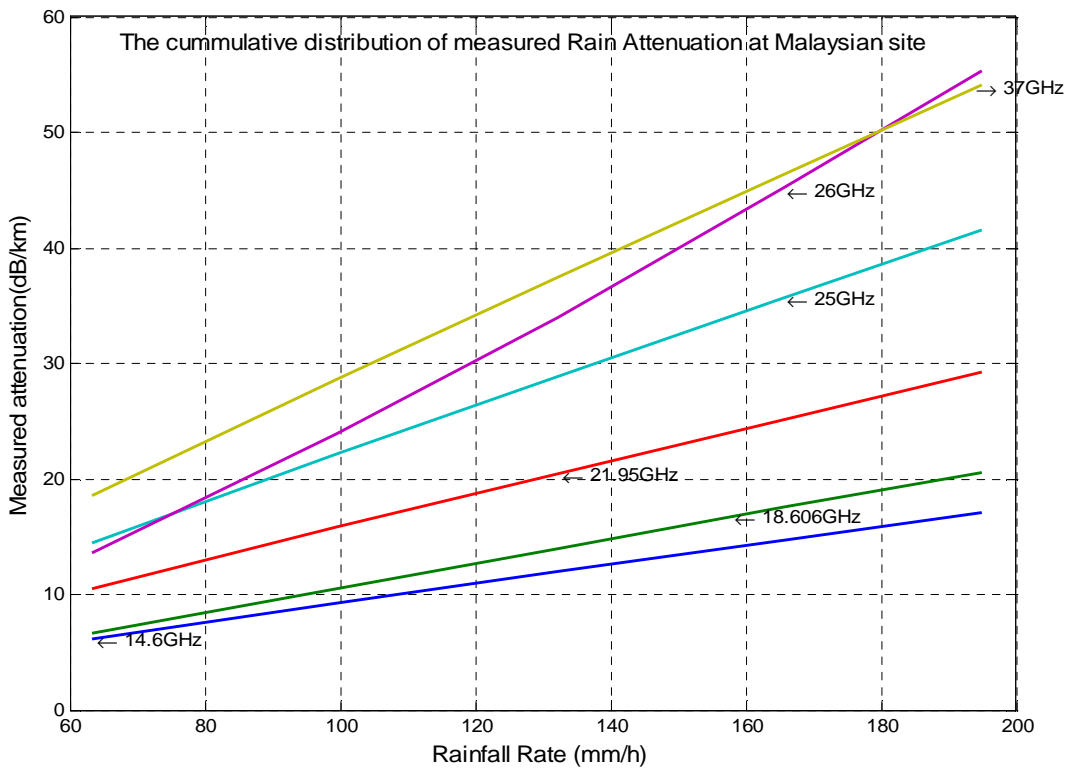
**Figure 3.21: The measured rain attenuation at Malaysian site,
for a short path 300meters microwave link with horizontal polarisation.**
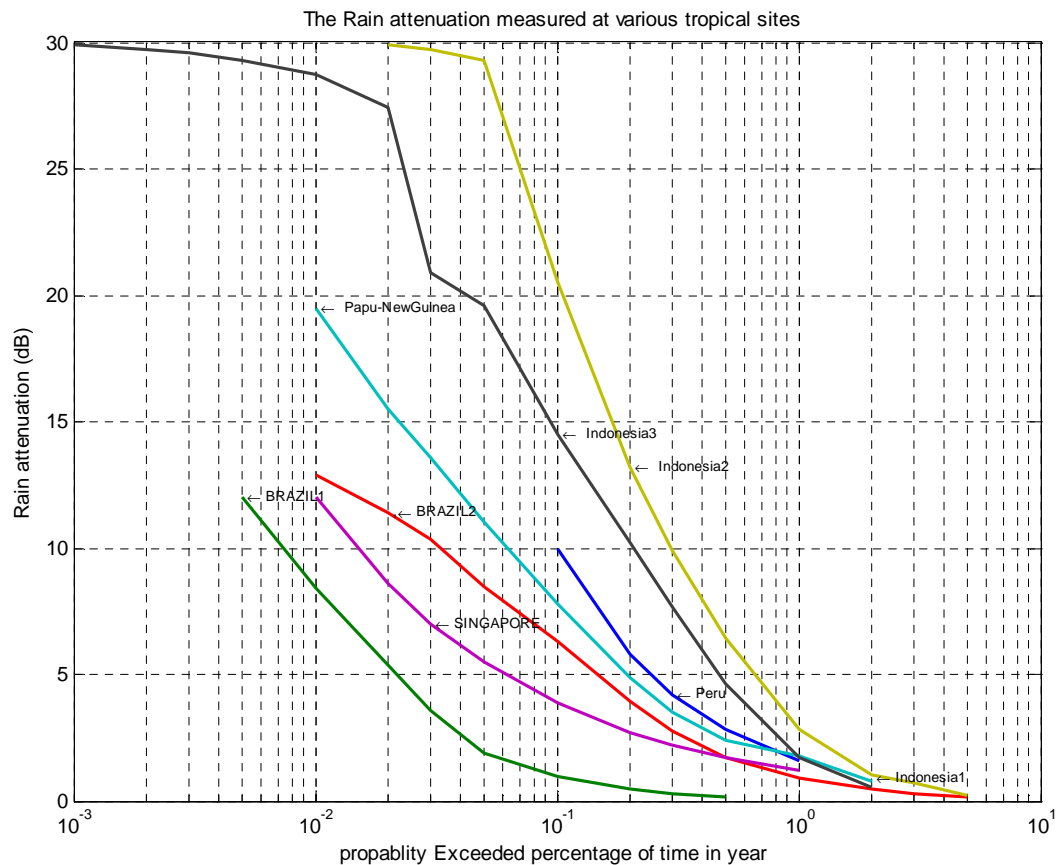
Figure 3.22: The rain attenuation using ITU-R study group three (DBSG3) Ku band data at Various tropical sites using satellite signal.

3.5.3. Moupfouma Rainfall Rate Model

According to Fidele Moupfouma, above a certain threshold of frequency, the excess attenuation due to rain fall becomes one of the most important limits of the performance of line-of-sight (LOS) microwave links [60]. In temperate climates this frequency threshold is about 10 GHz. In tropical climates in general and in equatorial climate particularly, since raindrops are larger than in temperate climates, the incidence of rainfall on radio links becomes important for frequencies as low as about 7 GHz. Estimate of rain attenuation are usually derived from the available information on rain rates observed in the geographical areas considered. Most of the many methods proposed for predicting rain induced attenuation make use of the rainfall cumulative distribution measured at a point. Certain authors have used the concept of equivalent path-averaged rain rate which is obtained by multiplying the point rain rate for the time percentage of interest by a reduction factor, while other authors use an effective path length the value of which is obtained in multiplying the actual path length by a reduction coefficient. This effective path length is

the hypothetical length of a path along which the attenuation for a given time percentage results from a point rainfall rate that occurs for the same time percentage. Rain intensity over this effective path length is assumed to be constant.

He had proposed a prediction method using effective path length and compared with the prediction method adopted earlier by the International Radio Consultative Committee (CCIR) during its XVth Plenary Assembly held in 1982.

The rain induced attenuation on a line of sight (Los) path can be expressed as

$$A(dB) \; = \; kR^{\alpha}L_{eff} \tag{3.38}$$

$$\text{with} \qquad L_{eff} = rl$$

Where l(km) is the actual path length, L_{eff} is the effective path length, and *r* a reduction coefficient having the well-known form.

$$r = \frac{1}{1 + Cl^{m}} \tag{3.39}$$

Where, C and *m* coefficients defined later.

The attenuation A(dB) and the one minute rain rate R(mm/h) are calculated for the same time percentage. k and α are the regression coefficients depending on frequency and polarization and allowing the calculation of the estimate specific attenuations through

$$v_R = k \, R^{\alpha} \tag{3.40}$$

The values of k and *a* used in the present work are those given by Fedi. To derive C and *m*, they used experimental data obtained in 30 terrestrial radio links in the 7-38 GHz band range with path lengths up to 58 km, located in the Congo, Japan, U.S., and Europe, with well-known fitting procedures. He found that C depends on probability level P(percent) of interest for which data are available, and *m* depends on the radio link path length on the one hand, and on its frequency on the other hand. Finally, the resultant formula for the path length reduction factor is given by

$$r = \frac{1}{1 + 0.03\left(\dfrac{P}{0.01}\right)^{-\beta} l^{m}} \tag{3.41}$$

with

$$m(F,l) = 1 + \psi(F) \log_e l \qquad (3.42)$$

and

$$\psi(F) = 1.4 \times 10^{-4} \, F^{1.76}$$

where, F(GHz) is the frequency. The β coefficient is given as result of a best fit by

$l < 50 \, km$

$$\beta = 0.45, \quad for \ 0.001 \leq P(percent) \leq 0.01$$
$$\beta = 0.6, \quad for \ 0.01 \leq P(percent) \leq 0.1$$

$l \geq 50 \, km$

$$\beta = 0.36, \quad for \ 0.001 \leq P(percent) \leq 0.01$$
$$\beta = 0.6, \quad for \ 0.01 \leq P(percent) \leq 0.1$$

The effective path length reflects the spatial in-homogeneity. Its frequency dependence which appeared here in the reduction coefficient **r,** results from both the non uniformity of the rain along the radio link path, and the nonlinear dependence of the specific attenuation rain rate.

3.5.4   Rain Attenuation Prediction Comparisons over Indian sub-continent

In this section, ITU-R model and Moupfouma models as discussed were used to predict the rain attenuation in Indian sub-continent region and compared. Substituting the above-mentioned $R_{0.01}$ and P% and all other required parameters into these prediction models in the uplink (29.75GHz) and downlink (19.75 GHz) direction, the variations of elevation angle vs. rain attenuation are obtained.

The knowledge of the mean rainfall distribution and the climate will provide a broad view on the expected rain attenuation. In order to calculate the rain attenuation prediction from the recommended measurements of local one-minute integration time of rain rate statistics are required.   Here we have presented the attenuation and related results for reference. All results for Indian cities calculated. Figure 3.23 shows a comparison of rain rate as provided in ITU for North and South India and calculated in Moupfouma method for sub tropical region. Figure 3.24 shows the rain rate in group 'A' cities as mentioned in the spot beam model by the Moupfouma method. It is found that the Moupfouma calculation rain rates are also comparable with the rain rate data collected from IMD.
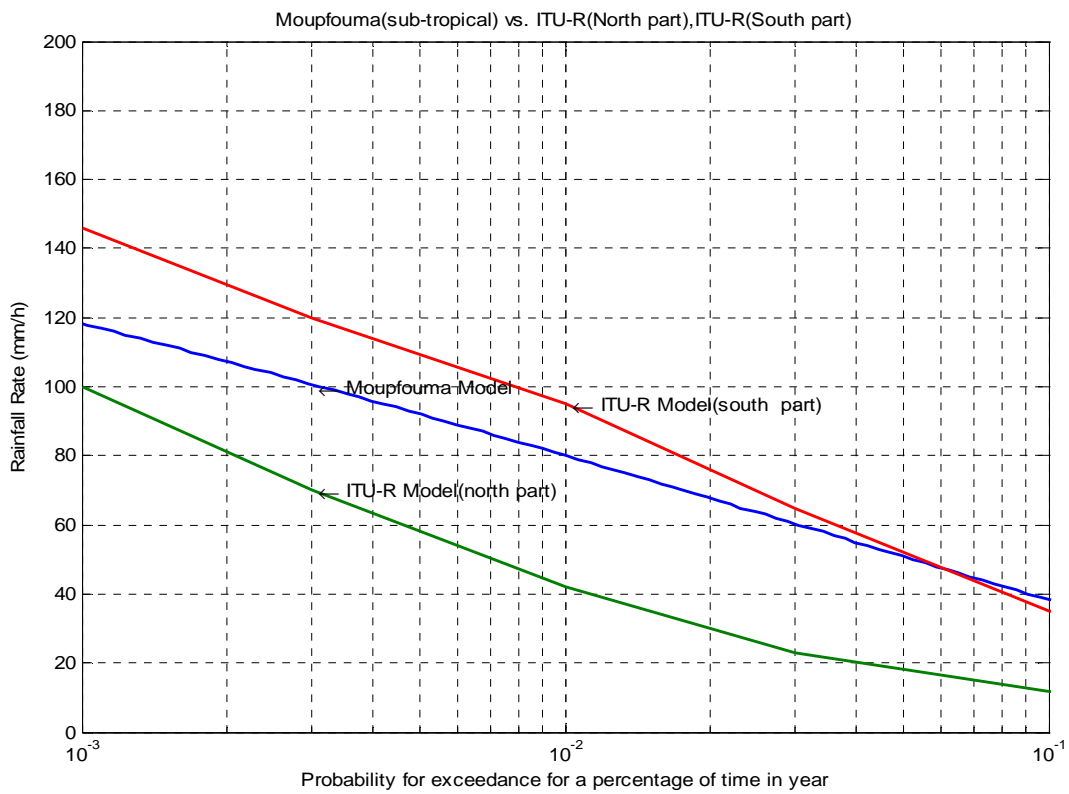
Figure3.23: Comparison of average one year cumulative distributions of rain rate R (mm/hr) in India(Southern and Northern part).
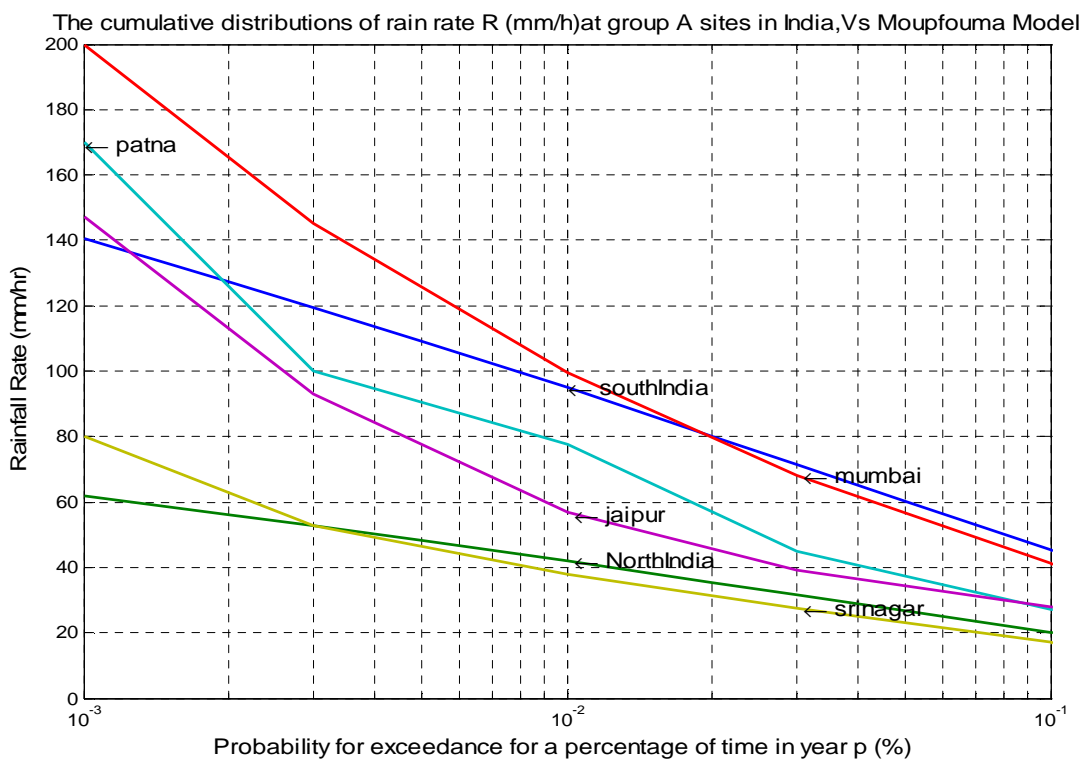
Figure 3.24 : Comparison of average one year cumulative distributions of rain rate R(mm/hr) in group A cities.
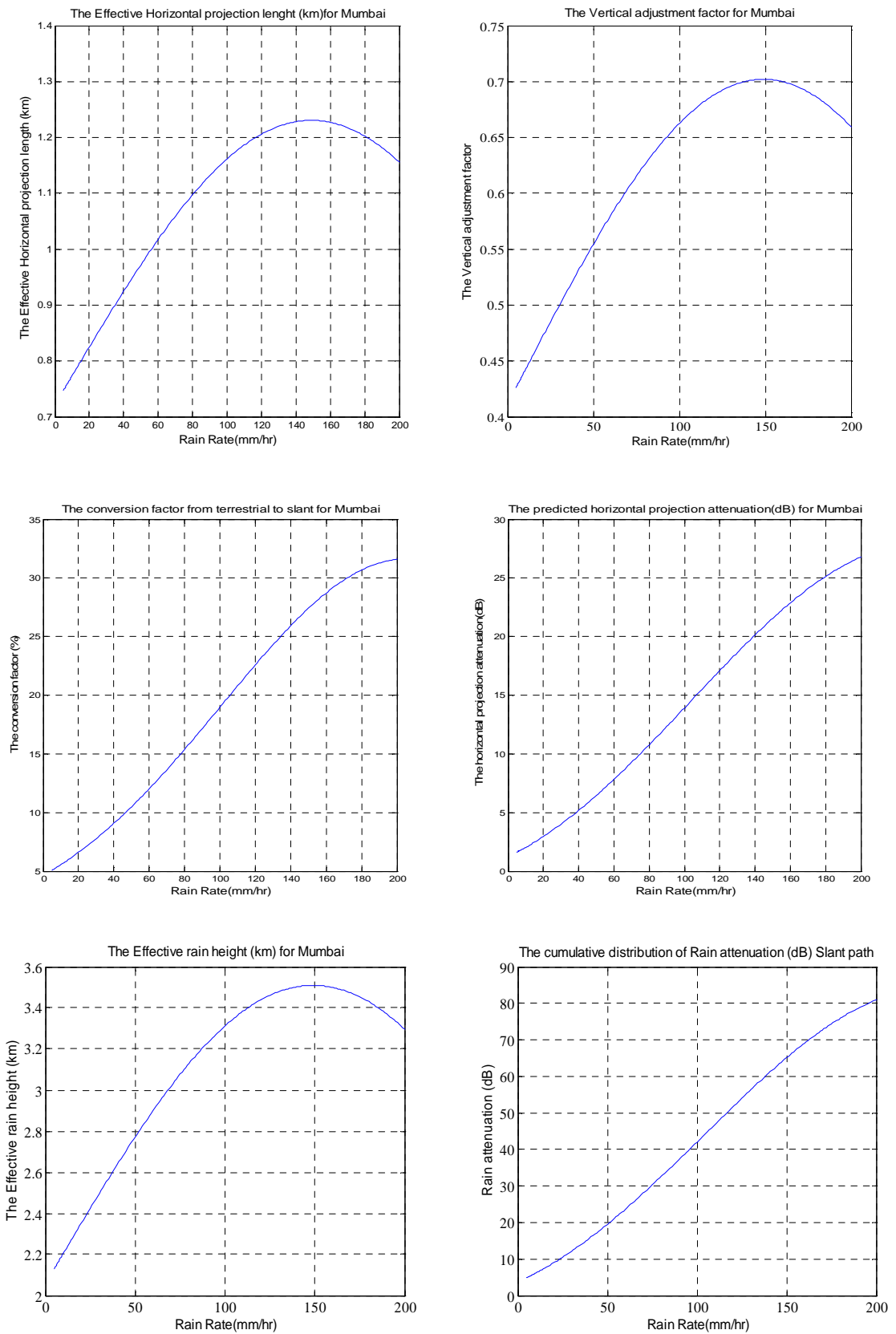
Figure 3.25: Intermediate parameters and attenuation of Moupfouma model for Mumbai as an example.

The figure 3.25 presented Intermediate parameters for a particular city Mumbai. Likewise we have got figures for a all the cities in 16 spot beam location by putting respective location data. The figure 3.26 represents the attenuation for percentage of time rain rate(mm) for group-I cities on basis of Moupfouma model.
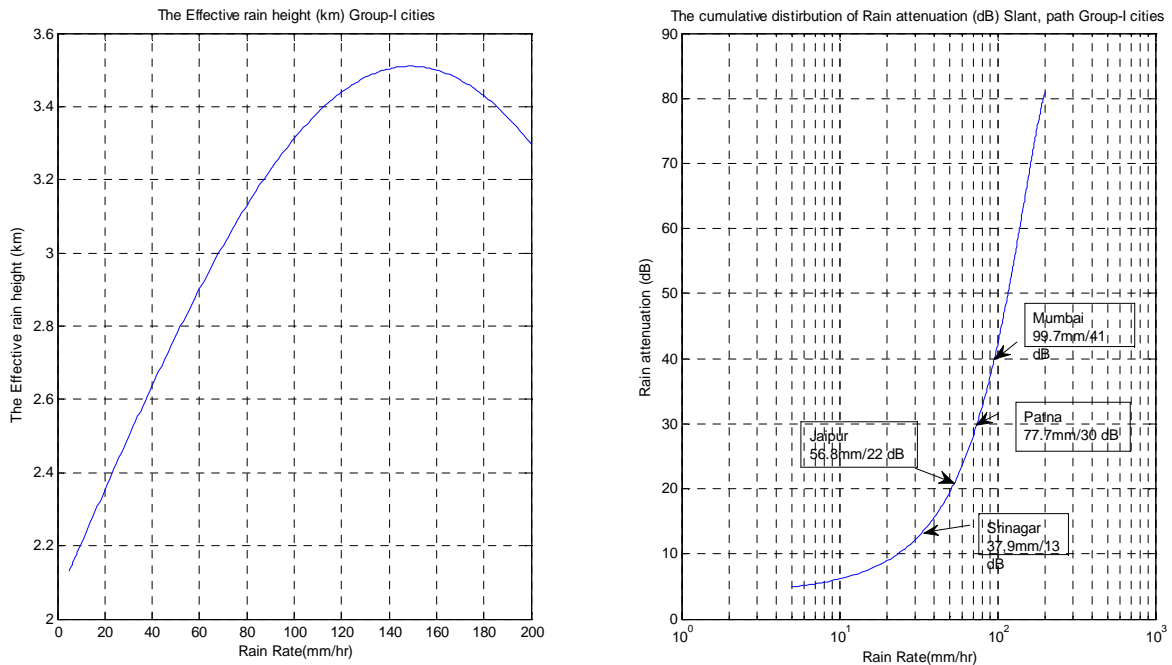
Figure 3.26: The rain attenuation in group 'A' cities by Moupfouma model.

3.6 Summary

In this chapter possible signal fade during rain specifically in Indian cities, at 16 spot-beam locations is focused. This analyses the terrestrial and slant path variation of rain heights and calculates different rain attenuations using mumbai (as a case) geographical and ITU parameters.We can also analyse this for all cities separately. It is found from the result that there is about 10 dB for the duration less than 0.1 (about 8.7 hrs) time and 30-55 dB rain attenuation occurs for less than 0.01% (about 53 minutes) over an average year. So 10 dB can be taken as the standard ateenuation level and it can be varied upto 30 dB statistically taking different attenuation level and demand of users in 16 spot-beams. The Moupfouma model calculation and ITU model attenuation are having close approximation with ITU model but, the Crane model shows a large variation.

Fade compensation and power control

4.1 Introduction

Satellite communication systems operating above 10 GHz undergo weather dependent path attenuation, primarily due to rain. This is severe for a significant period of time mainly in tropical regions. So systems can be designed to operate at an acceptable performance level by providing adequate power margins on the uplink and the downlink segments. This can be accomplished directly by increasing antenna size, the RF transmitting power, or both. Typically, power margins of 5 to 10 dB at C-band and 10 to 15 dB at Ku-band can easily be achieved with reasonable sized antennas and with RF power within acceptable limits [7]. RF power levels are most likely to be constrained by prime power limitations on the satellite, and by radiated power limitations on the ground fixed by international agreement. Here the path attenuation exceeds the available power margin that is 20-35 dB in the Ka- bands for many regions of India and earth. Additional methods must be considered to overcome the severe attenuation conditions and restore acceptable performance on the links.

Fixed line-of-site satellite restoration techniques can be divided into two types or classes. The first type, power restoration, does not alter the basic signal format in the process of restoring the link. The second type, signal modification restoral, is implemented by modifying the basic characteristics of the signal. Signal characteristics include carrier frequency, bandwidth, data rate, and coding scheme.

Compensation for rain fades in a satellite communications network is obtained by uplink power control mechanism incorporated in a master station or network operation Centre (NOC), which maintains a constant output power level of the satellite transponder without incorporating excessive static margins into the link power budget. A variable attenuator, which controls the output power of the master station's high power amplifier, is initially set at a prescribed level which will produce the EIRP for a "clear sky" condition [27]. The NOC monitors the output of the satellite amplifier and derives a measure of the SNR of down linked signals. Knowing the variable attenuator setting and the SNR of the downlink signal, the magnitude of attenuation of uplink signal to the satellite is

determined. In the event of a rain fade, the setting of the variable attenuator is adjusted by an amount that compensates for the fade and thereby causes downlink carrier frequency signal conveyed by the satellite amplifier device to remain effectively constant. An estimation of the error in the attenuator setting is preferably derived.

This chapter discussions hereby made on different methods of power control and fade mitigation techniques. This suggests the idea of power flow and enhancement to different spot beams in the proposed model by algorithm. It discusses the data rate adaptation to increase the service availability.

4.2. Power distribution and data flow to spot beam

The spot beams will be attended by the steerable antenna [43] to deliver the data taking accounts from the on board processor (OBP) in a TDM process. Here the power is estimated in every step on the basis of channel condition and the number of users accessing under the corresponding spot beam. We can regulate the power of antenna feeds, preferring revenue generating stations to get higher level of service (four metro cities). The data rate for individual channels can be decided statistically and keeping total outcome capacity of the system and spot beams constant. At any instant of time four distributed spot beams are focussed to deliver the data through four main lobes of the array antenna [4]. In the next time slot another four spot beams will be focussed and the process will go on rotation among four groups.

4.2.1 Concept of Data Flow to Spot-beams

We assume that each delivery session is identified by a unique data flow, and packets of several spots are queued at the NOC (fig. 4.1), which forwards them to the satellite at a rate limited by the uplink capacity of the system. An on-board processor switch forward the packets to one or multiple spot beam queues, duplicating the packets in the later case. A packet (may be regional) belonging to a single spot-beam queue, is forwarded to corresponding spot-beam location. In case of a multi-flow, i.e., the packets for multiple spot-beams are need to be duplicated and forwarded to multiple spot-beam queues at the satellite on-board. At every spot-beam queue, several flows share the total service rate of the queue. The rate-share of a flow that belongs to a particular queue depends on several factors, such as the number of flows currently active in that queue, the

type of the flows, and the rate allocation policy between different type of flows, i.e. audio, video, data etc. We call this rate-share as the supportable session rate of the flow at that particular queue [19].
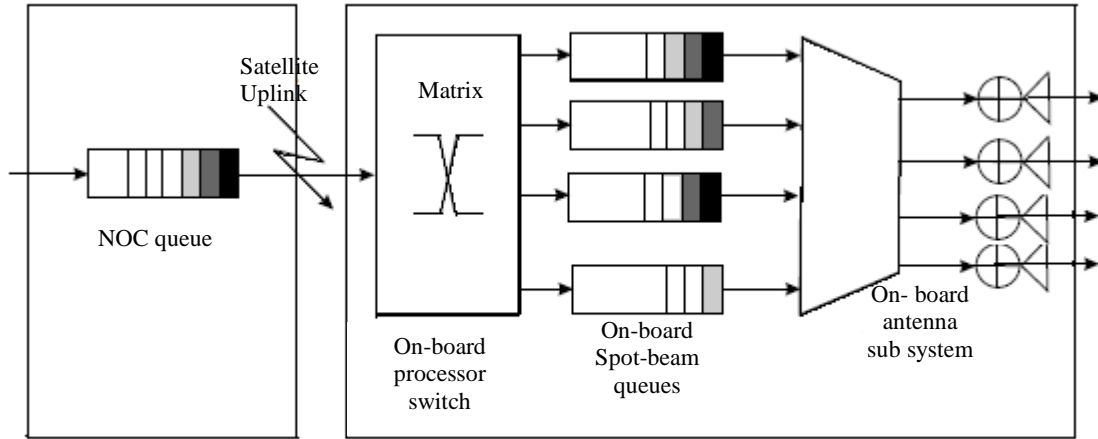
Figure 4.1: Concept of on-board satellite and spot beam queue.

In order to avoid over-flowing of any of the on-board queues, the input rate of a flow at the NOC queue have to be determined by the minimum rate the flow can be served at the spot-beam queues. We may refer to this rate as the maximum sustainable session rate of the flow. The service rate of each spot-beam queue varies as a function of the allocated power and the channel state, for a given modulation scheme and BER target. Therefore, not all queues can be served at the same effective rate.

Here the satellite spot beams are divided into four groups and radiate at four time slots. All antenna beams can be represented with an array. The four antennas are to attend all spot beams in 4 slots as in the following equations. So in the satellite, 4 steerable beams, total of 16 beams in TDM, multiplexed, interlinked through the on board processor.

$$\text{Antenna arrays} = \begin{bmatrix} A_1 & A_2 & A_3 & A_4 \\ B_1 & B_2 & B_3 & B_4 \\ C_1 & C_2 & C_3 & C_4 \\ D_1 & D_2 & D_3 & D_4 \end{bmatrix} \qquad (4.1)$$

$$\text{TIME SLOT 1} = \begin{bmatrix} A_1 & - & - & - \\ - & B_2 & - & - \\ - & - & C_3 & - \\ - & - & - & D_4 \end{bmatrix} \qquad (4.2)$$

$$\text{TIME SLOT 2} = \begin{bmatrix} - & A_2 & - & - \\ - & - & B_3 & - \\ - & - & & C_4 \\ D_1 & - & - & - \end{bmatrix} \tag{4.3}$$

$$\text{TIME SLOT 3} = \begin{bmatrix} - & - & A_3 & - \\ - & - & - & B_4 \\ C_1 & - & - & - \\ - & D_2 & - & - \end{bmatrix} \tag{4.4}$$

$$\text{TIME SLOT 4} = \begin{bmatrix} - & - & - & A_4 \\ B_1 & - & - & - \\ - & C_2 & - & - \\ - & - & D_3 & - \end{bmatrix} \tag{4.5}$$

At any moment the sum of power is constant

$$
\begin{aligned}
P_{TOT} &= A_1 + B_2 + C_3 + D_4 \\
P_{TOT} &= A_2 + B_3 + C_4 + D_1 \\
P_{TOT} &= A_3 + B_4 + C_1 + D_2 \\
P_{TOT} &= A_4 + B_1 + C_2 + D_3
\end{aligned} \tag{4.6}
$$

4.3   Operation and Power control of satellite systems

A satellite communication network operates with an uplink earth station from which uplink signals destined for a satellite are transmitted over an uplink communication channel. In the satellite, amplifier device (HPA), amplifies the signal and conveyed over a downlink channel to the ground station.

Controlling is carried out in the uplink station transmitter at carrier frequency, so as to cause the strength of the same conveyed from the output of satellite amplifier on board, to be effectively constant even in presence of rain fade between uplink earth station and satellite. The possible steps are

(i)   Setting the operation of uplink transmitter such that the strength of uplink signal conveyed from transponder amplifier device is at predefined signal strength.

(ii)   Monitoring, in the receiver provided at uplink earth station, uplink carrier frequency signals down linked from satellite to uplink earth station and deriving therefrom a measure of the signal-to-noise ratio (SNR) of the down linked signals.

(iii)   Determining a measure of attenuation of uplink signal transmitted from uplink station to the satellite in accordance with the measurement of the SNR derived.

(iv)   Compensate the strength of uplink signal transmitted by uplink transmitter by an amount that compensates for the measure of attenuation determined to effect uplink signal conveyed by satellite transponder to remain effectively constant.

So, the strength of uplink signals received at receiving ground station and, in response to the strength of monitored signals undergoing a reduction from the clear sky condition, an adjustment of power is provided to increase the strength of return link signals transmitted from satellite. The details are explained in the following sections.

4.3.1   Power control procedures

Power control refers to the process of varying transmitting power on a satellite link in the presence of path attenuation to maintain a desired power level at the receiver. Power control technique attempts to restore the link by increasing the transmit power during a rain fade event and then reducing power after the event back to its non-fade value during clear sky condition. The objective of power control is to vary the transmitted power in direct proportion to the attenuation on the link, so that the received power stays constant through severe fades. Power control can be employed on either the uplink or downlink, or both [53][46].

The maximum path attenuation that can be compensated by active power control is equal to the difference between the maximum output of the ground station or satellite power amplifier and the output required under non-fade conditions. The effect of power control on availability, assuming that control is perfect, is the same as having this power margin at all times. A perfect power control system varies the power exactly in proportion to the rain attenuation. Errors in power control result in added outages, effectively decreasing this margin [7].

The adaptive Power Control for Fade mitigation takes advantage of unused in-excess resource of the system [4]. Techniques sharing unused resource aim to compensate fading occurring on a given link in order to maintain or to improve the link

performance (required C/No). The following types of Power Control FMT can be considered:

1. Up-Link Power Control (ULPC),
2. Down-Link Power Control (DLPC)
3. On-Board Beam Shaping (OBBS).
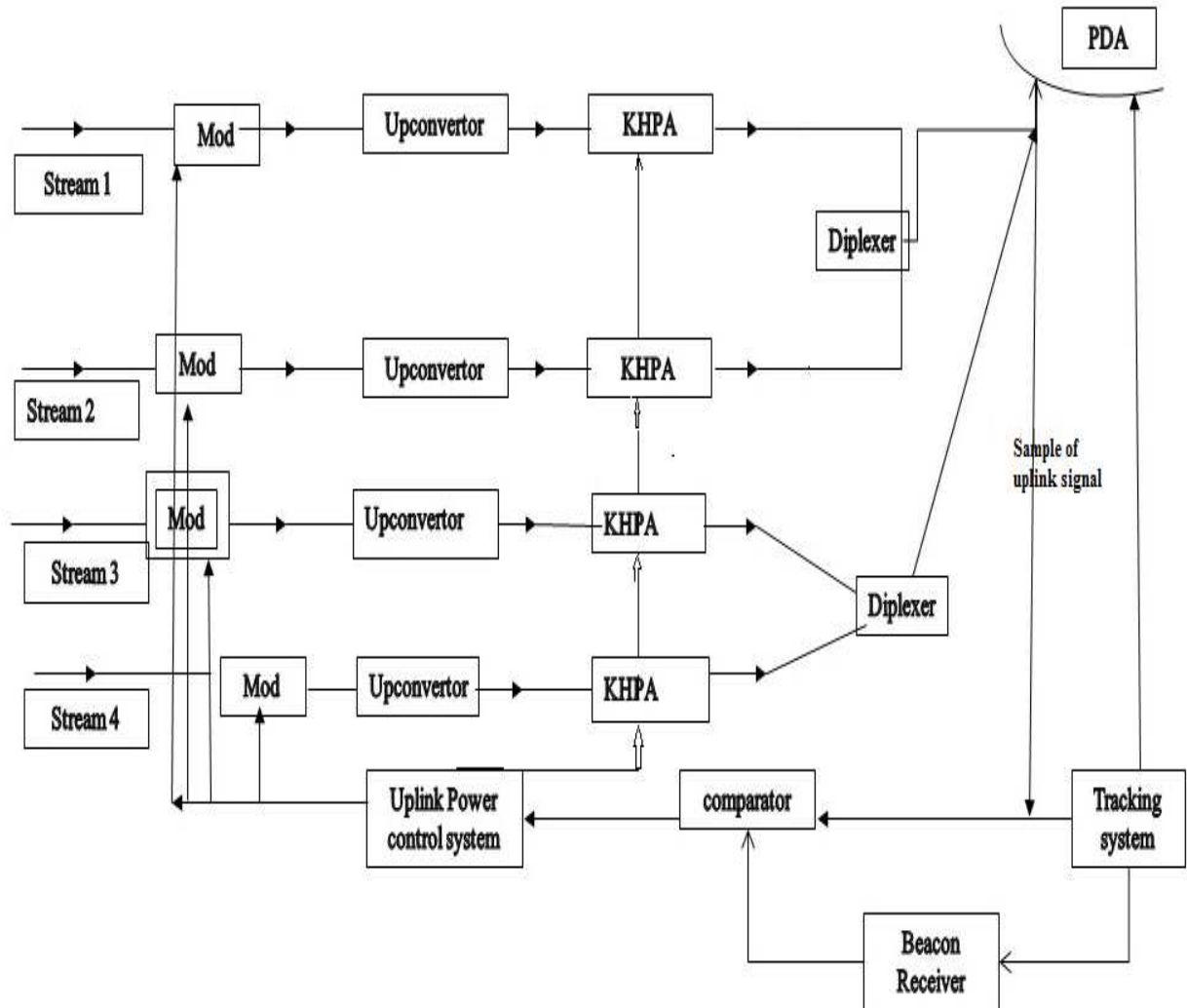
Figure 4.2 Block diagram of uplink power control system

The features of the block diagram for power adjustments are based on either a satellite beacon signal or a pilot carrier transmitted from the earth station. The transmit power adjustment levels compensate for differences between the beacon/return pilot carrier and the uplink carrier. Integrated carrier monitor verifies and refines the power adjustments for 'loopback' carriers i.e., the downlink carriers that are visible at the uplink earth station.

Open loop power control

In an open loop power control system, the transmit power level is adjusted by operation on a RF pilot control signal that itself undergoes path attenuation, and is used to overcome the attenuation experienced on the uplink. The radio frequency control signal can be one of the following:

  i.   the downlink signal

 ii.   a beacon signal at or near the uplink frequency

iii.   a ground based radiometer or radar.

```
┌─────────────────────────────┐
│     Receive the reference    │
│           signals            │
└─────────────────────────────┘
              ⇓
┌─────────────────────────────┐
│   Compared to pre-determined │
│           reference          │
└─────────────────────────────┘
              ⇓
┌─────────────────────────────────┐
│      Develop an error signal     │
└─────────────────────────────────┘
              ⇓
┌───────────────────────────────────────────────┐
│ Adjust feed link power to compensate for attenuation │
└───────────────────────────────────────────────┘
```
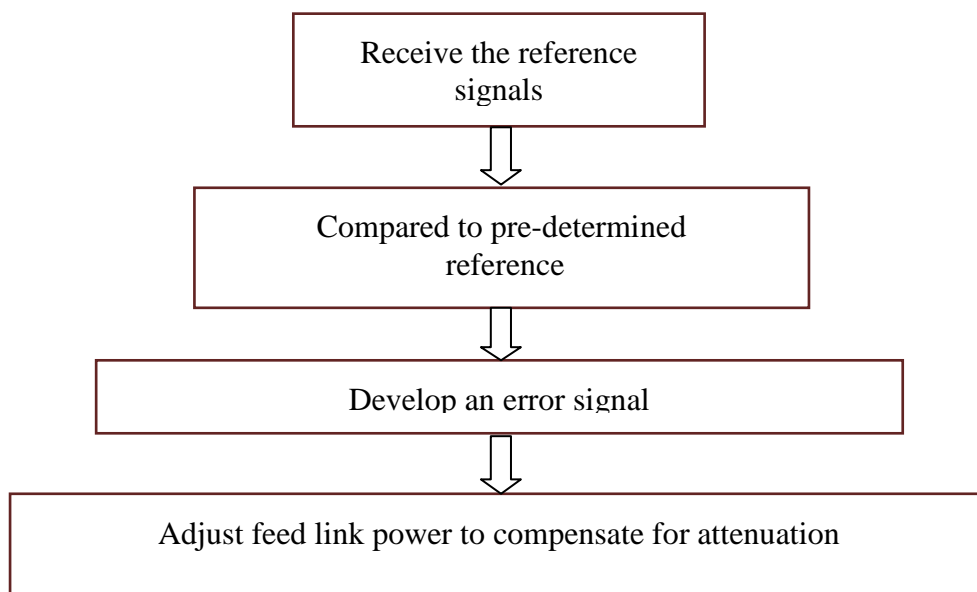
Figure 4.3: Flow chart of open loop power control.

In the downlink control signal system, the downlink signal level is continuously monitored and used to develop the controlling error signal for the high power transmitter. The control signal level is determined in the processor from rain attenuation prediction models, which compute the expected uplink attenuation at 30 GHz from the measured downlink attenuation at 20 GHz. The downlink control signal method is the most prevalent type of uplink power control, because of the availability of the downlink at the ground station and the relative ease of implementation [53][40].

In the beacon control signal system, a satellite beacon signal, preferably in the same frequency band as the uplink, is used to monitor the rain attenuation in the link [13]. The detected beacon signal level is then used to develop the control signal. Since the measured signal attenuation is at (or very close to) the frequency to be controlled, no

estimation is required in the processor. This method provides the most precise power control of the three techniques.

Close loop power control

A satellite communication system includes at least one satellite communication signal repeater, at least one ground station for transmitting a feeder link comprised of more than one signals to the satellite signal repeater. A number of user terminals each receiving

Typical flow chart

```
        ┌─────────────────────────┐
        │   Measure the quality of │
        │      reference signal    │
        └─────────────────────────┘
                    ⇩
        ┌─────────────────────────┐
        │   Transmit the above signal to │
        │        up-link station   │
        └─────────────────────────┘
                    ⇩
        ┌─────────────────────────┐
        │ Compare the above measured signal │◄──┐
        │   quality with target quality │      │
        └─────────────────────────┘          │
                    ⇩                          │
            ◇ Is available satellite ◇ ──No──┘
            ◇  capacity sufficient?  ◇
                    ⇩ Yes
        ┌─────────────────────────┐
        │ Adjust the NOC transmit power to compensate for │
        │ predicted variation in satellite gain but maintain │
        │ flux density above minimum threshold │
        └─────────────────────────┘
```
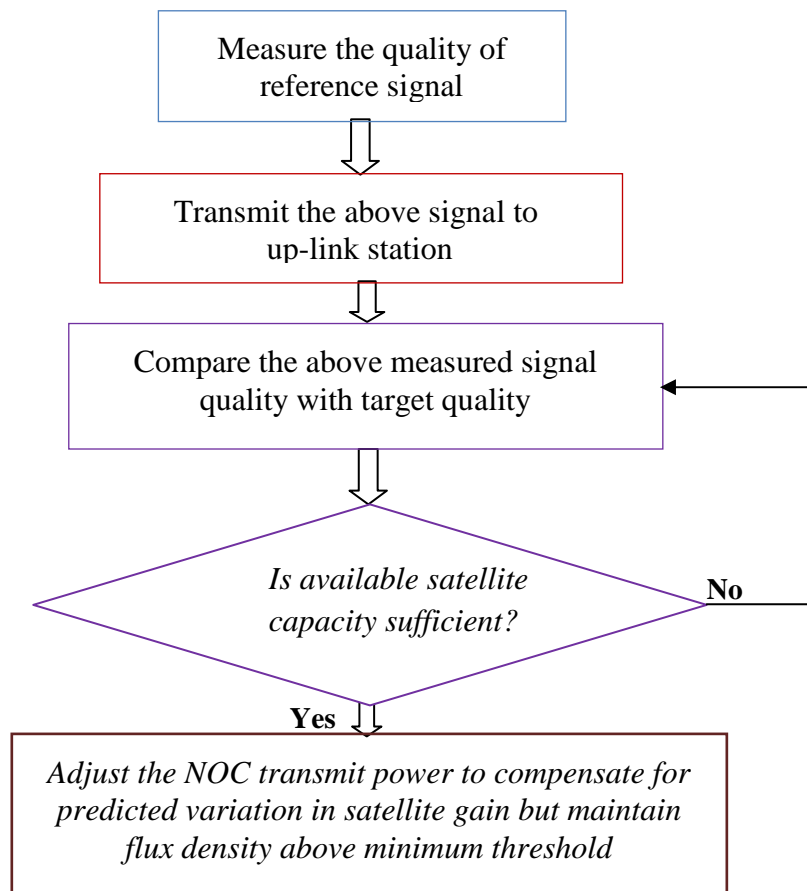
Figure 4.4: Flow chart of close loop power control for uplink.

one of the communication signals over a user link from the satellite transponder. The method includes steps of measuring the quality of at least one reference signal received by the user terminal, via the satellite transponder. Comparing the measured quality with a predetermined reference signal, the transmit power of the ground station is adjusted so that a flux density of the beam is substantially constant at the user terminal independent of the location of the user terminal of the beam.

On-Board Beam Shaping (OBBS)

OBBS technique is based on active antennas, which allows spot beam gains to be adapted to propagation conditions [7]. Actually, the objective is to radiate extra-power, and to compensate rain attenuation only on spot beams where rain is likely to occur. In case the signal is to focus on a small area with a large spectral density and high date rate as given in figure 2.5 required OBBS is used.

4.4 Algorithm for power distribution

The power distribution method is considered on the basis of following algorithm. Previously it has been defined that the variation in power is depends on two parameters

1. Channel condition
2. Number of users.

The steps are follows:

(i)   For a clear-sky condition, adjust the attenuator to a first setting at minimum power (P_{min}.) which causes uplink signals to be conveyed from the output of the transponder at prescribed clear-sky signal strength.

(ii)   By deriving a measure of the signal-to-noise ratio of down linked signals in accordance with the ratio of the square of the sum of signal plus noise to the square of the noise in down linked signals and the downlink power measure can be estimated by the ratio

$$C/N \ = \ ((S+N)^2 - (N)^2) \ / \ (N)^2 \tag{4.7}$$

The   expression for the output power EIRP of the satellite may be given by:

$$EIRP = EIRP_{NOC} - L_{fs,up} - F_{up} + G_{sat} - L_{upc} \qquad [dB] \tag{4.8}$$

Where,

$EIRP_{NOC,}$ is the NOC or uplink earth station   power out for satellite,

$L_{fs,up}$ is uplink free space loss,

F_{up} is uplink rain fade attenuation, G_{sat} is the satellite gain and

L_{upc} is the attenuation to be imparted by the uplink power correction mechanism using attenuator. On the downlink side, the received signal-to-noise ratio C/N may be expressed by:

$$C/N = EIRP_{sat} - L_{fs,dn} - F_{dn} + (G/T)_{NOC} - B_k \qquad [dB] \qquad (4.9)$$

Where,

$EIRP_{sat}$ corresponds to the desired satellite output power,

L_{fs},dn corresponds to the downlink free space loss,

F_{dn} is the downlink rain fade,

$(G/T)_{NOC}$ is the gain/temperature figure of merit of the NOC antenna

and B_k is Boltzmann's constant for thermal noise.

(iii) Determine the measure of attenuation of uplink carrier frequency signals transmitted from uplink earth station to satellite in accordance with the current setting of attenuator and first setting of the attenuator.

(iv) Adjust the attenuator in accordance with the corrected measure of SNR and the first setting of the attenuator.

4.4.1 Power Distribution Strategy

Power can be distributed among the spot beams in two ways. One is static power allocation and other is dynamic power allocation. Static power allocation implies that the input power to the beams is the same at any time of the satellite network operation, and clearly applies to clear sky and long-term precipitation models of the satellite links. All the users are receiving signal with adequate power, under clear sky conditions

The level of attenuation and corresponding compensation on the basis of two driving parameters as follows

1. Channel condition (As seen in chapter 3).
2. Number of users in the spot beam area (demand).

Equal antenna share (EAS):

$$P_{A_k} = P_{B_k} = P_{C_k} = P_{D_k} = P_{Tot}/4. \qquad for\ k = 1, 2, 3, 4. \qquad (4.10)$$

The total power of HPA is directed to four beams and all antenna beams are to radiate with equal power.

Balance Antenna share (BAS):

The antennas are to radiate with different powers maintaining a minimum threshold of P_{min}.

$$P_{TOT} - 4P_{Min} = P_s \qquad (4.11)$$

Where,

P_{TOT} is the total HPA power capacity to deliver to four antennas.

P_s is the extra power which can be shared unequally among all or some of the beams.

Assumptions for static power allocation:

i)   Number of users is fixed.

ii)   Channel condition is absolute.

Let, ζ =loss in dB

Channel condition in absolute and rainfade	Loss (ζ)	Fuzzy channel condition
0 dB = ζ_1	$\zeta_2 < \zeta < \zeta_1$	Excellent
-5 dB= ζ_2	$\zeta_3 < \zeta < \zeta_2$	Very good
-10 dB= ζ_3	$\zeta_4 < \zeta < \zeta_3$	Average
-15 dB= ζ_4	$\zeta_5 < \zeta < \zeta_4$	Good
-20 dB= ζ_5	$\zeta_5 < \zeta < \zeta_6$	Bad
-25 dB= ζ_6	$\zeta_6 < \zeta < \zeta_5$	Worst

Table 4.1: Fuzzy classification of channel condition due to fading
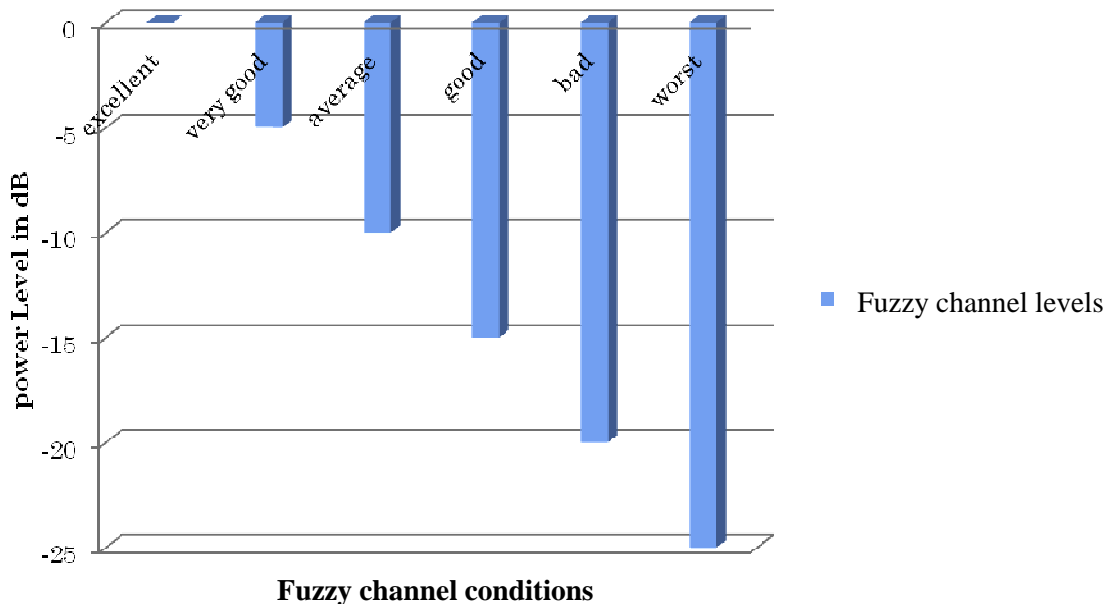

Figure 4.5: Power degradation levels due to impairment/fading.

Let P_{total} is the total capacity of the satellite to distribute power among four antenna beams and P_{min} is the minimum threshold power must be provided to each and every beam to get a desired flux density at the receiver terminal without any power

compensation during the clear sky condition. After this the extra power from the source will fulfil the requirement to compensate fading. Considering the maximum power capacity at the output of power amplifiers is 100 watts, this distributes to four antennas as follows.

Each sector or the spot beam antenna has an ideal acceptance power = 25 watts, From net power of four sectors (P_{tot}) = 25x4 =100 watts. Let P_{min} is 18 watts for this case. So during fading the power to an antenna beam is 18 W< P ≤ 25W.

The polling mechanism between the antennas and power supply loop will serve in a time division multiplexing (TDM) process. The polling procedure will look after the channel condition statistically in every 100ms and command the power reforms system to process the power level.

4.4.2 Compensation by static power allocation

The processor is to check the Channel condition in a sequence as following,

Sequence	
Set1:	A1,B2,C3,D4
Set2:	A2,B3,C4,D1
Set 3:	A3,B4,C1,D2
Set4:	A4,B1,C2,D3
Set1:	A1,B2,C3,D4
And so on….	

Let's define the absolute power to provide the corresponding rain fading logic.

0% power of P_s = p

8% power of P_s = q

16% power of P_s = r

24% power of P_s = s

32% power of P_s = t

40% power of P_s = u

So, **Ps = [0, 0.05Ps, 0.09Ps, 0.16Ps, 0.30Ps, 0.40Ps]** referenced to

[p   q   r   s   t   u] respectively.

The extra power can be statistically distributed among all the 4 antennas with 6 different power levels in 360 different combinations. The statistical distribution will depends on following and using a look up table.

There are three possible combinations of conditions as follows.

1. Number of users fixed

   Channel condition is variable

2. Channel condition is fixed

   Number of users is variable

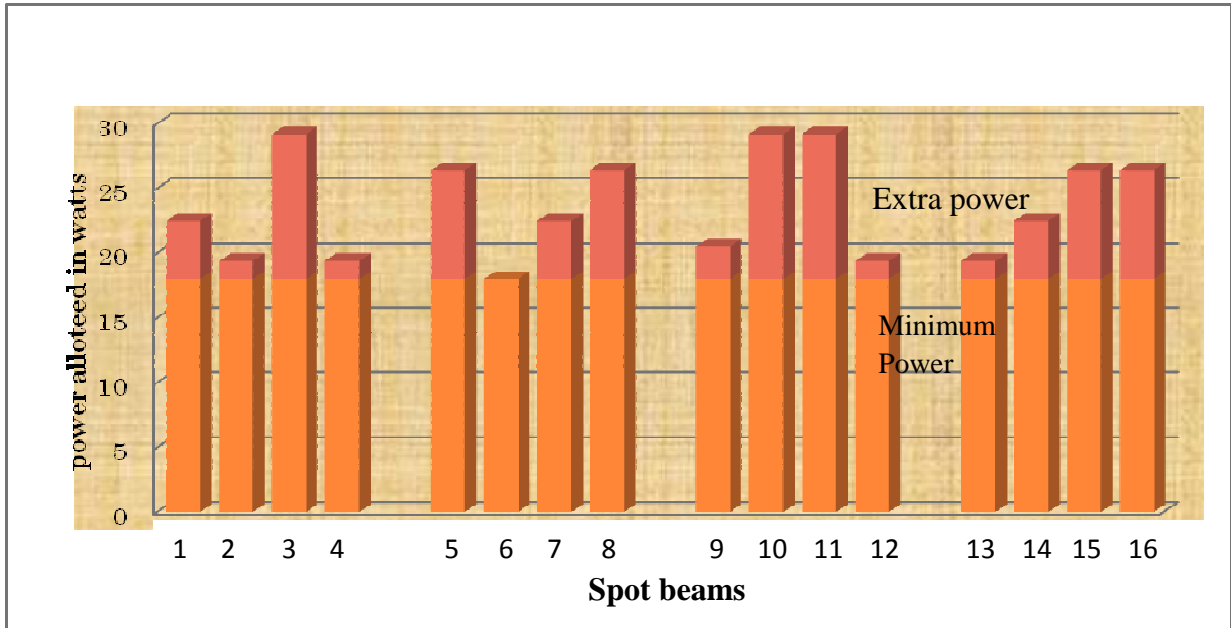3. Both Channel condition and number of users are variable

Figure 4.6: Static power allocation to spot beams.

Example of static power distribution

Let the total power of the satellite reserved for the four antennas to be delivered for 16 spot beams in TDM is 100 watt. And the minimum threshold power for each antenna in best channel condition is 18 watt.

So, $P_{total} = 100$ W

$P_{min} = 18$ W

And extra power Ps = P_{total} - $4P_{min}$ = 100-72= 28W

Finding the compensation levels

P = 0% of Ps = 0 W

q = 5% of Ps= 0.05*28= 1.4 W

r = 9% of Ps = 0.09*28=2.52 W

s = 16% of Ps= 0.16*28=4.48W

t = 30% of Ps=0.30*28=8.4 W

u = 40% of Ps=0.40 *28=11.20 W

Check slot 1 of antenna and 1st group of antenna beams.

Let A1 = q; B2 = p;   C3= u ;   D4= s   are the channel condition feedback.

So,   A1 will compensate with 1.4 watt, and will take 1.4+18= 19.40 watts.

C3 will compensate with 0 watt and will take 18 watts.

C3 will compensate with 11.20 watt and will take 11.20 + 18 =29.20 watt

D4 will compensate with 4.48 watt and will take 4.48 + 18 =22.48 watt

So, the minimum level of power is 18 watt and the maximum compensated power level of beam is 29.20 watt and there is a considerable increase in power level in C3 spot beam during fading.
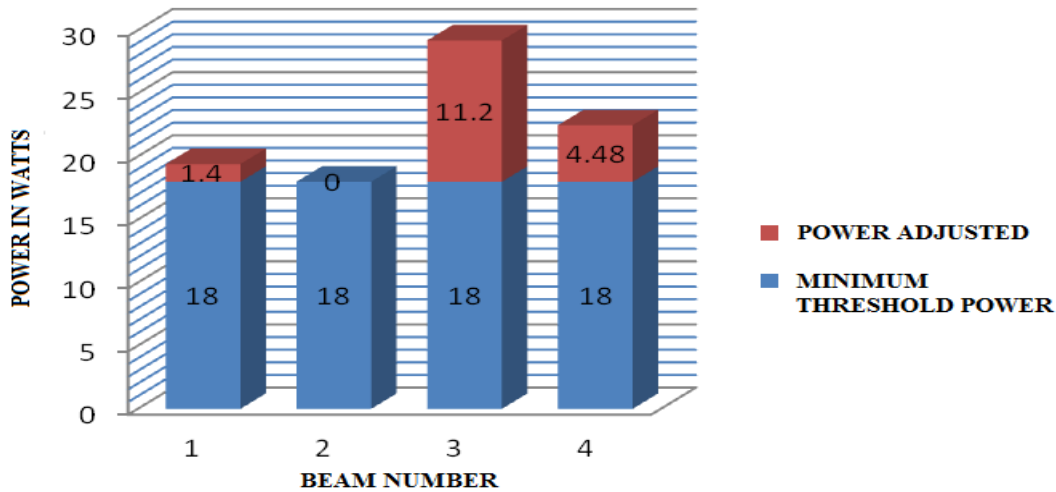

Figure 4.7: Static Power allocation to spot beams of one group based on example above.

4.4.3 Dynamic power allocation to 16 spot beams system

Simulation results of the proposed dynamic power allocation algorithm are presented here. Here we are presenting some results for hypothetical satellite network with multi-beam antenna having 16 beams. For simulation purpose the rainfall data from ITU-R rain model has been taken. The corresponding power threshold for every satellite terminal is set to -110 dBm. Three situations are assumed namely as allocation for clear sky condition, static and dynamic power allocation for rainy situation. For simulation purpose some beams are chosen rainy and other beams are chosen as non-rainy. In this simulation beam no. 1, 3, 5, 6, 7, 9, 13, and 15 are assumed as rainy beams i.e, beams undergoing attenuation due to rain. We can see here that dynamic power allocation is obviously different than static power allocation due to the fact that power is adapted to the current satellite channel conditions and rain attenuation predictions. Some beams have equal power distribution as for clear sky case, as it is expected for non-rainy beams. The basic

concept of the algorithm is that since rain attenuation changes significantly over time and space, the available satellite power must be distributed dynamically based on the rain attenuation instant value of each link [1].
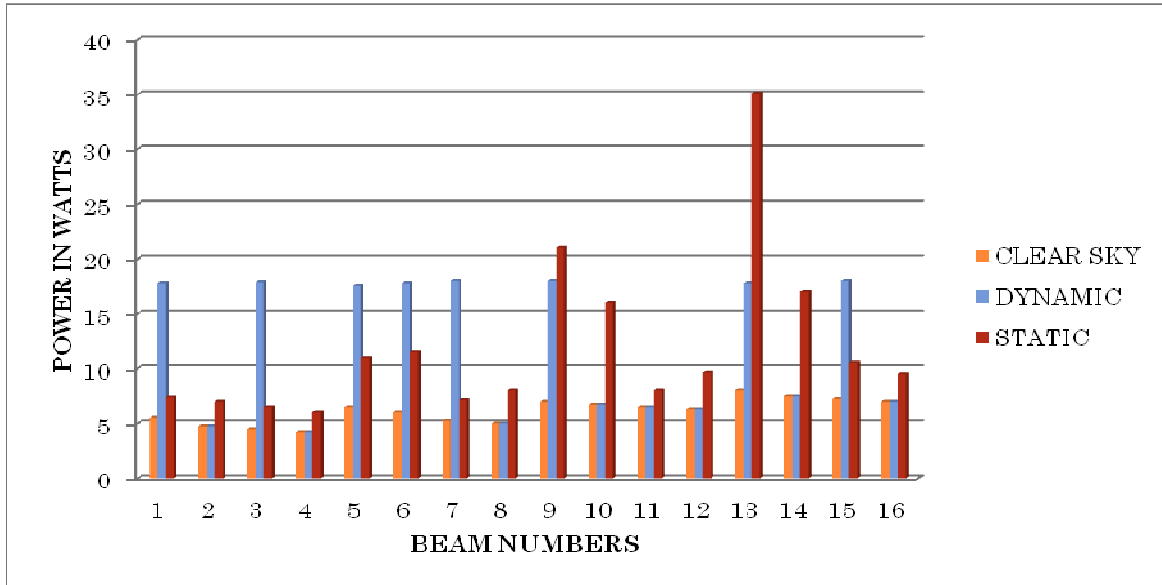

Figure 4.8: Typical clear sky, static and dynamic power allocation during rain fading

However, as real time reconfiguration is practically impossible, the objective is to allocate dynamically the power at specific time instants multi-beam antenna reconfiguration times and remain constant between two reconfiguration time instants [1]. More specifically, the rain attenuation at the next slot of beam reconfiguration is predicted for each link using either information from receiving ground terminals or meteorological data. This leads to significant reduction of the number of non served users of the system, especially when some of the region covered by the satellite suffers from heavy rain attenuation phenomena.

4.5 Summary

In this chapter we have introduced an outline for balancing the spot beam power level and data rate such that the sum of all power constant. User can get at least a minimum level of service during worst weather condition. The distribution of available system power among spot beams taking into account the load on the queues is the main factor. The balance antenna share does not impose any bound on the minimum power level for each spot beam in case of dynamic power design. For data rate and coding allocation a quality of service must be prefixed to determine the modulation and coding. So it is possible to manage the available power on board to provide a satisfactory service to all beams for almost all time in the year.

Conclusion and future Work

5.1 Conclusion

In this report a brief description of the major phenomena affecting radiowave propagation at earth satellite links in Indian region is given. Global models for long-term modelling of rain effect presented. This summarizes the thesis's contributions and overall integrated system design of Ka-band satellite system. Future work and suggestions are given here for further development in propagation study and fade mitigation.

This study provides terrestrial and slant path variation of rain heights and calculates rain attenuations using geographical parameters in various Indian locations. It is found from the result that there is about 10 dB attenuation for the duration less than 0.1% of time (about 8.7 hrs) and 20-30 dB rain attenuation occurs for less than 0.01% of time (about 53mints) over an average year. So this 10 dB can be taken as the standard attenuation level and it can be varied up to 30 dB statistically taking different attenuation levels and demand of users in 16 spot-beams. By adopting composite technique of mitigation the power level is maintained at a satisfactory level to the end user. The Moupfouma model calculations are having close approximations with ITU model, but the Crane model shows a large variation. In this paper possible rain attenuation and corresponding power allocation to provide uninterrupted service during rain specifically in Indian cities, over 16 spot-beam locations are focused.

We have presented a flexible beam allocation algorithm that combines the requirements to provide a minimum satellite gain with the need to provide a statistically balanced beam configuration for all users. Static power enhancement method can be used to maintain the power level constant for long duration depending upon predicted data. Adaptive power allocation to different spot beams has been shown to enhance the efficiency of satellite, by effective utilization of power and resource enabling user a higher data rate without degrading the average user throughput.

Here we have tried to analyse the effect of rain to Ka band broadcasting in Indian main land. But adequate data could have been collected from a ka band experimental satellite like ACTS or as planned in GSAT4. It would be a great achievement for all Indians if the system could work efficiently to cater needs of multitudes as envisaged.

5.2 Future work & Suggestions

Digital signal processing can be used to allocate power and data rate transmission to all beams for an effective output. The rain measurement seems to suggest possible shortcomings of the ITU-R theoretical model. So a long term measurement of rain attenuation should be performed in future with terrestrial and satellite path. In relation to this, it is proposed to attach a local meteorological station to the receiver providing on-site meteorological data. Data from two or more stations can also be compared to identify different rain events. The future possible works can be carried out with following problems

1. The design and development of electronically steerable phased array antenna will lead to steer among the spot beams to deliver the signal at desired power level.
2. The power allocation procedures would be simulated to get implemented. A more realistic scenario would be investigated taking into account the amount of power for a session using the dynamic power allocation.
3. Using DSP, the prediction of channel condition and power allocation to spot beams would be achieved.
4. The analysis of IP based user category and allocating variable bandwidth to individual user using DSP can be performed.

Dissemination of the Research Work

List of Publications

1. J .Jena, P.K, Sahu, "Rain fade and Ka-Band Spot Beam Satellite Communication in India", *IEEE International conference on "Recent trends in Space Technology Services and Climate Change-2010", ISRO and Indian Society of Remote Sensing (ISRS),ISBN-978-1-4244-7/10/3 p 304-306-2010, IEEE, (RSTS & CC -2010), Sathyabama University ,* Chennai, 14-17 Nov 2010.
(best paper in the session)

2. J. Jena, P.K, Sahu, "Rain Fade Calculation and Power Compensation for Ka-Band Spot Beam Satellite Communication in India", *NETCOM 2010 and COSIT-2011, 3-7 Jan 2011, Bangalore, CCSIT-2011,PART-II,CCIS132,PP-313-320,2011, "Springer" publication, Berlin ,* Heidenberg 2011.

3. J.Jena, P.K.Sahu, "Ka-Band Spot Beam Satellite Communication in India", *International Conference on Radio Science, International Centre for Radio Science (ICRS -2010),* Jodhpur, Rajasthan, 17-20 Dec -2010.

Bibliography

[1] Apostolos Destounis and Athanasios D. Panagopoulos, "Dynamic Power Allocation for Broadband Multi-Beam Satellite Communication Networks," *IEEE Communications letters, vol. 15, no. 4,pp. 380-382,* April-2011.

[2] K. Bandyopadhyaya, "GSAT-4, A step towards Indian advanced communication satellite," *IWSSC*, IIT, Kharagpur, Oct-2008.

[3] J. S. Ojo, M. O. Ajewole, and S. K. Sarkar, "Rain rate and rain attenuation prediction for satellite communication in Ku and Ka bands over Nigeria," *Progress In Electromagnetics Research B*, Vol. 5, 207-223, 2008.

[4] Sangeeta Kamboj, and Dr. Ratna Dahiya, "Adaptive Antenna Array for Satellite Communication Systems," *Proceedings of the International Multi-Conference of Engineers and Computer Scientists 2008, Vol. II ,IMECS 2008, pp.19-21*, Hong Kong, March, 2008.

[5] Ana Yun, Ana Jalón, Josep Prat, Borja de la Cuesta, Alejandra Carla Salas, and Cedric Baudoin, "Next generation on board pay load architecture," *IEEE International Conference, Information Society Technologies, 978-1-4244-2204-3/08*, *pp.246-250, IEEE-* 2008.

[6] Sarat Kumar K, Vijaya Bhaskara Rao S, and D Narayana Rao, "Prediction of Ku Band Rain Attenuation Using Experimental Data and Simulations for Hassan, India," *IJCSNS - International Journal of Computer Science and Network Security, VOL.8 No.4,pp.10-15 ,*April 2008.

[7] L.J.Ippolito Jr., "Satellite communications Systems Engineering," *John Wiley & sons publication, Third edition-*2008.

[8] Timothy Pratt, Charles Bostian, and Jeremy Alnutt, "Satellite communications," *Wiley and sons, 2nd edition-*2007.

[9] Mohamad H. Ostovarzadeh and Forouhar Farzaneh, "A proposed Multi beam Ka-band Satellite for providing high-speed Internet service for Iranian Universities and Educational Institutions," *Proceedings of the 2007 IEEE International Conference on Telecommunications and Malaysia International Conference on Communications,* Penang, Malaysia, 14-17 May 2007.

[10] T. S. Rappaport, "Wireless communications: Principles and practice," *Prentice Hall, New Jersey,* 2007.

[11] S. B. Ahmad, "Frequency scaling of rain attenuation," *Master's Thesis,* May-2007.

[12] K. faisal, and Al-tabatabaie, "Long-term rain attenuation probability and site diversity Gain prediction formulas," *Master's Thesis*, May-2007.

[13] Cornelis Jan Kikkert, "The Design of a Ka band Satellite Beacon Receiver,*" IEEE Proceedings of ICICS*, *978-1-4244-2182-4/08, pp.598-601*, 2007.

[14] Recommendation ITU-R P.676-7, "Attenuation by atmospheric gases", *P Series, International Telecommunication Union,* Geneva, Switzerland, 2007.

[15] Emanuela Falletti, Fabrizio Sellone,Candida Spillard, and David Grace, "A Transmit and Receive Multi-Antenna Channel Model and Simulator for communication from High Altitude Platforms,*" International Journal of Wireless Information Networks, Vol. 13, No. 1, pp. 59-71*, January- 2006.

[16] C. E. Bobadilla-Del-Villar, and J. L. Cuevas-Ruíz, "Compute rain attenuation. An approach supported in ITU-R recommendations for the Ku- Band," *Proceedings of the 16th IEEE International Conference on Electronics, Communications and Computers (CONIELECOMP 2006)0-7695-2505-9/06, IEEE, pp. 1-4,-*2006.

[17] Dennis Roddy, "Satellite Communications," *Fourth International Edition, McGraw-Hill Publication,* 2006.

[18] Damodar Madgum, "Application of propagation models to design Geo-stationary satellite link operating in ka-band over Indian rain zones," *CSSTEAP-UN, SAC, ISRO,* Ahmedabad, 2005.

[19] Gun Akkor, "Multicast communication support over satellite networks," *Doctoral Thesis, University of Maryland,* 2005.

[20] Ayman. A. Alwarfalli, "The effect of rain rate modelling for the prediction of Satellite propagation in Malaysia," *Master's Thesis,* Nov-2005.

[21] Rens Baggen, Sybille Holzwarth, Martin Bottcher, and Michael Eube, "Phased Array Technology: Trends & Developments," *GeMiC*, Germany, 2005.

[22] C. A. Balanis, "Antenna Theory, Analysis and Design,*" John Wiley & Sons, Inc*. New Jersey, 2005.

[23] Recommendation ITU-R P.835-4, "Reference standard atmospheres," *P Series, International Telecommunication Union, Geneva,* Switzerland, 2005.

[24] Ashok Kumar Baldotra and I. S. Hudiara, "Rain Attenuation Statistics Over Terrestrial Microwave Link at 19.4 GHz at Amritsar," *IEEE Transactions on Antennas and Propagation, vol. 52, no. 6, pp. 1505-1508,* June-2004.

[25] Dennis Lee, Andrew Gray, and Edward Kang, "A Gigabit per second Ka band demonstration," *IEEE, AC paper- 1403, Version 4,* Dec- 2004.

[26] Recommendation ITU-R P.618-7, "Propagation Data and Prediction Methods Required for the Design of Earth-Space Telecommunications Systems," Geneva, 2003.

[27] Recommendation ITU-R S.827, "Maximum permissible level of off-axis E.I.R.P. density from very small aperture terminals (VSATs)," Geneva, 2003.

[28] Recommendation ITU-R P.837, "Characteristics of precipitation for propagation modelling," Geneva, 2003.

[29] Recommendation ITU-R P.838, "Specific attenuation model for rain for use in prediction," Geneva, 2003.

[30] Recommendation ITU-R R P.618-8, "Propagation data and prediction methods required for the design of Earth-space telecommunication systems," Geneva, 2003.

[31] ITU, "Handbook on Satellite Communications," *3rd Edition, Wiley, New York,* 2002.

[32] Sungtek Kahng, Man Seok Uhm and Seong Pal Lee, "A Dual Mode narrow band channel filter and group Delay equaliser for ka Band Satellite transponder," *ETRI Journal, Vol. 25,No. 5, pp.379-386.1-9,*2003.

[33] Asoka Dissanayake, "Ka band propagation modelling for fixed satellite applications," *Comsat Laboratory, pp.1-5, space journal-fall,* 2002.

[34] Recommendation ITU-R P.839, "Rain height model for prediction methods," 2002.

[35] Mario A. Blanco and Marc N. Richard, "Waveform Design for Ka-band SATCOM High Data Rate Links," *The MITRE Corporation Bedford, MA 01730,* USA-2002.

[36] Sasa T. Trajkovic, "Ka band transmitter for IP transfer over satellite," *Master's Thesis, University of Belgrade,* April- 2002.

[37] Feng, Y., "Resource Allocation in Ka-band Satellite Systems," *Master's Thesis, University of Maryland, College Park,* Maryland, U.S.A., 2001.

[38] Saxena Poonam and T.K. Bandyopadhyaya, "Rain induced attenuation of millimeter waves radio link in Indian continent," *RRL,CSIR*, Bhopal-2001.

[39] Recommendation ITU-R 530-10, "Propagation prediction techniques and data required for the design of terrestrial line-of-sight systems," *International Telecommunication Union*, 2001, *pp. 271-295, P Series*, Geneva, Switzerland, 2001.

[40] Tah-Hsiung Chu, Chao-Hsiung Tseng, Shin-Der Yang and Chung-I Chi, "A ka-band receiving terminal for measuring Rocsat-1 ecp beacon signals," *Journal of the Chinese Institute of Engineers, Vol. 24, No. 1, pp. 29-36,* 2001.

[41] Gert Cuypers, "Noise in satellite links," *Belgian Microwave roundtable*, 2001.

[42] Krishna Kumar, and K.D. Kumar, " Feasibility of using statellites in nonequatorial 24- hour circular orbits for Communications," *51st IAF congress-Acta Astronautwa Vol. 48, No. 5-12, pp 589-596, Elsevier Science Ltd.,* IIT Kanpur 2001.

[43] R.Acosta,S.Johnson,and O.Sands,"Ka-Band Phased Array System Characterization," *Glenn Research Center, NASA STI Program, Vol. 40,* Cleveland, Ohio, Nov.-2001.

[44] Simon Haykin, "Communication Systems,"*4th Edition, John Wiley & sons, Singapore,* 2001.

[45] Yuei-an Liou, "Radiometric Observation of Atmospheric Influence on Space-to-Earth Ka-Band Propagation in Taiwan," *Proc. Natl. Sci. Counc. ROC (A), Vol. 24, No. 3, pp. 238-247,* 2000.

[46] Dennis G. Sweeney, and Charles William Bostian, "Implementing Adaptive Power Control as a 30/20-GHz Fade Countermeasure," *IEEE Transactions on Antennas and Propagation, Vol. 47, No. 1 ,pp. 40-46,* January-1999.

[47] Gargione.F., Iida.T., Valdoni.F., and Vatalaro.F.,"Services, Technologies, and Systems at Ka band and Beyond-a survey," *Communications, IEEE Journal, Vol. 17 (2), pp. 133–144,* Feb-1999.

[48] James Yoh, Charles C. Wang and Gary W. Goo, "Survey of ka-band satellites for wideband communications," *The Aerospace Corporation Proceedings of IEEE,pp.1-7,* 1999.

[49] John D. Kraus, "Antennas,*" McGraw-Hill,* New York, 1998.

[50] A. Dissanayake, J. E. Allnutt, and F. Haidara, "A Prediction Model that Combines Rain attenuation and Other Propagation Impairments along Earth-Satellite Paths," *IEEE Transaction on Antennas and Propagation, Vol. 45. No. 10,pp.1546-1558,* October-1997.

[51] Patrick S. Young, "Ka band services and technologies," *The Institution of Electrical Engineers*-1997.

[52] Recommendation ITU-R S.1329, "Frequency sharing of the bands 19.7-20.2 GHz, and 29.5-30.0GHz between systems in the mobile-satellite service and systems in the fixed-satellite service," Geneva, 1997.

[53] Dissanayake, A.W., "Application of open-loop uplink power control in Ka-band satellite links," *IEEE Journals, Vol. 85, Issue 6, pp. 959 -969,* June 1997.

[54] J.Beaver, J.Turk, V.N Bringi "Ka band propagation measurement from the Advanced Communications Technology Satellite (ACTS*)," Geoscience and Remote Sensing Symposium*, *Vol-1,pp. 79-81*,*IEEE*, 1994.

[55] R. L. Olsen, D. V. Rogers, R. A. Mys , and m. M. Z. Khar, "Interference due to Hydrometeor Scatter on Satellite Communication Links," *Proceedings of the IEEE. Vol.81, no. 6, pp 914-922,* June-1993.

[56] L.J. Ippolito, Thomas a. Russell, "Propagation Considerations for Emerging Satellite Communications Applications," *Proceedings of the IEEE, vol. 81, no. 6*, June 1993.

[57] J.E. Allnutt, "Satellite-to-ground radiowave propagation: Theory, practice and system impact at frequencies above 1 GHz," *Peter Peregrinus Ltd.,* London, 1989.

[58] Pratt,T., and Bostian, C., "Satellite Communications," *John Wiley & Son, New Jersey,* 1986.

[59] Crane, R.K., "Prediction of Attenuation by Rain," *IEEE Transactions on Communications, Vol. COM-28, No. 9, pp. 1717-1733,* Sept-1980.

[60] Fidele Moupfouma, "Improvement of rain attenuation prediction method for terrestrial microwave links," *IEEE Transaction on Antennas and Propagation, Vol.AP-32, No.12, pp.1368-1372,*Dec-1984.